Determining the mechanism by which PZA exerts its antimycobacterial activity against *Mycobacterium tuberculosis*

A DISSERTATION

SUBMITTED TO THE FACULTY OF THE GRADUATE SCHOOL

OF THE UNIVERSITY OF MINNESOTA

BY

Nicholas Allen Dillon

IN PARTIAL FULFILLMENT OF THE REQUIREMENTS

FOR THE DEGREE OF

DOCTOR OF PHILOSOPHY

Advisor: Anthony Baughn, PhD

February 2017

Acknowledgements

I could not have made it to this point without the support of my friends and family. I don't know how many "this experiment took way longer than I thought, I'll be late" messages I had to send over the years. It kind of became a running joke, where everyone just assumed I'd leave lab 2 hours after I said I would, problem is, they were usually right.

I would especially like to thank my mentor Tony. I wouldn't be where I am without his guidance. In fact I'd probably still be setting up some giant experiment with every condition possible being tested, only to find out that I used the wrong conditions since I never did a pilot. Tony has helped me focus, helped me learn to ask the questions that need to be answered, and then design experiments to address those questions. I have thoroughly enjoyed our 1 hour meetings that usually last 2-3 hours, and the great discussions we have had over the years. I can unequivocally say that Tony has helped me become a better scientist, and I'm extremely thankful for his guidance and mentorship over the years.

Throughout the years I have relied on the support and friendships I have built with my labmates. From daily trips to the hospital cafeteria for coffee/tea, to our always entertaining group lunches, we commiserated or celebrated with each other based on the outcome of our experiments. We had epic lab ball tournaments, that helped lively up some of those slow Minnesota winter days, and we created a convoluted verbal betting

scheme based off of awarding “Pride Points”. Nothing made a normally boring meeting more exciting then when pride points were on the line.

I have been fortunate to be surrounded by a great group of friends throughout my life, from friends that I have known since high school, to friends that I didn’t meet until graduate school. We had a lot of fun over the years going discing, playing games, and just hanging out. The time I have spent with them has been crucial to letting me unwind from the long weeks in the lab.

I would not be where I am without the help and love of my amazing wife. She has patiently listened to me complain about failed experiments and she has slept through a lot of my practice talks at home just so I could have someone sitting in the audience. She has long tolerated the schedule that graduate school demands. In the early days Laurie would occasionally pick me up from work. She ended up spending a lot of time sitting in the car waiting for me, since I was never ready when I said I would be. We eventually made a compromise and we’d go out to eat every time she had to wait on me, we went out to eat a lot. I treasure the nights and weekends that I spend with Laurie and our son Ryker, and I look forward to all of the adventures that are ahead of us.

Dedication

This thesis is dedicated to my friends and family. I couldn’t have done it without them.

Abstract

Pyrazinamide (PZA) is one of the four first line drugs used to treat *Mycobacterium tuberculosis* infections. For PZA to be active against *M. tuberculosis* the drug must be enzymatically converted into pyrazinoic acid (POA) by the *M. tuberculosis* amidase PncA. *In vitro* PZA susceptibility requires concurrent exposure to stress, potentially linking the extracellular environment of *M. tuberculosis* to the drug's mechanism of action. While the production of POA is required, its molecular target is unknown. Multiple models have been proposed to explain the anti-mycobacterial activity of POA, yet, confirmatory evidence is required for their validation. We evaluated each of the proposed models to assess their validity. Our findings refute the previously proposed models leading us to conclude that the mechanism of action of PZA was still undefined. While studying drug susceptibility in a pantothenate auxotrophic strain of *M. tuberculosis* we discovered that supplementation with metabolites of the pantothenate/coenzyme A pathway antagonized the activity of PZA. In further characterization of this phenomenon, we found that some metabolic precursors to pantothenate also antagonized PZA only when the precursors could be used for the synthesis of pantothenate. Based on the recent identification of a novel PZA resistance mutation we set out to use a library of transposon mutagenized *M. tuberculosis* to select for PZA resistance. To our surprise, we identified transposon insertions in over 150 genes that had no previous association with PZA resistance. Compiling a list of the most frequent genomic positions that contained the transposon we uncovered a relationship between PZA susceptibility and the sigma factor E (SigE) regulon. SigE activation in *M. tuberculosis* occurs in response to

extracyotplasmic stress. When examining the impact of extracyotplasmic stress on PZA activity we found that POA worked synergistically with H_2O_2 against *M. tuberculosis*. Based on our studies we hypothesize that the synergy occurs through increased hydroxyl radical production from the interaction of POA and iron complexes with H_2O_2. Increasing cellular oxidative stress would negatively impact multiple metabolic processes and could lead to a reduction in free coenzyme A (CoA). A recent study found a reduction in CoA levels after PZA treatment further linking the drug to this crucial cofactor. Combining our data we hypothesize that POA reduces free CoA availability through increased oxidative stress, leading to the eventual killing of *M. tuberculosis* through an inhibition of global metabolic functions.

Table of Contents

List of Tables

List of Figures

Chapter 1

Introduction

Tuberculosis

Infectious diseases were the primary cause of death in humans until the advent of modern medicine in the mid 20th century. Through improvements in hygiene, vaccination and therapeutic interventions, many of the old-world diseases were defanged, reducing their modern mortality rates to near-negligible levels. Tuberculosis (TB) represents one of the outliers, an ancient disease that continues to ravage humanity into the 21st century.

Infections with *Mycobacterium tuberculosis*, the causative agent of TB, are the leading cause of death due to an infectious agent in 2016[1]. Annually, an estimated 10.4 million patients are newly diagnosed with active *M. tuberculosis* infections and approximately 1.45 million deaths are attributed to the disease[1]. While new active infections are highest in sub-Saharan Africa and Asia, there are still approximately 10,000 cases in the U.S. on an annual basis[1].

Due to its co-evolution with the human immune system *M. tuberculosis* has multiple adaptations that permit its survival within the host. In addition to a thick peptidoglycan layer, mycobacteria also possess a relatively impermeable outer layer of long-chain fatty acids termed mycolic acids. While serving as a physical barrier, mycolic acids may also play a role in the immunoevasion mechanisms employed by *M. tuberculosis*[2]. The characteristic slow growth rate of *M. tuberculosis*, requiring 20-24 hours for a single replication cycle *in vitro*, is also thought to enhance its survival in the host by limiting the pathogen's initial exposure to the immune system[3].

M. tuberculosis is spread through aerosolized droplets that are typically expelled from infected individuals through coughing. Once inhaled by a *naïve* host, the pathogen survives and replicates within host phagocytes. It is estimated that as little as one bacillus is sufficient to establish an active *M. tuberculosis* infection[4]. While the lungs are the most common site of mycobacterial residence, approximately 15% of cases will also establish extra-pulmonary infections[1].

Immunological control of the active infection is not associated with mycobacterial sterilization within the host which permits the establishment of a latent infection. During latency *M. tuberculosis* is effectively sequestered within host-derived granulomas where it can persist for decades prior to reactivation[5]. Latently infected individuals harbor an approximate 5-10% lifetime risk of the mycobacteria reactivating [6]. Once reactivation occurs, infectious bacilli will again be present in the sputum, permitting transmission of the pathogen in the population. As there are no known environmental reservoirs for *M. tuberculosis*, infected individuals represent the only infectious reservoir for the disease. Estimates indicate that 1/3 of the entire human population is latently infected by *M. tuberculosis*, providing an infectious reservoir of approximately 2 billion people[1].

Although *M. tuberculosis* is considered a causative agent of TB, the disease can manifest in response to infections by other mycobacteria. The group of mycobacteria that can cause the disease are referred to as the *Mycobacterium tuberculosis* complex. The members of the complex are ever-changing[7], but it notably contains *M. tuberculosis, M. africanum, M. bovis,* and *M. canetti* amongst others. *M. africanum* and *M. canetti* are both found predominantly in Africa, where immunosuppression due to the AIDS pandemic is at its highest. Although *M. africanum* has the same transmission potential as *M. tuberculosis,* its association with disease progression is reduced in immunocompetent individuals[8]. However, in a study in Gambia, when compared to *M. tuberculosis,* AIDS patients were twice as likely to have *M. africanum* infections, and *M. africanum* infected individuals were 3.5 times more likely to have HIV[9].

Given the similarity between the species, *M. tuberculosis* was originally thought to have derived from *M. bovis*[10]; however, comparative genomics has revealed that the two species deviated from a common ancestor approximately 15,000-20,000 years ago[11,12]. Prior to the widespread use of pasteurization in dairy products, it was estimated that *M. bovis* infections were responsible for 20-40% of the cases of TBs in the United Kingdom[13]. *M. bovis* still accounts for up to 7% of the TB cases in areas of the southern United States where consuming unpasteurized milk is more commonplace[14]. Unlike *M. tuberculosis*, *M. bovis* transmission between humans is extremely rare[15].

Symptoms, immune response, *in vivo* environment of *M. tuberculosis*

M. tuberculosis has evolved in conjunction with the human immune response to permit its survival and replication within the host. Interactions between the immune system and the bacterium occur soon after inhalation when the pathogen is phagocytosed by alveolar macrophages and other phagocytes. Once within the phagosome, *M.*

tuberculosis arrests phagosomal maturation and blocks phagosomal-lysosomal fusion through the production of multiple interfering molecules that appear to be dependent on the ESX-1 secretion pathway[16]. Modulation of this initial intracellular environment prohibits phagosomal acidification, permitting bacterial growth[17]. Induction of adaptive immunity doesn't occur until approximately 42 days in humans[18] and 14 days in mice[19] during this stage of the infection due to multiple molecular stratagems employed by *M. tuberculosis*[20–22].

The onset of adaptive immunity marks the turning point for the end of the active infection and the eventual control of *M. tuberculosis*. Through a largely T_h1-driven response, infected macrophages are able to overcome the arrested phagosomal maturation and induce phagosome lysosome fusion[23]. Once activated, macrophages increase their production of reactive oxygen species and reactive nitrogen species in response to interferon-γ [24,25] and tumor-necrosis factor-α [26,27]. Through their immunomodulatory function both interferon-γ[28,29] and tumor-necrosis factor-α[30] are crucial for controlling an *M. tuberculosis* infection.

Although the active infection is controlled upon the onset of adaptive immunity, the latency phase of the infection ensues due to the inability of the immune system to fully eliminate the pathogen. To sequester the bacilli and prevent reactivation, the host encapsulates the pathogen within an aggregate of immune cells called a granuloma. Multiple immune cell types can be found within granulomas including macrophages, both CD4 and CD8 T-cells, neutrophils, and B-cells[31]. While walled off within granulomas, *M. tuberculosis* can survive and persist. Caseous necrotic granulomas can release their bacterial contents into the extracellular environment inducing increased mycobacterial growth and potential reactivation[32,33]. Reactivation can occur in an immuno competent individual but the rates are much higher in immuno compromised patients due to an inability to maintain the granuloma. Patients who are coinfected with HIV therefore have a higher risk for *M. tuberculosis* reactivation due to the virus associated loss in CD4 activity[34].

Intracellular environment occupied by *M. tuberculosis* in the host

Due to the host immune system the intracellular niche that *M. tuberculosis* occupies is an environment rife with multiple sources of stress. While residing within the phagosome *M. tuberculosis* is exposed to reactive oxygen species (ROS), reactive nitrogen species (RNS), an acidic extracellular environment, and nutrient limitation. *M. tuberculosis* has evolved multiple mechanisms to counteract these host derived stresses. Acidic pH and nutrient limitation stunt phagosomal pathogenic growth while the release of RNS and ROS directly eliminate invading bacteria. Through the evolution of efficient nutrient acquisition systems and by blocking phagosomal-lysosomal fusion *M. tuberculosis* is able to combat nutrient limitation and avoid the extremely acidic extracellular environment associated with the phagolysosome. Therefore the release of RNS and ROS is thought to play the crucial role in controlling *M. tuberculosis* infections within the host.

The immunological response to an *M. tuberculosis* infection in the mouse is dependent on the production of RNS[35]. The primary RNS produced is nitric oxide (NO) that is generated by an inducible NO synthase (iNOS) through a two-step reaction that produces NO and L-citrulline through the oxidation of L-arginine[36]. NO production is induced by multiple host cytokines in response to the infection[25,37]. Loss of NO production in murine iNOS mutants is associated with an increased susceptibility and mortality post *M. tuberculosis* exposure[35]. RNS production is critical in the mouse yet its relevance for the response in humans has been questioned due to an absence of iNOS associated activity in human alvelor macrophages[38].

The production of ROS plays a central role in the human response to an *M. tuberculosis* infection. Superoxide is generated in the phagosome by the NADPH oxidase complex through the transfer of an electron to molecular oxygen. Once produced superoxide dismutates into the more stable hydrogen peroxide (H_2O_2). Hydroxyl radicals are then produced through the interaction of H_2O_2 with metal ions. Hydroxyl radical exposure can lead to the damage of multiple cellular components including proteins, DNA, and lipids. Loss of NADPH oxidase function is associated with increased susceptibility to mycobacteria in humans[39,40] but not in mice[41]. ROS does seem to have an early role in murine models however, since NADPH mutants have higher initial mycobacterial loads[41]. Through the production of the catalase KatG *M. tuberculosis* is able to survive exposure to host derived ROS in mice[42]. Loss of function mutations in *katG* promote susceptibility to the murine host induced oxidative burst indicating that *M.*

tuberculosis resists ROS in mice by inactivating it[42]. ROS therefore seems to play a complimentary role in mice but a crucial role in humans.

Drug regimen

An efficacious multi-drug regimen is used to treat patients with drug-susceptible *M. tuberculosis* infections. Multiple drug combinations were evaluated in extensive clinical trials through the 1970s to find a regimen that could shorten the standard therapy and reduce the rate of relapse[43]. The optimal regimen that prevailed was a four-drug cocktail that included isoniazid, rifampin, pyrazinamide, and ethambutol[43]. The treatment lasts for six months with all four drugs given for two months, followed by a four-month continuation phase of isoniazid and rifampin. Implementation of the new short-course therapy reduced the relapse rate from 27% to 2% when compared to the previous standard treatment[44].

Through targeting multiple essential mycobacterial functions, the four-drug short-course therapy is able to boast an approximate 90% success rate for clearing *M. tuberculosis* infections[1]. Isoniazid, discovered in 1952, is activated by the bacterial catalase KatG to form an NAD adduct that interferes with mycolic acid synthesis by inhibiting the enoyl ACP reductase involved in mycolic acid synthesis[45]. Isoniazid is considered one of the most potent agents in the regimen due to its strong bactericidal activity against replicating cells. Disruption of the synthesis of the cell wall is also the mechanism by which ethambutol exerts its anti-mycobacterial activity. Ethambutol disrupts the formation of arabinogalactan by targeting arabinosyl transferase, an enzyme required for the synthesis of the polysaccharide[46]. Rifampin has strong bactericidal activity and plays a crucial role in inducing mycobacterial sterilization within the host[43]. Rifampin is a broad spectrum antibiotic that binds to DNA-dependent RNA polymerase to inhibit RNA synthesis[47]. Unlike the other three drugs in the regimen, pyrazinamide (PZA) is active via a hitherto undefined mechanism. Understanding the mechanistic basis for susceptibility and resistance of *M. tuberculosis* to these drugs will be paramount in the discovery of novel agents with improved activity and in the development of molecular tools that will permit rapid drug susceptibility testing.

Drug resistance in *M. tuberculosis*

Although the first line regimen has a high success rate its future efficacy is threatened by the emergence of drug resistance in *M. tuberculosis*. There are two main classifications of drug resistance in *M. tuberculosis* that are based upon the resistance profile of each strain. Multi-drug resistance (MDR) is classified as resistance to both rifampin and isoniazid[1], two of the most potent bactericidal drugs in our arsenal. Extensively-drug resistant (XDR) isolates are classified as being resistant to at least one fluoroquinolone and one of the injectable second line drugs in addition to both rifampin and isoniazid[1]. Although not an official classification, totally-drug resistant infections, those resistant to all known mycobacterial drugs, have been detected in multiple parts of the world[48,49].

Drug resistant *M. tuberculosis* infections are associated with increased treatment duration in addition to an increased mortality rate. Treatment with the first line regimen is typically for a duration of 6 months while treatment of an MDR infection takes a minimum of 18 months of therapy[1]. Increased treatment duration is associated with increased patient non-compliance on the recommended treatment regimen[50], further promoting the development of resistance in *M. tuberculosis*. MDR and XDR infections have a high mortality rate at 40% and 60% respectfully[1]. Based on historical data untreated *M. tuberculosis* infections are associated with an approximate 70% mortality rate[51].

The prevalence of drug resistance in *M. tuberculosis* is low compared to the total number of infections but it is still not clear if the rates of resistance are increasing. A new *M. tuberculosis* infection has a 3.9% chance of being classified as an MDR infection as of 2015[1], compared to a 3.7% chance in 2012[52]. While drug resistance would appear to be increasing based on the given rates, the reported rates are an estimation due to poor MDR testing and reporting around the world[1]. Some countries that have done successive MDR rate reporting have shown increases in the rates of MDR from 2014 to 2015[1]. Only 20% of patients with MDR infections were enrolled in the MDR WHO recommended thereapy in 2015[1], potentially compounding the future prevalence of MDR infections.

The enigma that is pyrazinamide

The identification of PZA as a TB drug can be attributed to the discovery of antimycobacterial properties of a structurally similar compound. The original screen that identified PZA was enacted based upon a serendipitous discovery by Ernst Huant in 1945 when he attempted to protect lung tumor patients' mucosal layers from radiation therapy with nicotinamide[53]. Using nicotinamide, a PZA structural analog, he found that although he did not observe the desired mucosal protective effect he had anticipated, he did find that patients with concurrent TB infections had reduced TB associated lung lesions post administration of this compound[53]. This led him to conclude that nicotinamide had potential as an anti-mycobacterial drug. Considering streptomycin, the first TB drug, was only discovered in 1944[54], there was considerable excitement for nicotinamide as a potential additional agent. Subsequently, screens were conducted by multiple groups to identify structural analogs of nicotinamide with improved anti-mycobacterial activity. Out of these screens came both isoniazid[55] and pyrazinamide[56] in 1952.

The clinical efficacy of PZA treatment has been documented for more than 60 years, but the mechanism behind its anti-mycobacterial effects has been elusive. While initial studies demonstrated effectiveness in guinea pigs[57], mice[58], and humans[59], *in vitro* susceptibility to the drug was unattainable until the requirement for an acidic growth medium was realized[60]. *In vitro* experiments have demonstrated that PZA is not bactericidal for *M. tuberculosis*, leading to its classification as a bacteriostatic agent in the first-line regimen. PZA was initially given to TB patients in monotherapy, where it was found to induce bacterial clearance[59]. These early *in vivo* observations contradict the bacteriostatic dogma that has persisted within the PZA literature to date and suggest that host environment is critical for revealing the bactericidal activity of this drug.

The efficacy of PZA treatment requires that the drug is converted into the activated form pyrazinoic acid (POA). Formation of POA occurs through the hydrolysis of PZA by the mycobacterial pyrazinamidase/nicotinamidase PncA[61]. PncA is involved in the NAD salvage pathway in *M. tuberculosis* through its hydrolysis of nicotinamide to form nicotinic acid. PZA resistance-promoting mutations in *pncA* are common due to the dispensability of the NAD salvage pathway for *M. tuberculosis* viability[62]. Although POA has activity *in vitro* against *M. tuberculosis,* it is ineffective when administered *in vivo*, likely due to its high rate of clearance from the host[63].

Resistance to PZA

Resistance to PZA was observed in *M. tuberculosis* during its first use in humans[59], yet our identification of the mutations that promote resistance is still incomplete. Clinical resistance to PZA occurs in approximately two thirds of the cases through loss of function mutations in *pncA.* Loss of *pncA* function precludes the conversion of PZA to POA thereby preventing the enzymatic activation of PZA that is required for the drug's activity. *M. tuberculosis* can tolerate the loss of PncA, and its crucial role in the NAD salvage pathway, due to its capacity to synthesize NAD *de* *novo*[64,65]. However, a subset of clinical isolates maintain wild type *pncA* yet are presumably resistant to PZA through, as yet, unidentified mechanisms.

Determining the genetic basis for resistance to PZA is complicated in clinical isolates by the absence of suitable parental strains for DNA sequence comparison. Generation of resistant mutants in characterized laboratory strains yields mutations that can be readily identified due to the availability of the previously sequenced parental strains. Through the analysis of isolated spontaneous resistant mutants from an H37Rv background, a novel PZA resistance mutation was identified in *panD*[66]. *panD* encodes an aspartate decarboxylase that functions in the conenzyme A (CoA) biosynthesis pathway. Although detected *in vitro*, the *in vivo* relevance of *panD* mutations has been challenged due to their absence in characterized collections of PZA resistant clinical isolates[67]. Clinical data therefore indicates that up to a third of PZA resistant clinical isolates are resistant through an unknown mechanism. The identification of PZA resistance promoting mutations is presented in Chapter 3 of this thesis.

Previously proposed models for the mechanism of action of PZA

Multiple models for the mechanism of action of PZA have been proposed. The four most prevalent models are that PZA targets: fatty acid synthesis[68], intrabacterial pH homeostasis[69,70], a ribosomal rescue mechanism[71], and pantothenate biosynthsis[72]. All four models will be discussed below.

Fatty acid synthesis is disrupted by the PZA structural analog 5-chloropyrazinamide (5-Cl PZA) through the inhibition of fatty acid synthase I (FAS-I)[68,73,74]. Based upon the potent inhibition by 5-Cl PZA it was proposed that PZA was also an inhibitor of FAS-I[68]. However, some reports indicate that POA is not an inhibitor of FAS-I[73] and while PZA treatment does result in inhibition of FAS-I activity[68,74,75], POA has an IC_{50} for FAS-I that is >1000x then that of 5-Cl PZA[74]. While an impact on fatty acid synthesis may still be a facet of PZA activity it is unlikely to target FAS-I directly.

Prior work in *M. tuberculosis* had found an association between *in vitro* PZA susceptibility and concurrent exposure to an acidic pH[76]. Based upon this association with low pH it was hypothesized that POA functioned as a proton ionophore leading to eventual acidification of the mycobacterial cytoplasm[77]. This model is consistent with the observation that *M. tuberculosis* is especially susceptible to various acids during *in vitro* culturing[69]. PZA treatment is also associated with a disruption in membrane transport[77] and ATP synthesis[78], both of which are predicted to occur through a loss of proton motive force due to POA functioning as a proton ionophore. Evidence is presented in Chapter 2 refuting this model for the mechanism of action of POA.

In a search for molecular targets of POA it was reported that a binding interaction had been detected between POA and a ribosomal subunit that inhibited the ribosomal rescue mechanism of *trans*-translation[71]. This study was enacted based upon the low PZA resistance seen in the *M. tuberculosis* strain DHMH444 that encodes a wild type copy of *pncA* but was found to have a polymorphism in *rpsA*, which encodes the ribosomal protein S1 (RpsA) [71]. *trans*-Translation is a mechanism used by bacteria to release ribosomes that have stalled on mRNA transcripts. Using isothermal titration calorimetry the proponents of the model suggested direct binding between POA and RpsA, and inhibition of *trans*-translation in a cell free assay[71]. Evidence is presented in Chapter 2 that refutes this model.

The aforementioned resistance studies demonstrated a relationship between PanD activity and PZA susceptibility[66]. This led to the suggestion that PZA targeted PanD directly[66,72]. In support of this model levels of CoA are reduced upon PZA treatment[79]. While reduced levels of CoA in *M. tuberculosis* could be due to an impact on its production, direct interaction between PanD and PZA, or POA, has not been demonstrated. This model is assessed in Chapter 3 of this thesis.

Identification of the mechanism of action of PZA

PZA treatment affects multiple biological processes in *M. tuberculosis* that may indicate potential targets for the drug. PZA treatment has been previously linked to disruption of membrane potential[80], reduced ATP synthesis[78], and coenzyme-A depletion[79]. *M. tuberculosis in vitro* PZA susceptibility is also enhanced when the cells are in stationary phase compared to logarithmic growth[81]. An impact on the metabolic rate of *M. tuberculosis* seems to be a unifying theme in the various conditions associated with PZA activity. Identification of the mechanism of action of PZA will require addressing the effect of the drug on these biological processes in addition to defining the basis for its increased potency *in vivo*.

We now propose a new model for the mechanism of action of PZA against *M. tuberculosis* based upon evidence contained within this thesis. In our model POA increases oxidative stress within *M. tuberculosis* through enhancing the host induced oxidative burst. We further hypothesize that the increased production of ROS reduces the availability of the cofactor coenzyme A leading to an inability of the bacterium to conduct its required metabolic functions. This model has the potential to explain the multiple biological process that are affected by PZA treatment, as increased oxidative stress would have a global cellular impact, as well as the synergy that is observed between PZA and the host immune system.

Chapter 2

Previously proposed models do not adequately explain the mechanism of action of PZA.

Since its discovery in the 1940s and 1950s PZA has been a black box to modern medicine. It is a drug with a clear *in vivo* efficacy yet it is a poor anti-mycobacterial in laboratory culture. Multiple studies have sought to characterize the mechanism of action of PZA. In this chapter we evaluate fundamental aspects of two of the prevailing models that are described in the literature and accepted by many in the tuberculosis research community.

The first model that we addressed was the proton ionophore model. This model contended that POA acts as a proton ionophore leading to the eventual acidification of the bacterial cytoplasm. This model was based on the requirement for an acidic extracellular environment for *in vitro* PZA activity. In our 2015 publication in Antimicrobial Agents and Chemotherapy we were able to demonstrate that PZA activity does not require an acidic extracellular environment and the bacterial cytoplasm does not rapidly acidify as is seen with characterized ionophores. I contributed to this manuscript by conducting the experiments involving PZA susceptibility in buffer. I also participated in the overall design and focus of the study. The other experiments in the paper were conducted by Nicholas Peterson and Brandon Rosen. I was the third author on this manuscript.

The second model that we addressed was the *trans*-translation model in which POA was suggested to block the ribosomal rescue mechanism of *trans*-translation. The initial model was formulated based on a clinical PZA resistant isolate that had a mutation within the gene encoding the ribosomal subunit RpsA. The proponents of this model contended that POA bound to RpsA blocking the ribosome freeing capacity of *trans*-

translation. The model was based off of the observation that RpsA was found to be associated with POA when binding partners with the drug were pulled out of *M. tuberculosis* whole cell lysates and when direct binding was examined using isothermal titration calorimetry (ITC). We recreated the reported mutation in isogenic strains of *M. tuberculosis* finding no difference in the susceptibility to PZA. Using the same method employed by the previous studies, isothermal titration calorimetry (ITC), we detected no binding between POA and RpsA while we did detect binding between RpsA and its previously reported binding partner ssRNA. In collaboration with the Keiler laboratory at the Pennsylvania State University we confirmed in an *in-vitro trans*-translation assay that POA had no effect on *trans*-translation while an interfering oligonucleotide blocked *trans*-translation. I am listed as the first author of this manuscript and I contributed to this manuscript by doing the majority of the experiments that were presented within the paper as well as aiding in the overall design and the writing of the paper. Nicholas Peterson also aided in the experiments that are presented in this manuscript. The manuscript is submitted and we are awaiting a decision on its acceptance.

Uncoupling environmental pH and intrabacterial acidification from pyrazinamide susceptibility in *Mycobacterium tuberculosis*

Abstract

Pyrazinamide (PZA) is a first-line anti-tubercular drug for which the mode of action remains unresolved. *Mycobacterium tuberculosis* lacks measurable susceptibility to PZA under standard laboratory growth conditions. However, susceptibility to this drug can be induced by cultivation of the bacilli in an acidified growth medium. Previous reports have suggested that the active form of PZA, pyrazinoic acid (POA), operates as a proton ionophore that confers cytoplasmic acidification when *M. tuberculosis* is exposed to an acidic environment. In this study, we demonstrate that over-expression of the PZA-activating enzyme PncA can confer PZA susceptibility in *M. tuberculosis* under neutral and even alkaline growth conditions. Further, we find that wild type *M. tuberculosis* displays increased susceptibility to POA relative to PZA in neutral and alkaline medium. Utilizing a strain of *M. tuberculosis* that expresses a pH-sensitive GFP we find that unlike the *bona fide* ionophores monensin and carbonyl cyanide 3-chlorophenylhydrazone, PZA and POA do not induce rapid uncoupling or cytoplasmic acidification under conditions that promote susceptibility. Thus, based on these observations, we conclude that the anti-tubercular action of POA is independent of environmental pH and intrabacterial acidification.

Introduction

The first-line anti-tubercular drug pyrazinamide (PZA) is an essential component of tuberculosis (TB) short-course therapy. Inclusion of PZA in this regimen has yielded a significant reduction in relapse rates and has shortened treatment duration from 9 to 6 months[82]. Yet, the increasing global burden of multidrug-resistant and extensively drug-resistant TB threatens the durability of anti-tubercular therapy[83]. Acquisition of a better understanding of the requirements for PZA susceptibility in *M. tuberculosis* will facilitate the optimization of treatment regimens. Further, elucidating the mode of PZA action will guide the discovery of mechanistically related novel compounds to improve TB therapy and circumvent drug resistance.

PZA is a pro-drug whose anti-mycobacterial activity necessitates hydrolysis to pyrazinoic acid (POA) by the *M. tuberculosis* nicotinamidase/pyrazinamidase PncA[63,84]. PncA is a component of the NAD^+ salvage pathway in *M. tuberculosis*, which is nonessential for growth as the bacilli express a *de novo* NAD^+ biosynthesis pathway[65,85]. Loss-of-function mutations in *pncA* confer no discernible fitness defect and represent the primary molecular mechanism for PZA resistance in clinical and laboratory isolates of *M. tuberculosis*[84]. As recently reviewed by Zhang and colleagues[86], additional PZA resistance mechanisms have been suggested from *in vitro* studies, including enhanced POA efflux, structural alterations in the ribosomal protein RpsA[71], and alterations in the pantothenate/coenzyme A biosynthetic pathway[66,72,87]. The overall contribution of these latter putative resistance mechanisms has yet to be confirmed in a clinical setting or in mammalian models of TB infection.

While PZA exerts a sterilizing bactericidal effect against *M. tuberculosis* in humans and in animal models of infection[44,56,57,59], it shows no notable activity against bacilli under standard laboratory growth conditions[88]. *In vitro*, PZA-mediated bacteriostasis of *M. tuberculosis* can be induced by incubation under conditions of mild acidity[89] and co-incubation with efflux pump inhibitors[80]. Further, bactericidal activity of PZA can be induced under acidic incubation conditions by nutrient limitation[90], anaerobiosis[91] and exposure to compounds that interfere with energy metabolism[77]. It is conceivable that a common feature of these conditions is that they all promote cytoplasmic accumulation of POA, yet this model has not been experimentally evaluated.

Several models have been proposed to explain the mechanistic basis for the anti-tubercular action of PZA[68,71,72,77]. Of these, POA-mediated proton shuttling leading to cytoplasmic acidification of the bacilli remains the most widely accepted model for PZA action[77,86,92]. In this model, PZA passively diffuses across the mycobacterial wall and inner membrane where it is hydrolyzed to POA by the cytoplasmic amidase PncA. Negatively charged POA (pK_a of 2.9) is then eliminated from the cytoplasm by an unidentified mechanism. Once in the mildly acidic extracellular milieu (typically pH ~6 for PZA susceptibility assays[93]), a small proportion of extracellular POA becomes protonated and passively diffuses back into the cytoplasm. In the slightly alkaline cytoplasm (pH 7.4)[94] POA becomes deprotonated completing the cycle. Through repeated rounds of cycling, POA drives equilibration of the extracellular and intracellular pH, resulting in cytoplasmic acidification and pleiotropic impairment of cellular metabolism.

Recent reports have revealed that the acid-dependence for PZA action can be diminished through co-incubation with efflux pump inhibitors[80,81] or by over-expression of PncA[75]. Nonetheless, proton shuttling resulting in cytoplasmic acidification remains a plausible, but untested model for PZA action. Thus, in this study, we chose to more thoroughly examine the link between pH and PZA susceptibility. In the context of *pncA* over-expression we establish that PZA susceptibility is independent of environmental pH. Moreover, by monitoring intrabacterial pH using an intravital fluorescent reporter, we find that POA does not display robust proton ionophore (protonophore) activity. Thus, we conclude that *M. tuberculosis* growth inhibition by PZA or POA can be uncoupled from extracellular and intracellular pH, and is not likely attributable to proton shuttling and cytoplasmic acidification.

Methods.

Bacterial strains and culture conditions. *M. tuberculosis* strains H37Ra and H37Rv were gifts from W.R. Jacobs, Jr., of the Albert Einstein College of Medicine. Strains were grown in Middlebrook 7H9 medium (Difco) supplemented with 10% (vol/vol) oleic acid-albumin-dextrose-catalase (OADC) (Difco), 0.2% (vol/vol) glycerol, 0.05% (vol/vol) tyloxapol, and 50 µg/ml kanamycin and 150 µg/ml hygromycin as necessary. For nutrient-limited PZA survival assays *M. tuberculosis* H37Ra was incubated in PBS (pH 7.0) containing 0.05% (vol/vol) tyloxapol.

Construction of *pncA* over-expression vectors. *M. tuberculosis pncA* was amplified by PCR from pTIC6a::*pncA* (28) with primers 5'-CATCCCGGCGTTGATCTGTG-3' and 5'-TAATCGCGGCCTCGAGCAAG-3', digested with *Hin*dIII and *Nhe*I, and ligated into mycobacterial replicative and integrative expression vectors pUMN002 and pUMN007, respectively. Recombinant plasmids were propagated in DH5α and maintained with kanamycin selection. *M. tuberculosis* strain H37Ra was transformed with the *pncA* expression plasmids by electroporation and selected on supplemented 7H10 agar containing kanamycin.

Antimicrobial susceptibility assays. Antimicrobial susceptibility was determined by measuring optical density of respective cultures at 600 nm (OD_{600}). Susceptibility testing was performed using supplemented 7H9 medium at pH 5.8. The minimum inhibitory concentration (MIC_{90}) for antimicrobial compounds was defined as the minimum concentration required for inhibition of at least 90% of growth, relative to the no antimicrobial control. Exponentially growing cultures of *M. tuberculosis* were diluted to an OD_{600} of 0.01 in 5 ml of supplemented 7H9 medium in 30 ml square Nalgene bottles. Antimicrobial compounds were added to the final concentrations indicated in the text. Cultures were incubated at 37°C with shaking on a rotary platform at 100 rpm for 14 days. After incubation, 20 µl aliquots of the no antimicrobial control and antimycobacterial MIC_{90} cultures were removed and spotted on pH paper to determine culture pH.

Survival kinetics and dose response. Exponentially growing cultures of *M. tuberculosis* H37Ra were centrifuged and resuspended in phosphate buffered saline (PBS, pH 7.0) containing tyloxapol (0.05%). Cultures were starved for 2 days then diluted to an OD_{600} of 0.01 in 5 ml of PBS with tyloxapol (0.05%) in 30 ml square Nalgene bottles. PZA was added at specified concentrations. For acid survival exponentially growing cultures of *M. tuberculosis* were diluted to an OD_{600} of 0.01 in 5 ml of supplemented 7H9 medium at pH 5.8 in 30 ml square Nalgene bottles. At the indicated time points, culture aliquots were plated for colony forming unit (cfu) enumeration. For dose response determinations, starved cultures were diluted to an OD_{600} of 0.01 in PBS (pH 7.0) containing tyloxapol (0.05%) and specified PZA concentrations. Cell suspensions were incubated for 3 weeks and viability was monitored by plating for cfu.

Pyrazinamidase assays. Pyrazinamidase activity was determined as previously described[75]. Briefly, mid-exponential phase cultures of *M. tuberculosis* grown in supplemented 7H9 (pH 6.8) were treated with 2 mM PZA and incubated at 37ºC with shaking. At various time points 1 ml of culture was removed, centrifuged (13,000 x g, 10 min), and 100 µL of 200 mM fresh ferrous ammonia sulfate (Sigma-Aldrich) was added. Samples were incubated at 4ºC for 24 hours and then centrifuged (13,000 x g, 5 min) and OD_{468} measured. A millimolar extinction coefficient of 0.68 was used to determine POA concentration[75].

Quantitative RT-PCR. For quantification of *pncA* expression, quantitative reverse transcription-PCR (qRT-PCR) was performed. Briefly, mid-exponential phase *M. tuberculosis* was harvested via centrifugation. Cell pellets were resuspended in 500 µL TRIzol (Intitrogen) containing 1% polyacryl carrier (Molecular research center) and RNA was extracted by bead beating with 0.1 mm zirconia beads. Remaining DNA was removed by treatment with TURBO DNA-free™ kit (Ambion). Gene specific primers for qRT-PCR were designed with Primer3 software (bioinfo.ut.ee/primer3). qRT-PCR was performed with the QuantiFast® SYBR® Green RT-PCR kit (Qiagen). qRT-PCR reactions were prepared with 2X QuantiFast SYBR Green RT-PCR master mix, 10 µM primers, 0.1 µl QuantiFast RT Mix, 1 ng RNA and were run on a LightCycler®480 with following cycle conditions: 50°C for 10 min, 95°C for 5 min, 35 cycles of 95°C for 10 s, 60°C for 10 s, and 72°C for 20 s with fluorescence quantification for each cycle. A melting curve cycle of 95°C for 15 s, 60°C for 15 s, and 95°C with a 2% ramp rate was used to determine product specificity. To test for contaminating DNA, control qRT-PCR lacking reverse transcriptase was performed.

Intrabacterial pH determination. pH-GFP was a gift from Sabine Ehrt of Weill Cornell Medical College. H37Ra pUMN007 and H37Ra pUMN007::*pncA* were transformed with pH-GFP and selected on supplemented 7H10 containing 150 µg/ml hygromycin and 50 µg/ml kanamycin as needed. Transformants were propagated in supplemented 7H9 containing hygromycin and kanamycin as necessary. Intrabacterial pH was determined as previously reported[94] with modification. Briefly, mid-exponential phase H37Ra expressing pH-GFP was transferred to acidified or neutral medium by centrifugation

(3000 rpm, 10 min) and resuspension to a final OD_{600} of 0.1 in 5 ml supplemented 7H9 medium at pH 5.8 or 7.0 in 30 ml square Nalgene bottles. Anti-mycobacterial compounds and ionophores were added to the final concentrations indicated in the text. At specified time points, 200 µL of culture was removed to a black walled 96 well plate and fluorescence was assessed by excitation at 395 nm and 475 nm and recording emission at 510 nm using a Molecular Devices SpectraMax M2 plate reader. Ratios of emission obtained from excitation at 395 and 475 were correlated to pH using a standard curve that was generated by placing 20 µL of total protein extract of H37Ra expressing pH-GFP in 200 mM sodium phosphate, 100 mM citrate buffer at pH intervals from 5.5 to 8.5 in 0.5 increments. A sigmoidal Hill equation was fit to the 395:475 ratios using GraphPad Prism 6 for pH calculation.

Membrane potential determination. Membrane potential was assessed as previously described[95] with modification. Briefly, mid-exponential *M. tuberculosis* H37Ra grown in supplemented 7H9 was transferred to acidic or neutral medium by centrifugation (3000 rpm, 10 min) and resuspension to a final OD_{600} of 0.1 in 5 ml supplemented 7H9 medium at pH 5.8 or 7.0 in 30 ml square Nalgene bottles. Anti-mycobacterial compounds and ionophores were added to the final concentrations indicated in the text and incubated at 37 ºC. At 30 minutes 180 µl was removed and 20 µl of 150 µM 3,3-diethyloxicarbocianide chloride ($DiOC_2(3)$) added and incubated at room temperature for 30 minutes. Cells were then washed, resuspended in supplemented 7H9, and transferred to a black walled 96 well plate and analyzed in a Molecular Devices SpectraMax M2 plate reader, fluorescence was assessed by excitation at 488 nm and recording emission at 530 nm and 610 nm. Ratios of 610:530 were calculated.

Results

***pncA* over-expression confers susceptibility to PZA at neutral and alkaline pH.** To further evaluate the association between environmental pH and PZA susceptibility in *M. tuberculosis*, we over-expressed *pncA* from a constitutive mycobacterial promoter[96]. *pncA* over-expression by 100-fold was confirmed using quantitative real time PCR (qRT-PCR), which was further corroborated by PncA activity assays confirming a 100-fold increase in the rate of cell-mediated conversion of PZA to POA (Table 2-1). Consistent with previous results[75,97], *M. tuberculosis* H37Rv over-expressing *pncA* demonstrated PZA hyper-susceptibility in acidic growth medium (Table 2-1). In addition, *pncA* over-expression also conferred PZA susceptibility under neutral and alkaline growth conditions (Table 2-1). This PZA susceptibility phenotype is in contrast to *M. tuberculosis* with wild-type *pncA* expression levels, which demonstrated PZA susceptibility in acidic medium and resistance to greater than 13 mM PZA in neutral and alkaline media (Table 2-1). In addition, we found that wild type *M. tuberculosis* showed increased susceptibility to POA, relative to PZA, in both neutral and alkaline medium (Table 2-1). Considering these PZA and POA susceptibility studies were conducted in 7H9 medium, which has a weak buffering capacity, we evaluated culture pH at the conclusion of susceptibility testing. There was no notable change in pH for growth-inhibited pH 5.8 or pH 7.0 cultures. However, pH 8.0 cultures at the PZA and POA MIC_{90} had decreased slightly to pH 7.5.

***pncA* expression is not acid inducible and demonstrates no significant strain disparity.** Considering that over-expression of *pncA* can confer PZA susceptibility at neutral and alkaline pH, we performed qRT-PCR to determine if *pncA* expression is acid-responsive. Exponential phase cultures of *M. tuberculosis* were sub-cultured to acidified supplemented 7H9 medium (pH 5.8) for 24 hours at which point RNA was extracted and qRT-PCR was performed. There was no significant change in *pncA* expression levels under acid incubation in either *M. tuberculosis* strain H37Ra or H37Rv (Fig. 2-1).

PZA is bactericidal for *M. tuberculosis* in nutrient-limited, neutral pH medium. Consistent with previous findings[90], we observed that PZA produces a bactericidal effect against nutrient-limited *M. tuberculosis*. Yet, while previous reports describe bactericidal activity of PZA under nutrient-limited acidic conditions, we find that this bactericidal activity can occur at neutral pH (Fig. 2-2A and B). Under nutrient-limiting, neutral pH conditions, physiologically relevant PZA concentrations become bactericidal against *M. tuberculosis* after 5 days of incubation (Fig. 2-2A), while there is no discernable bactericidal activity in nutrient replete acidic medium (Fig. 2-2C). Additionally, bactericidal activity of PZA at neutral pH demonstrates dose dependent activity with a minimum bactericidal concentration of 1.6 mM (Fig. 2-2B).

Table 2-1. *M. tuberculosis* PZA susceptibility is independent of environmental pH.

Strain	PZA MIC_{90}[a] (mM)			POA MIC_{90}[a] (mM)			PZA Turnover (nmol/min/ ml of cells [OD_{600}])
	pH 5.8	pH 7.0	pH 8.0	pH 5.8	pH 7.0	pH 8.0	
H37Ra pUMN002	0.4	>13	>13	1.6	3.2	>6.4	0.099 ± 0.001
H37Ra pUMN002::*pncA*	0.4	1.6	1.6	1.6	3.2	>6.4	11 ± 1
H37Rv pUMN002	0.8	>13	>13	1.6	3.2	6.4	ND[b]
H37Rv pUMN002::*pncA*	0.05	1.6	3.2	1.6	3.2	6.4	ND[b]

[a]MIC_{90}, minimum concentration that inhibited ≥90% of growth relative to the no drug control over 2 weeks of incubation. [b]ND, not determined.

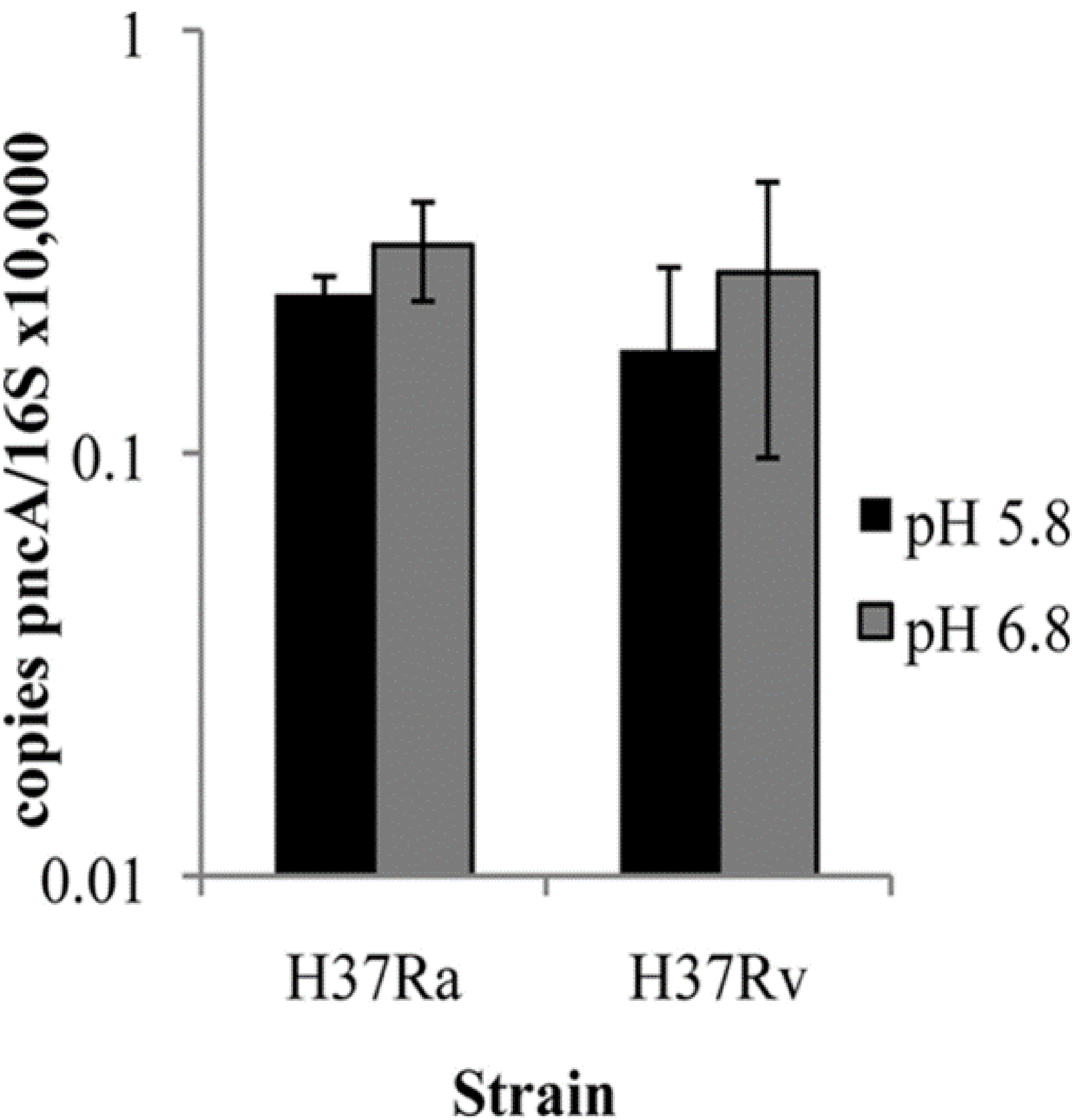

Figure 2-1: qRT-PCR analysis of *pncA* expression in acidified medium. Mid-exponential-phase *M. tuberculosis* H37Ra or H37Rv cells were transferred to acidified or neutral supplemented 7H9 medium for 24 h, after which RNA was extracted. Expression of *pncA* was quantified by qRT-PCR. The *pncA* expression level was normalized to the 16S rRNA level. Data are the means ± standard deviations of data from 3 independent experiments.

The effect of PZA and POA on *M. tuberculosis* cytoplasmic acidification. To address the long-standing question of whether POA functions as a protonophore we utilized a pH-sensitive green fluorescent protein (pH-GFP)[94,98] that enabled us to monitor the intrabacterial pH of live *M. tuberculosis*. Our rationale was that POA should function in a similar fashion to the characterized protonophore carbonyl cyanide 3-chlorophenylhydrazine (CCCP)[99]. Growing *M. tuberculosis* was treated with CCCP, the sodium ionophore monensin[100], POA (Fig. 2-3A) and PZA (Fig. 2-3B) at the MIC and 10-fold above and below the MIC. CCCP and monensin induced rapid and dose-dependent acidification of the cytoplasm (Fig. 2-4A and B). Indeed, mild cytoplasmic acidification was observed at concentrations 10-fold below the MIC for these ionophores. In stark contrast, POA did not induce measurable cytoplasmic acidification over 2 hours of incubation when included at the MIC (Fig. 2-4C). However, slight acidification was observed when POA was present at 10-fold above the MIC (Fig. 2-4C). Similar to results obtained with POA, no significant cytoplasmic acidification was observed with PZA even at the highest concentration tested (Fig. 2-4D). When *M. tuberculosis* was exposed to PZA and POA over several days, there was slow and subtle acidification of the cytoplasm (Fig. 2-4E and F). To determine if this slow acidification was associated with PZA-mediated inhibition of *M. tuberculosis*

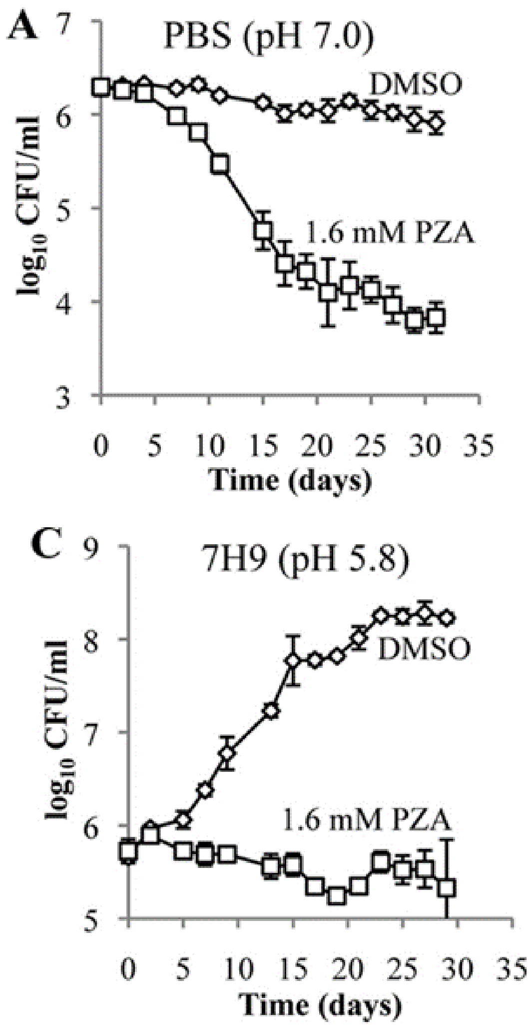

Figure. 2-2 Survival kinetics and dose response of nutrient-limited and -replete *M. tuberculosis* cells treated with PZA. *M. tuberculosis* strain H37Ra cells were inoculated in PBS (pH 7.0) containing tyloxapol (0.05%) (A and B) or in 7H9 medium containing OADC (10%), glycerol (0.2%), and tyloxapol (0.05%) at pH 5.8 (C). Cells were treated with dimethyl sulfoxide (DMSO) (diamonds) or PZA (squares) at the indicated concentrations. Survival kinetics were determined by plating for CFU at the indicated time points (A and C). For the PZA dose response under nutrient limitation conditions, bacilli were incubated for 3 weeks in the presence of the indicated concentrations of PZA, after which cells were plated for CFU enumeration (B). Data shown are the means ± standard deviations of data from 3 independent experiments.

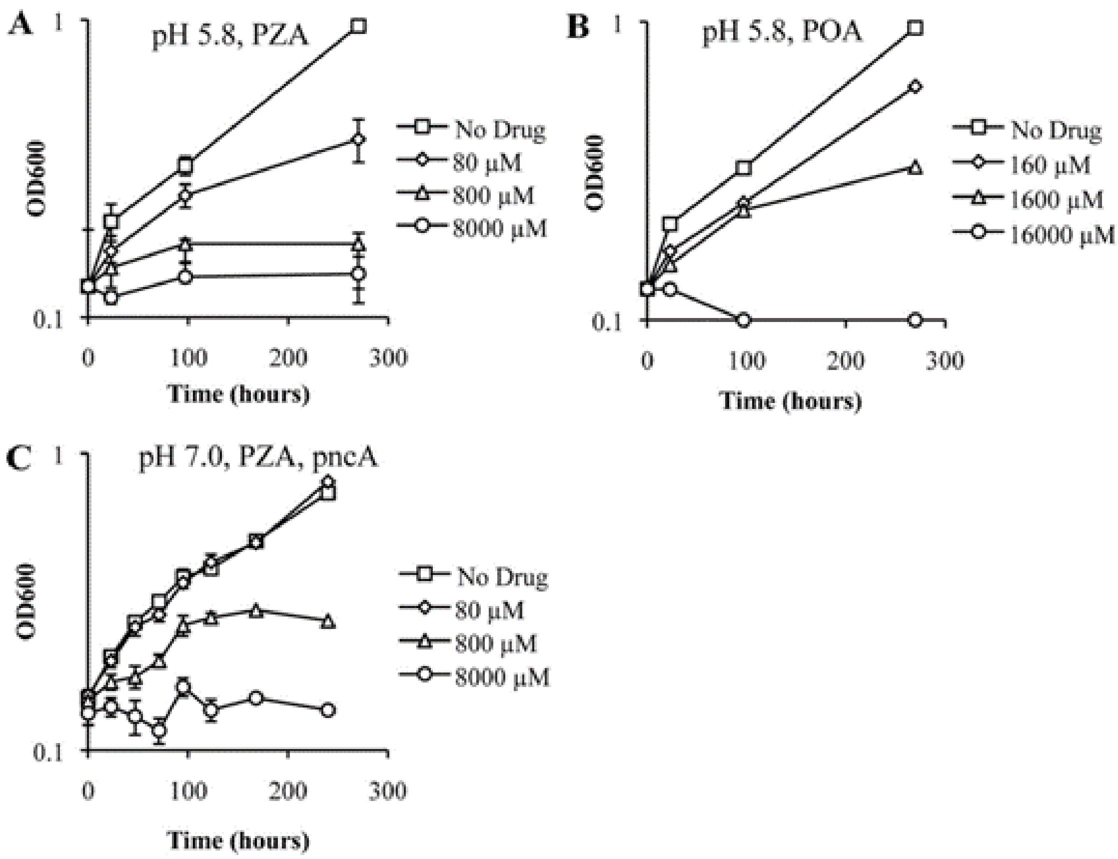

Figure 2-3 Growth kinetics of *M. tuberculosis* treated with PZA or POA at pH 5.8 and 7.0. The growth of *M. tuberculosis* strain H37Ra (A and B) or H37Ra/pUMN007::*pncA* (C) in 7H9 medium containing OADC (10%), glycerol (0.2%), and tyloxapol (0.05%) at pH 5.8 (A and B) or pH 7.0 (C) is shown. The cultures were treated with no drug (squares) or with either PZA (A and C) or POA (B) at concentrations 10-fold below the MIC (diamonds), at the MIC (triangles), and 10-fold above the MIC (circles). Data are the means ± standard deviations of data from 3 independent experiments.

growth or a secondary consequence of PZA action, we monitored the intrabacterial pH of PZA-treated *M. tuberculosis* over-expressing *pncA* at neutral pH. PZA treatment resulted in growth inhibition (Fig. 2-3C) with mild cytoplasmic acidification only at the highest concentrations of PZA examined (Fig. 2-4G). Significantly, lower PZA concentrations that fully inhibited growth did not induce cytoplasmic acidification (Fig. 2-4G).

The impact of POA on membrane potential in acidic medium. Given the lack of cytoplasmic acidification we proceeded to evaluate the previous suggestion that POA disrupts the membrane potential of *M. tuberculosis*[77]. Growing *M. tuberculosis* H37Ra was treated with 10 µM CCCP as a control or POA at 0.1, 1.0 and 10-fold the MIC followed by incubation with the membrane permeable fluorescent dye $DiOC_2(3)$. Consistent with previous reports and our evaluation of intrabacterial pH, CCCP induced significant loss of membrane potential[95], while concentrations of POA 10-fold above the MIC failed to significantly modify the membrane potential of *M. tuberculosis* at acidic pH (Fig. 2-5).

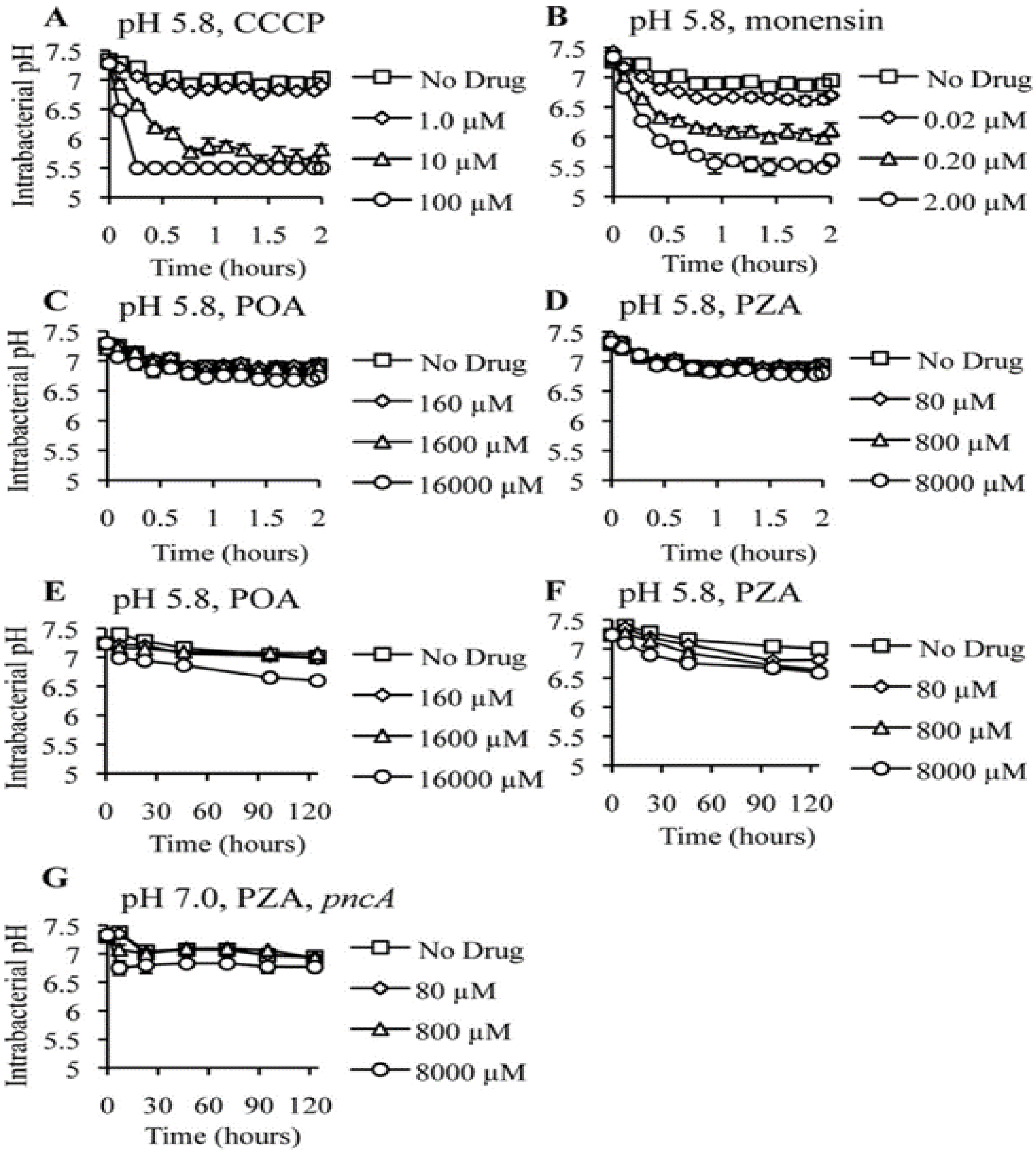

Figure 2-4 Cytoplasmic acidification kinetics of *M. tuberculosis* treated with CCCP, monensin, POA, or PZA at pH 5.8 and 7.0. The intrabacterial pH of *M. tuberculosis* strain H37Ra (A to F) or H37Ra/pUMN007::*pncA* (G) expressing ratiometric pH-sensitive GFP in 7H9 medium containing OADC, glycerol (0.2%), and tyloxapol (0.05%) at pH 5.8 (A to F) or pH 7.0 (G) is shown. The cultures were treated with no drug (squares) or with CCCP (A), monensin (B), POA (C and E), or PZA (D and F) at concentrations 10-fold below the MIC (diamonds), at the MIC (triangles), and 10-fold above the MIC (circles). pH 5.5 was the limit of detection. Data are the means ± standard deviations of data from 3 independent experiments.

Discussion and conclusions.

The increasing threat to TB therapy posed by drug-resistant strains of *M. tuberculosis* necessitates a deeper understanding of PZA action and potentiation. Therefore, in this study we investigated the dependence on environmental pH for PZA susceptibility in *M. tuberculosis*. Over-expression of PncA in *M. tuberculosis* conferred hyper-susceptibility to PZA at acid, neutral, and alkaline pH. Furthermore, PZA bactericidal activity against *M. tuberculosis* under nutrient limitation at neutral pH was observed. These observations demonstrate that an acidic environment is not essential to sensitize *M. tuberculosis* to PZA. Accordingly, while acidic incubation conditions potentiate the action of PZA, growth inhibition by POA is far less dependent upon acidic pH. Indeed, we found that *M. tuberculosis* is susceptible to POA at neutral and alkaline pH. A possible explanation for the disparity in pH requirements for POA and PZA action could lie in differences in the rate of accumulation of a critical concentration of POA. Indeed, it has been demonstrated that POA accumulates more readily under acidic incubation conditions[80].

Additionally, the disparity in pH requirements could possibly be explained by differing mechanisms of action at acidic and neutral pH. It has previously been reported that *Streptococcus bovis* lowers its internal pH to prevent significant anion accumulation and thereby enables growth at reduced pH in the presence of abundant organic acids[101].

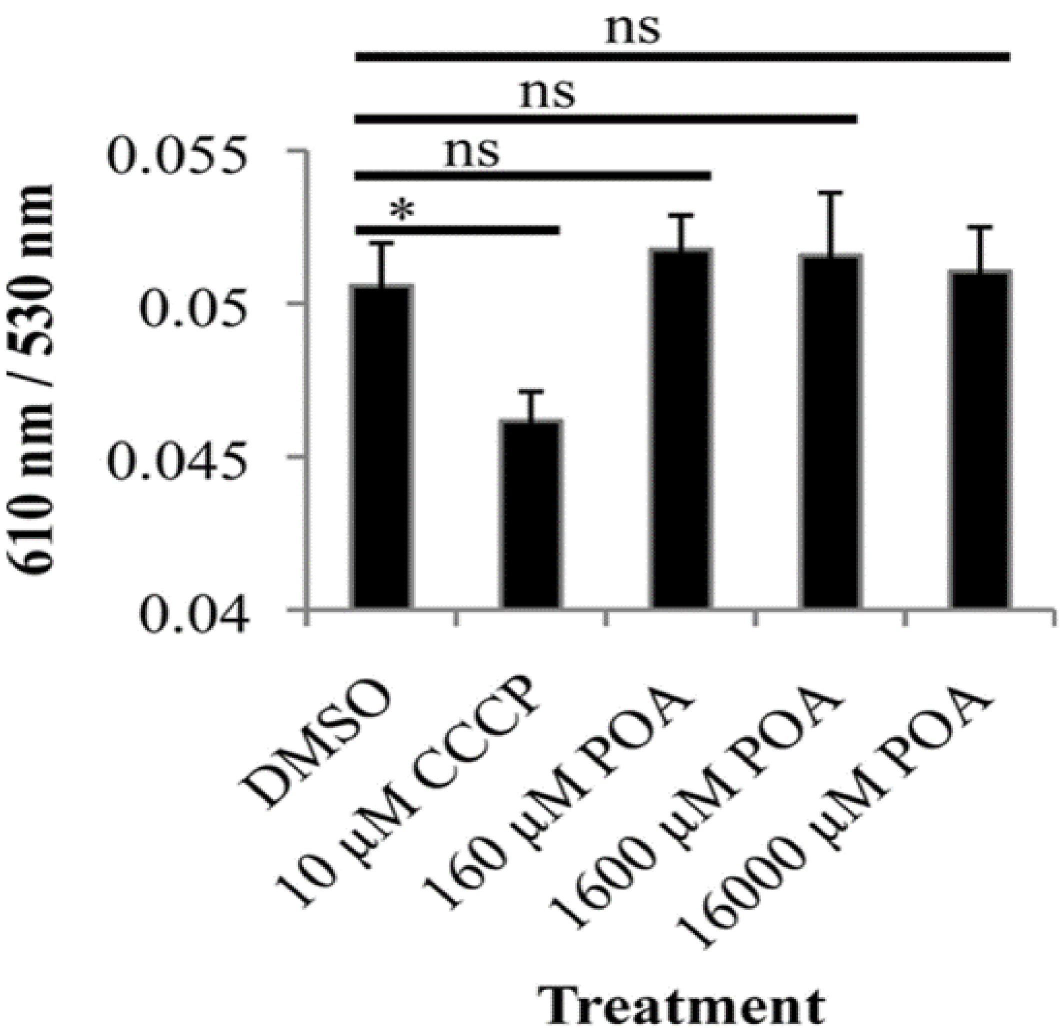

Figure 2-5 Membrane potential of *M. tuberculosis* treated with CCCP and POA at pH 5.8. *M. tuberculosis* cells in 7H9 medium containing OADC, glycerol (0.2%), and tyloxapol (0.05%) at pH 5.8 were treated with CCCP or POA at the indicated concentrations for 30 min. After 30 min of treatment, the fluorescent dye $DiOC_2(3)$ was used to assess membrane potential by monitoring the ratio of red fluorescence (610 nm) to green fluorescence (530 nm). A shift from green (530 nm), dependent on cell size, to red (610 nm), dependent on cell size and membrane potential, indicates the presence of membrane potential. Data are the means ± standard deviations of data from 3 independent experiments (*, $P < 0.05$; ns, not significant).

Therefore, growth inhibition under neutral pH conditions could be due to significant POA anion accumulation. Though, the observation that POA inhibits growth at neutral and alkaline pH suggests that this model is unlikely and that the intracellular target(s) of POA requires a critical concentration of POA for inhibition.

Significantly, acid-mediated potentiation of PZA susceptibility is independent of changes in expression of *pncA* in both attenuated and virulent strains of *M. tuberculosis*, H37Ra and H37Rv respectively. It is worth noting, though, that H37Ra carries a single nucleotide polymorphism in *phoP* conferring a non-synonymous serine to leucine change at position 219 in PhoP that compromises its DNA binding function[102]. *phoP* encodes the DNA response regulator PhoP of the two component signal transduction system PhoPR. Previous studies have demonstrated a role for PhoPR in the acid stress response[103]. Considering that H37Ra and H37Rv have similar *pncA* expression levels, activation of PZA does not appear to be a consequence of PhoP or acid pH, though these findings do not exclude the possibility that other PhoPR acid responsive targets could have relevance in PZA activity. Changes in the PhoP regulon could provide a possible explanation for the discrepancy in PZA MICs at pH 5.8 between H37Ra and H37Rv.

A key facet of the proton ionophore model of PZA action is the suggestion that POA drives acidification of the *M. tuberculosis* cytoplasm. While previous studies have reported acidification of the *M. tuberculosis* cytoplasm upon treatment with PZA, these studies were conducted under nutrient limitation and extreme acid stress (pH 4.5)[104]. In contrast to these findings, we observed only minimal acidification of the *M. tuberculosis* cytoplasm following PZA or POA treatment in nutrient replete, moderately acidic medium (pH 5.8). Importantly, PZA and POA showed a drastically delayed and less substantial degree of acidification relative to the well-characterized ionophores monensin and CCCP which exhibited rapid and dose-dependent acidification. Additionally, concentrations of POA that were at least 1600-fold greater than the molar equivalent concentration of CCCP that confers cytoplasmic acidification demonstrated no appreciable acidification. Furthermore, POA failed to significantly alter the membrane potential at acid pH, suggesting that the active form POA does not appear to function as a robust protonophore.

Prolonged incubation of *M. tuberculosis* with PZA or POA eventually resulted in modest acidification. Acidification of the cytoplasm after extended incubation with POA is not surprising considering POA has been demonstrated to reduce ATP production in *Mycobacterium bovis*[78], which could ultimately compromise membrane potential and allow cytoplasmic acidification as a secondary consequence. Conversely, acidification conferred by PZA treatment could involve PncA-dependent production of ammonia. A previous report suggested that ammonia produced by PncA hydrolysis of PZA could contribute to eventual acidification of the cytoplasm through bacterial efflux of ammonia and proton accumulation[97]. This phenomenon could explain the initial acidification observed with the highest concentration of PZA tested. Notably, though, inhibitory concentrations of POA and PZA do not lead to a marked decrease in intrabacterial pH, suggesting that growth arrest does not necessitate cytoplasmic acidification. Taken together, these data demonstrate that *M. tuberculosis* PZA and POA susceptibility is independent of environmental pH and is not attributable to cytoplasmic acidification and proton shuttling.

Acknowledgements

This work was supported by a grant from the NIAID (7UM1 AI068636-07) and institutional startup funds from the University of Minnesota to ADB. BCR was supported by an ASM Undergraduate Research Fellowship and a UROP Fellowship from the University of Minnesota. NAD was supported by an institutional training grant from the NHLBI (T32 HL07741). We thank Dr. Sabine Ehrt for providing plasmid pUV15-pHGFP, and Dr. William R. Jacobs, Jr. for providing *M. tuberculosis* strains H37Ra and H37Rv. We thank Dr. Dean Crick for helpful comments and thoughtful discussions.

Anti-tubercular Activity of Pyrazinamide is Independent of *trans*-Translation and RpsA

Abstract

Pyrazinamide (PZA) is a first line anti-tubercular drug for which the mechanism of action remains unknown. Recently, it was proposed that the active form of PZA, pyrazinoic acid (POA), disrupts the ribosome rescue process of *trans*-translation in *Mycobacterium tuberculosis*. This model suggests that POA binds to ribosomal protein S1 (RpsA) and inhibits *trans*-translation leading to accumulation of stalled ribosomes. In this study, we demonstrate that POA does not interact with RpsA. Further, we demonstrate that the *rpsA*ΔA438 polymorphism that was previously identified in a PZA resistant isolate of *M. tuberculosis* does not confer PZA resistance when reconstructed in a laboratory strain. Similarly, we find that over-expression of *rpsA* does not alter PZA susceptibility. Utilizing an *in vitro trans*-translation assay with purified *M. tuberculosis* ribosomes we find that an interfering oligonucleotide can inhibit *trans*-translation, yet POA does not inhibit *trans*-translation. Thus, we conclude that the action of PZA is independent of RpsA and *trans*-translation in *M. tuberculosis*.

Introduction

Pyrazinamide (PZA) is a first line anti-tubercular drug that has enabled a reduction in tuberculosis (TB) treatment duration from 9 to 6 months and has played a critical role in lowering relapse rates[82,105]. Efficacy of PZA is dependent on hydrolysis to pyrazinoic acid (POA) by the *Mycobacterium tuberculosis* encoded nicotinamidase/pyrazinamidase PncA[61]. As PncA is non-essential for growth and pathogenesis of *M. tuberculosis*, 90 % of PZA resistant clinical isolates harbor loss-of-function mutations in *pncA*[106]. While PZA shows sterilizing activity against *M. tuberculosis* in humans and in animal models of TB infection[56,57,59], it shows no notable effect on growth of *M. tuberculosis* in standard laboratory culture medium[88]. Since stresses such as acidic pH[60], nutrient limitation[107] and anaerobiosis[91] enhance the anti-tubercular action of PZA, it has been suggested that this drug selectively targets slowly growing and non-growing populations of *M. tuberculosis*[70]. However, it is important to note that PZA and POA also show inhibitory activity against actively replicating *M. tuberculosis*[107,108], indicating that the function(s) disrupted by POA is critical for fitness of the bacilli regardless of their growth status. Understanding the mechanistic basis for action of this important drug will guide discovery efforts for next generation compounds that show improved activity and circumvent emerging resistance.

Recently, it was suggested that POA acts by inhibiting *trans*-translation[71], a process used by bacteria to liberate ribosomes that have stalled on mRNA transcripts lacking an in-frame stop codon[109]. This pathway requires small protein B (SmpB) for recruitment of the dual function transfer-messenger RNA (tmRNA) that promotes release of the stalled ribosome from its non-stop mRNA with subsequent tagging and release of the incomplete nascent peptide[109]. Evidence for POA-mediated inhibition of *trans*-translation in *M. tuberculosis* included *1)* an apparent interaction between POA and ribosomal protein S1 (RpsA) as demonstrated through the use of isothermal titration calorimetry (ITC), *2)* the PZA resistant clinical isolate DHMH444 (PZA MIC of 300 μg/ml) was found to have a polymorphism in *rpsA* (*rpsA*ΔA438; deletion of alanine codon 438), *3)* five-fold over-expression of *rpsA* in *M. tuberculosis* strain H37Ra conferred resistance to PZA (MIC of 500 μg/ml), and *4)* POA appeared to inhibit *trans*-translation in a cell-free assay[71]. As *trans*-translation is important for growth and stress tolerance of many bacteria[110–112], this model could explain the ability of PZA to target growing and non-growing populations of *M. tuberculosis*.

Despite its plausibility, this model is inconsistent with previous reports of the role of RpsA in *trans*-translation and the PZA and POA resistance of *M. tuberculosis* strain DHMH444. First, while RpsA has been shown to interact with tmRNA, it does not appear to be required for the *trans*-translation pathway in *Escherichia coli*[113] or *Thermus thermophilus*[114,115]. In addition, it has been shown that *M. tuberculosis* strain DHMH444 bearing the *rpsA*ΔA438 polymorphism maintains PZA susceptibility in a murine model of infection[116]. This strain is also fully susceptible to POA *in vitro*, and its moderate *in vitro* PZA resistance has previously been attributed to its reduced PncA activity[117]. Moreover, a strain of *M. tuberculosis* altered for *trans*-translation showed enhanced susceptibility to antibiotics that interfere with translation, yet, displayed no difference in PZA susceptibility relative to the parental control[118]. To resolve these inconsistencies, we further examined the role of RpsA in PZA susceptibility of *M. tuberculosis* and biochemically evaluated interaction of POA with RpsA and the *trans*-translation complex.

Materials and Methods

Bacterial strains and growth conditions. *Mycobacterium tuberculosis* strain H37Ra was grown in Middlebrook 7H9 medium (Difco) supplemented with 10% (vol/vol) oleic acid-albumin-dextrose-catalase (OADC) (Difco), 0.2% (vol/vol) glycerol, and 0.05% (vol/vol) tyloxapol. *Escherichia coli* strains DH5α used for the propagation of phasmids and plasmids and BL21 (DE3)[82] used for overexpression and purification of protein were grown in Lysogeny Broth (LB). Antibiotics hygromycin (150 μg ml^{-1}) and kanamycin (50 μg ml^{-1}) were used as necessary.

RpsA Expression and Purification. For RpsA expression and purification, *M. tuberculosis* encoded *rpsA* was amplified by PCR, digested with BamHI and HindIII, and ligated into pET-28b+ digested with the same enzymes. The recombinant plasmid was transformed and propagated in BL21(DE3) selected with kanamycin. Growing BL21(DE3) containing pET-28b+*rpsA* was induced with 0.25 mM isopropyl β-D-1-thiogalactopyranoside (IPTG) for 3 hours at 37°C. Induced cells were harvested via centrifugation and resuspended in 50 mM NaH_2PO_4, 300 mM NaCl, 10 mM imidazole (pH 8.0). Cells were disrupted by sonication and debris pelleted via centrifugation. Supernatant was bound to Ni^{2+}-NTA resin (Qiagen), previously washed and equilibrated with 50 mM NaH_2PO_4, 300 mM NaCl, 20 mM imidazole (pH 8.0), by mixing at 4°C. Resin supernatant slurry was packed into a chromatography column and washed with 20 column volumes of 50 mM NaH_2PO_4, 300 mM NaCl, 20 mM imidazole pH 8.0. Bound RpsA was eluted with 5 column volumes of 50 mM NaH_2PO_4, 300 mM NaCl, 250 mM imidazole pH 8.0. Eluted RpsA was dialyzed with 800 ml 10 mM phosphate buffer twice for 3 hours and once for 16 hours. Overexpression and purification were confirmed via SDS-PAGE gel.

Isothermal titration calorimetry (ITC) assay. The ITC interaction assays were conducted on the MicroCal VP-ITC at 25.0 ^{o}C. POA, RpsA, and the polyC-RNA positive control were dissolved in 10 mM phosphate buffer (pH 7.4). The pH of the POA buffer solution was adjusted to pH 7.4 to account for any pH change due to POA, unless otherwise indicated. The drugs were loaded into the syringe at the indicated concentrations. Each experiment consisted of 26 10 µl injections over a 2 second duration into 1449.7 µl of ligand within the cell. The solution mixtures were stirred at 300 rpm and the interval between injections was set at 500 seconds. Origin 7 software (Origin®) was used to collect and analyze the data.

qRT-PCR. For quantification of *rpsA* overexpression quantitative reverse transcription-PCR (qRT-PCR) was performed. Briefly, mid exponential phase *M. tuberculosis* was harvested via centrifugation. Cell pellet was resuspended in 100 µl 10 mM Tris-HCl, 1 mM EDTA, 15 mg/ml lysozyme and incubated at 37°C for 16 hours. RNA was extracted using the E.Z.N.A.™ bacterial RNA kit (Omega Biotek). Remaining DNA was removed by treatment with TURBO DNA-free™ kit (Ambion). Gene specific primers for qRT-PCR were designed with Primer3 software. qRT-PCR was performed with the QuantiFast® SYBR® Green RT-PCR kit (Qiagen). qRT-PCR reactions were prepared with 2X QuantiFast SYBR Green RT-PCR master mix, 10 µM primers, 0.1 µl QuantiFast RT Mix, 1 ng RNA and were run on a LightCycler®480 with following cycle conditions: 50°C for 10 min, 95°C for 5 min, 35 cycles of 95°C for 10 s, 60°C for 10 s, and 72°C for 20 s with fluorescence quantification each cycle. Melting curve cycle of 95°C for 15 s, 60°C for 15 s, and 95°C with 2% ramp rate to determine product specificity. No reverse transcriptase qRT-PCR reaction performed to test for contaminating DNA.

Cloning of allelic exchange and overexpression strains. To generate the *rpsA* ΔA438 polymorphism in *M. tuberculosis rpsA* was first cloned into p0004s using PCR amplification followed by a 4 piece ligation. The 5' flank was amplified with the primers *rpsA*_5'_F and *rpsA*_5'_R and digested with PacI and NheI. The 3' piece was then amplified via PCR with the primers *rpsA*_3'_F and *rpsA*_3'_R and digested with NcoI and NdeI. The primers designed for the *rpsA*ΔA438 quick change, *rpsA*ΔA438_F and *rpsA*ΔA438_R, were then used to introduce the alanine deletion in *rpsA* via PCR amplification. The resulting cosmid was then inserted into pHAE159 and was introduced into *M. tuberculosis* via specialized transduction.

For RpsA overexpression, *M. tuberculosis* encoded *rpsA* was amplified by PCR with primers indicated in Table 1, digested with NheI and XbaI, and ligated into mycobacterial replicative expression vector pMV261 digested with XbaI. The recombinant plasmid was transformed and propagated in DH5α selected with kanamycin. For RpsA overexpression H37Ra was electroporated with *rpsA* overexpression plasmid and selected on supplemented 7H10 containing kanamycin.

Pyrazinamide susceptibility testing. Antimicrobial susceptibility was determined by measuring optical density of respective cultures at 600 nm (OD_{600}). PZA susceptibility testing was performed using supplemented 7H9 medium adjusted to pH 5.8. The minimum inhibitory concentration (MIC_{90}) for antimicrobial compounds was defined as the minimum concentration required for inhibition of at least 90% of growth, relative to the no antimicrobial control. Growing *M. tuberculosis* H37Ra was diluted to an OD_{600} of 0.01 in 5 ml of supplemented 7H9 medium in 30 ml square Nalgene bottles. Antimicrobial compounds were added to the final concentrations indicated in the text. Cultures were incubated at 37°C with shaking on a rotary platform at 100 rpm for 14 days. All results presented are from a minimum of three independent determinations.

Ribosome purification. Cells were grown in supplemented 7H9 until mid exponential phase (OD_{600} of 0.5) and lysed by French pressure lysis. The lysate was cleared by centrifugation at 30,000 x g for 20 min, and crude ribosomes were harvested from the supernatant by centrifugation at 100,000 x g for 2 h. The pellet was washed 3 X in Buffer II (20 mM Tris-HCl [pH 7.6], 1 M ammonium acetate, 10 mM magnesium acetate, 6 mM ß-ME), and resuspended in Buffer I (10 mM Tris-HCl [pH 7.6], 100 mM ammonium acetate, 10 mM magnesium acetate, 6 mM ß-ME). 70S ribosomes were isolated by sucrose density fractionation (10-40% sucrose in 10 mM Tris-HCl [pH 8.0], 30 mM KCl, 10 mM magnesium acetate).

Isolation of *M. tuberculosis* tmRNA and SmpB. *M. tuberculosis ssrA* was amplified by PCR using primers MtbSsrAF and MtbSsrAR to place it under control of a T7 promoter. The product was gel purified and used as template in a second PCR reaction with primers MtbSsrAF and MtbSsrAR. The product was transcribed *in vitro* and purified as described previously for *E. coli* tmRNA[119]. *M. tuberculosis smpB* was amplified by PCR using primers TB_SmpB_F and TB_SmpB_R, digested with HindIII and NdeI, and ligated into pET28b that had been digested with the same enzymes. SmpB was produced and purified as described previously for *E. coli* SmpB [119].

In vitro *trans*-translation assays. Template construction and reaction conditions were as previously described [119], with the following modifications. DHFR-stop and DHFR-NS templates were made by PCR using T7 universal primer and either Stop_UTR_DHFR_FL or NS_UTR_DHFR_FL. *trans*-translation reactions used the PURExpress ribosome-free kit (New England Biolabs) with 50 nM *M. tuberculosis* ribosomes, 150 nM *M. tuberculosis* tmRNA, 150 nM *M. tuberculosis* SmpB, and 640 nM template DNA. Where applicable, pyrazinoic acid (Sigma) was added to 1 mM or anti-SsrA oligo was added to 2 µM. Reactions were incubated at 37 °C 3 h and analyzed by SDS-PAGE followed by phosporimaging [119].

Results and Discussion

Using isogenic *M. tuberculosis* laboratory strains we assessed the impact of the *rpsA*ΔA438 polymorphism on PZA susceptibility. Utilizing specialized linkage transduction[120] we reconstructed the *rpsA*ΔA438 polymorphism in the *M. tuberculosis* laboratory strain H37Ra. Three independent *rpsA*ΔA438 and two matched wild type strains were verified by full genome resequencing. The PZA minimum inhibitory concentration (MIC) for these strains was found to be indistinguishable from that of the parental strain (Fig. 2-6). To further evaluate the connection between RpsA and PZA resistance, *rpsA* was over-expressed using an analogous mycobacterial expression vector as previously described[71]. Quantitative real time PCR confirmed 10-fold over-expression in this strain (Fig. 2-6), however, similar to the *rpsA*ΔA438 strains, over-expression of *rpsA* conferred no change in PZA susceptibility (Fig. 1). Next, we utilized ITC to

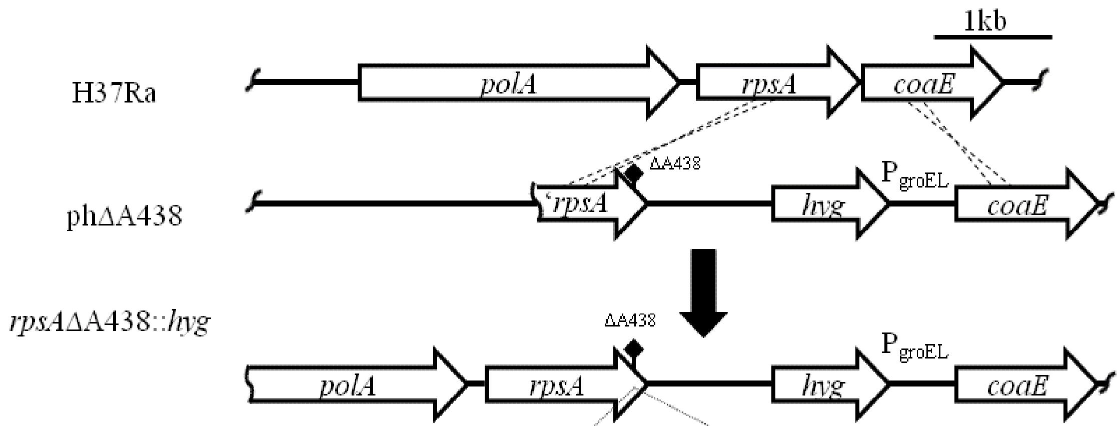

Strain	PZA MIC$_{90}$ (µg/ml)	Sequence of *rpsA* nucleotides 1282-1332 (Corresponding protein sequence in parenthesis)
H37Ra	100	CACACCGCGCACATGGAGAAGTTCGCCGCCGCCGAGGCGGCTGGACGCGGC
H37Ra *rpsA*::*hyg*	100	CACACCGCGCACATGGAGAAGTTCGCCGCCGCCGAGGCGGCTGGACGCGGC
H37Ra *rpsA*ΔA438::*hyg*	100	CACACCGCGCACATGGAGAAGTTCGCCGCC---GAGGCGGCTGGACGCGGC
H37Ra pMV206::*rpsA*	100	CACACCGCGCACATGGAGAAGTTCGCCGCCGCCGAGGCGGCTGGACGCGGC
H37Ra pMV206	100	
		(HisThrAlaGlnMetGluLysPheAlaAla**Ala**GluAlaAlaGlyArgGly)

Figure 2-6. *rpsA*ΔA438 polymorphism and *rpsA* over-expression do not confer PZA resistance in *M. tuberculosis*. Schematic representation of specialized linkage transduction used to introduce the *rpsA*ΔA438 mutation and corresponding nucleotide sequences of the *rpsA* locus of respective strains. Wild type and *rpsA*ΔA438 mutant strains were tested for the minimum concentration of PZA that was required to inhibit at least 90% of growth relative to the no drug control (MIC$_{90}$) over 2 weeks of incubation in supplemented 7H9 medium (pH 5.8). All MIC$_{90}$ and qRT-PCR assays were conducted with at least three independent replicates. Three independent isolates bearing the *rpsA*ΔA438 polymorphism, confirmed by full genome sequencing, were assessed.

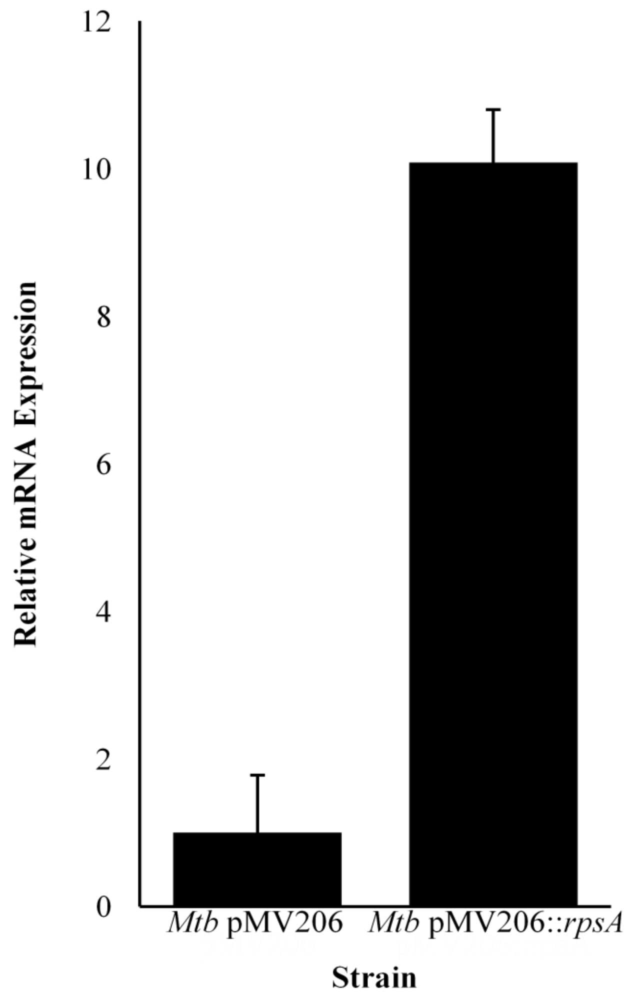

Figure 2-7. Over-expression of *rpsA* in *M. tuberculosis*.

qRT-PCR was performed on RNA extracted from *M. tuberculosis* strains H37Ra and H37Ra pMV206::*rpsA*. Relative mRNA expression was calculated using *sigA* transcripts for normalization.

examine the purported interaction between *M. tuberculosis* RpsA and POA. During protein synthesis, RpsA aids in translation initiation via direct binding of single stranded mRNA[121].

E. coli RpsA has been shown to have two RNA binding sites with varying affinity for polyC RNA[121–123]. Utilizing purified recombinant *M. tuberculosis* RpsA and polyC RNA as a ligand, we observed a bimodal association curve consistent with the presence of two high-affinity RNA binding sites on RpsA (Fig. 2-8A). Fitting the data to a multi binding site model we determined that the higher affinity site bound the polyC RNA with $K_a = 8.91\times10^7 \pm 5.42\times10^7\ M^{-1}$ while the lower affinity site bound the polyC RNA with $K_a = 8.48\times10^6 \pm 1.85\times10^6\ M^{-1}$ (Fig. 2-8A). These data demonstrate that the purified RpsA is folded and has the expected biochemical properties. Despite this robust interaction with polyC RNA and in contrast to that which was described previously[71], no interaction between POA and RpsA was observed (Fig. 2-8B). These data indicate that RpsA is not directly associated with POA action in *M. tuberculosis*.

ITC is an extremely sensitive approach for measurement of thermodynamic binding parameters, and injection of a weak acid, such as POA, into a modestly buffered solution could generate a robust signal due to pH dependent proton dissociation. Indeed, saturated POA, as used in the previous study[71], produced a strong signal due to proton dissociation and not interaction with RpsA (Fig. 2-9A). The signal, though, was abrogated when the pH of the saturated POA was adjusted to that of the diluent buffer (Fig. 2-9B). Thus, we conclude that the previously reported ITC signal for RpsA and POA was not due to interaction between these ligands, but was instead due to heat of proton dissociation of the weak acid POA.

To specifically address whether POA can inhibit the tagging activity mediated by the *trans*-translation pathway, we utilized an *in vitro trans*-translation assay[119]. A gene encoding dihydrofolate reductase (DHFR) lacking a stop codon (DHFR-NS) was used as a template in a transcription/translation assay containing *M. tuberculosis* ribosomes, tmRNA and SmpB. Expression of DHFR-NS with *M. tuberculosis* components resulted in tagging of the DHFR-NS demonstrating that *trans*-translation functions *in vitro* with *M. tuberculosis* components (Fig. 2-10). Incubation with 1 mM POA resulted in no substantial reduction in the tagging activity of *trans*-translation (1.6 ± 4 %), while incubation with an anti-sense ssrA oligonucleotide exhibited >90 % reduction in tagging activity (Fig. 2-10).

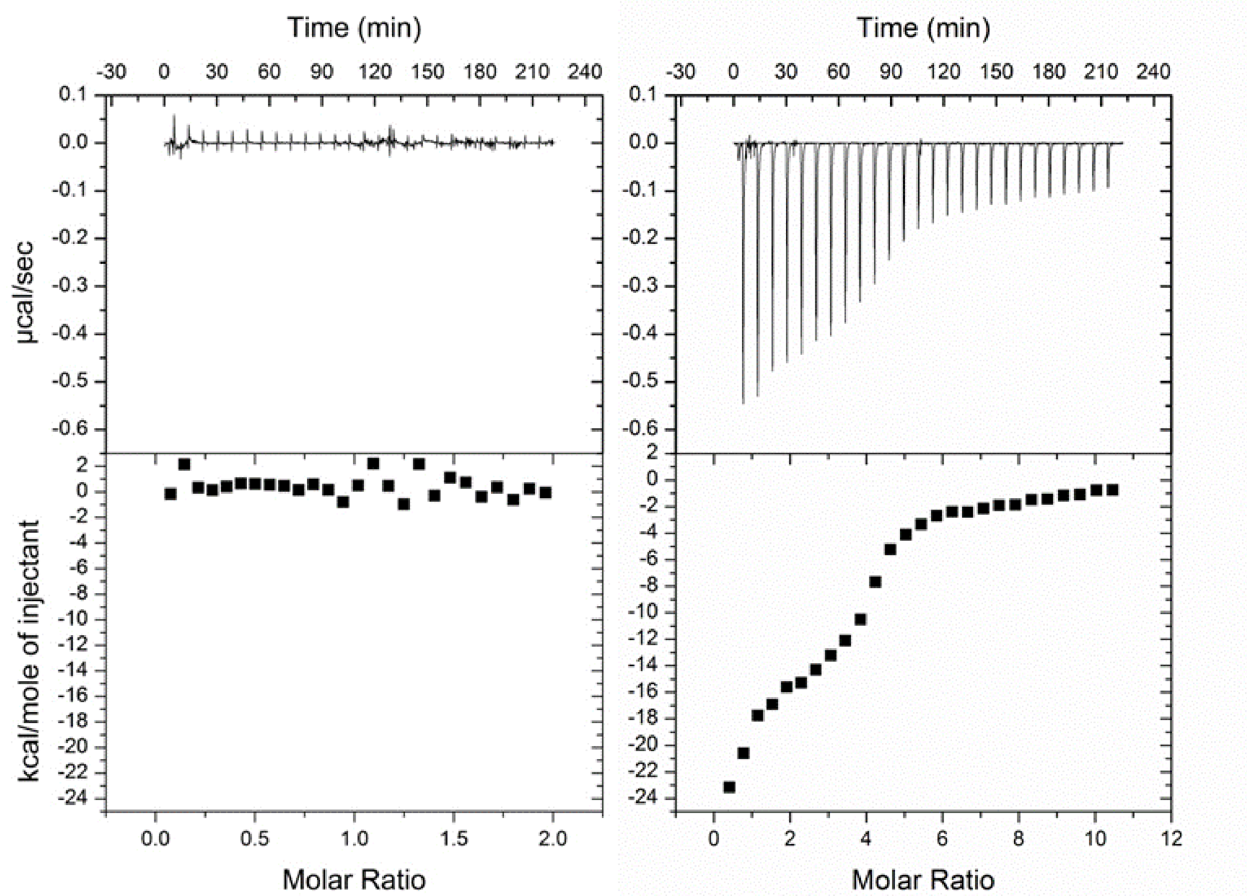

Figure 2-8. ***M. tuberculosis*** **RpsA interacts with polyC RNA, but not with POA.**

Isothermal titration calorimetry was used to assess the binding between RpsA and either polyC RNA (A) or POA (B). In each plot, the top panel represents the heat produced per injection as µcal/sec while the bottom panel shows the change in enthalpy (kcal/mole) as a function of the molar ratio of the two ligands. Titrations were performed at 25ºC using 10 mM PB (pH 7.4). POA and polyC RNA solutions were adjusted to pH 7.4.

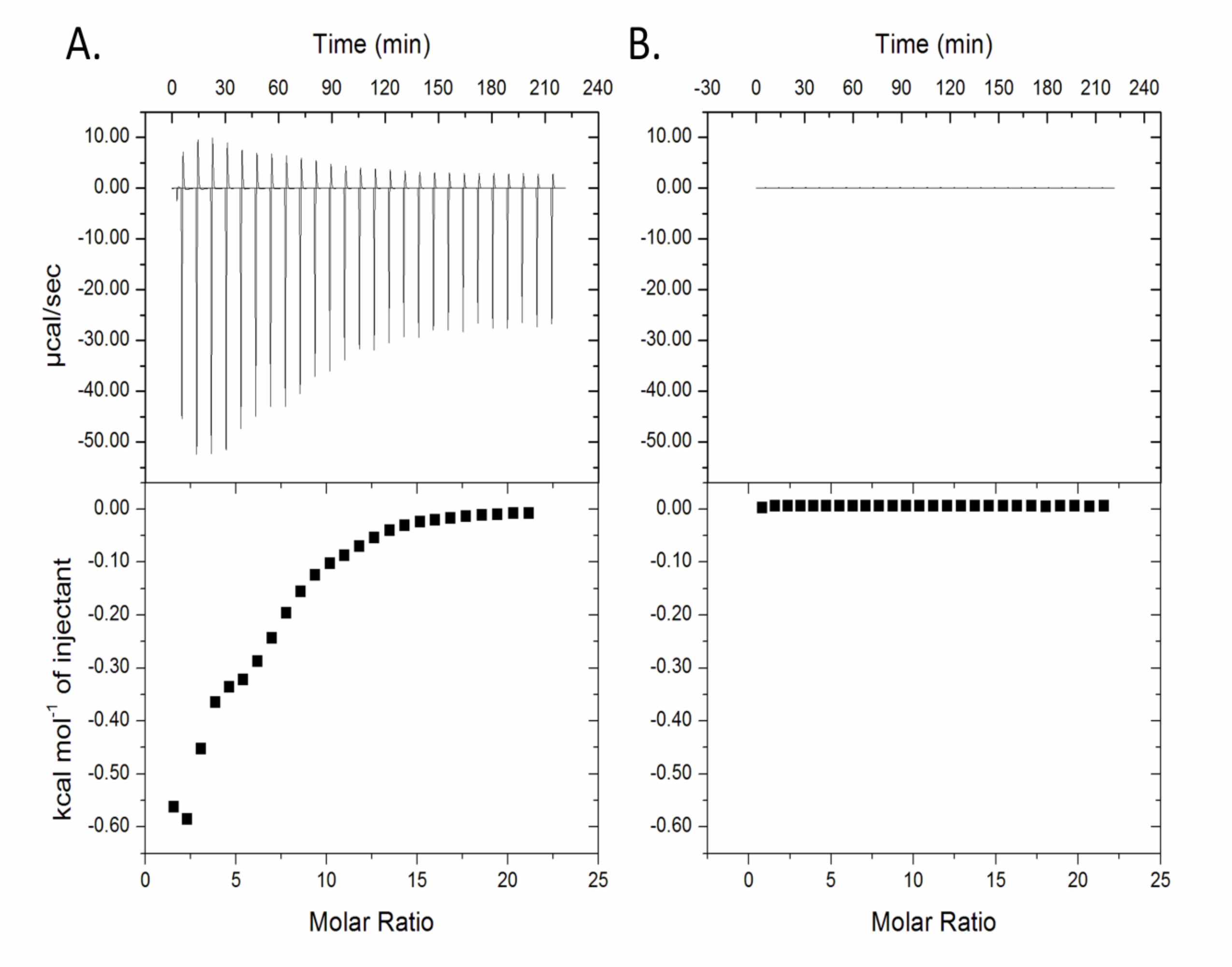

Figure 2-9. Unbuffered POA gives a robust ITC signal when titrated into neutral buffer. Saturated POA (A, unadjusted pH 2.3; B, pH adjusted to 7.4) was injected into 10mM pH 7.4 PB.

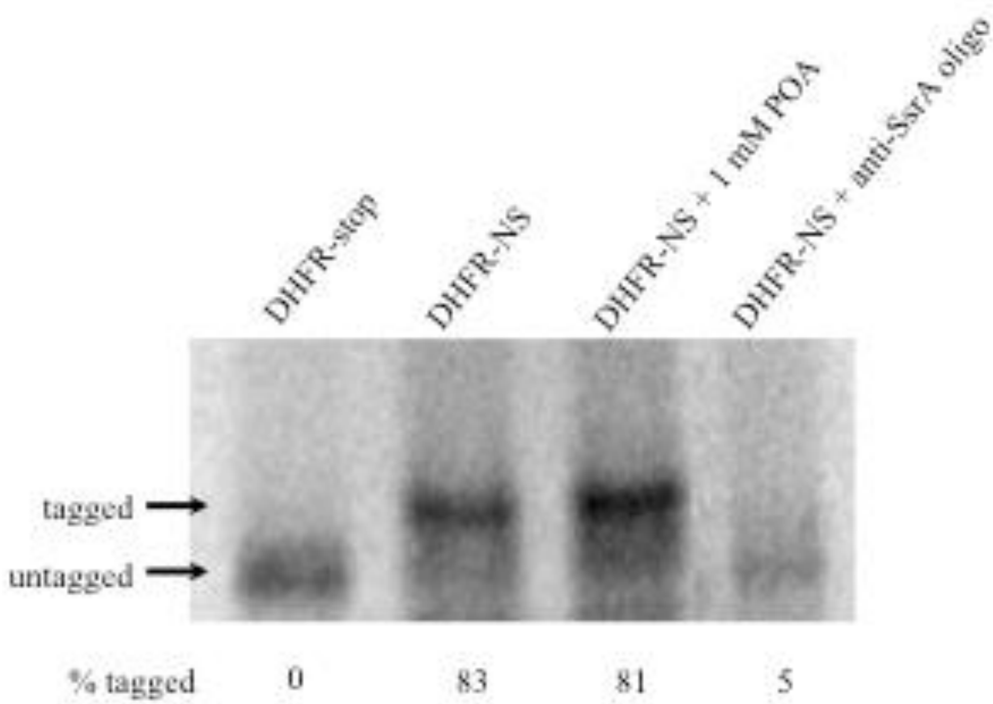

Figure 2-10. POA does not inhibit *trans*-translation *in vitro*. *trans*-Translation reactions with 50 nM *M. tuberculosis* ribosomes, 150 nM *M. tuberculosis* tmRNA, 150 nM *M. tuberculosis* SmpB, and 640 nM template DNA. Where indicated pyrazinoic acid (Sigma) was added to 1 mM or anti-SsrA oligonucleotide was added to 2 µM. Reactions were incubated at 37 °C 3 h and analyzed by SDS-PAGE followed by phosporimaging.

Collectively, these observations indicate that RpsA and *trans*-translation do not have a role in the mode of action of PZA and that the mechanistic basis for PZA susceptibility remains to be elucidated. Considering the unparalleled *in vivo* sterilizing activity of PZA and the increasing global burden of multi-drug and extensively drug resistant TB, elucidating the requirements for susceptibility of *M. tuberculosis* to key drugs such as PZA is paramount for the optimization of impactful treatment regimens.

Table 2-2. Oligonucleotide primers used in this study.

Name of oligonuleotide	Sequence 5' to 3'
MtbSsrAF	GAAATTAATACGACTCACTATAGGGGCTGAACGGTTTCGACTT
MtbSsrAR	TGGTGGAGCTGCCGGGAATC
TB_SmpB_F	CGCGGCAGCCATATGGTGTCCAAGTCGTCGCGTG
TB_SmpB_R	CTCGAGTGCGGCCGCAAGCTTCAGGTCATGCCCTTAGCGC
Anti-SsrA	ATGTGAATCGGCGCTTATT
*rpsA*_5'_F	TTAATTAAACATCGGCAAGGAGATCGAG
*rpsA*_5'_R	GCTAGCTCAAGCGCTGCCGGCGAGTTTTTCCC
*rpsA*_3'_F	CCATGGGCCGGCAGCGCTTGATCTTG
*rpsA*_3'_R	CATATGTCGTTCAGGGACGCCAGTG
*rpsA*ΔA438_F	GAGGCGGCTGGACGCGGCGCGGACGATCAGTC
*rpsA*ΔA438_R	GGCGGCGAACTTCTCCATCTG

Acknowledgements:

This work was supported by grants from the NIH (AI123146) and Bill & Melinda Gates Foundation (Grand Challenges Explorations), and institutional startup funds from the University of Minnesota to ADB. K.C.K. and H.A.F. were supported by grant GM068720 from NIH. N.A.D was supported by an institutional training grant from the NIH (HL007741). We thank Dr. William R. Jacobs, Jr. for providing *M. tuberculosis* strains H37Ra and H37Rv, Dr. Yusuke Minato for assistance in analyzing mutant strains of *M. tuberculosis*, and Chris Rae who helped provide reagents for *in vitro trans*-translation assays.

Chapter 3

Alterations in CoA biosynthesis and mycobacterial stress responses confer PZA resistance

Resistance to PZA has been documented since its first use in therapy during the 1949-1952 human trials, yet, it was not until genetic sequencing was implemented that the primary resistance conferring mutation was mapped. Mutations in *pncA*, the gene encoding the amidase that is required for conversion of PZA to POA, were identified as the primary PZA resistance mechanism in *M. tuberculosis*. Loss-of-function mutations in *pncA* account for about two thirds of PZA resistance mutations found in *M. tuberculosis* clinical isolates. The remaining third of PZA resistance mutations are currently unidentified.

A recent manuscript found a link between PZA resistance and mutations in the aspartate decarboxylase encoding gene *panD*. Based on this finding a model was proposed that hypothesized POA targeted PanD. PanD is an essential component of the CoA biosynthesis pathway and is involved in the synthesis of β-alanine. We had previously found that pantothenate, produced by the ligation of β-alanine and pantoate, antagonized the action of PZA. Endeavoring to define the mechanistic basis for pantothenate antagonism of PZA we sought to examine other metabolites of the CoA biosynthesis pathway to evaluate their impact on drug activity. β-alanine was found to antagonize PZA, but only when it could be utilized in the synthesis of pantothenate thereby linking pantothenate, or a further downstream product, as being the essential component for antagonism. This paper was published in 2014 in Antimicrobial Agents and Chemotherapy. I did the majority of the experiments and I was the primary author of the manuscript. Nicholas Peterson and Brandon Rosen also aided in conducting the experiments that were shown in the final manuscript.

Mutations in *panD* accounted for some, but not all, of the remaining PZA resistance clinical isolates. We sought to use a transposon mutaganized library of H37Rv to select for drug resistance conferring mutations on inhibitory concentrations of POA. After the initial characterization of a select group of randomly selected PZA resistant isolates, we determined that our library had many mutations that had never been previously linked to PZA resistance. We therefore employed a next-generation sequencing based approach to identify the resistance conferring mutations in approximately 2,200 isolated colonies. We found over 150 new genes which, when mutated, conferred PZA resistance. When ranking the genes hit with the highest frequency we found a preponderance of mutations in *sigE* and its regulon. A *M. tuberculosis* Δ*sigE* mutant strain was confirmed to be resistant to PZA, and introduction of *sigE* on an integrating vector restored PZA susceptibility of this strain. This paper is nearly ready for submission and I am the first author. I did the majority of the experiments and I am responsible for composing the manuscript. Dr. Yusuke Minato aided in the analysis of the sequencing data.

Pantothenate and pantetheine antagonize the anti-tubercular activity of pyrazinamide

Abstract

Pyrazinamide (PZA) is a first line tuberculosis drug that inhibits growth of *Mycobacterium tuberculosis* via an as yet undefined mechanism. A *M. tuberculosis* laboratory strain that was auxotrophic for pantothenate was found to be susceptible to PZA and to the active form pyrazinoic acid (POA). To determine whether this phenotype was strain or condition specific, the effect of pantothenate supplementation on PZA activity was assessed using prototrophic strains of *M. tuberculosis*. It was found that pantothenate and other β-alanine-containing metabolites abolished PZA and POA susceptibility, suggesting that POA might selectively target pantothenate synthesis. However, when the pantothenate auxotrophic strain was cultivated using a sub-antagonistic concentration of pantetheine, *in lieu* of pantothenate, susceptibility to PZA and POA was restored. In addition, we found that β-alanine could not antagonize PZA and POA activity against this strain, indicating that this antagonism is specific to pantothenate. Moreover, pantothenate-mediated antagonism was observed for structurally related compounds including *n*-propyl pyrazinoate, 5-chloropyrazinamide and nicotinamide, but not for nicotinic acid or isoniazid. Taken together, these data demonstrate that while pantothenate can interfere with the action of PZA, pantothenate synthesis is not directly targeted by PZA. Our findings suggest that targeting of

pantothenate synthesis has the potential to enhance PZA efficacy and possibly restore PZA susceptibility in isolates with *panD*-linked resistance.

Introduction

Pyrazinamide (PZA) is one of four first line drugs used in standard short course combination therapy for tuberculosis (TB). Due to its role in reducing relapse rates and in shortening treatment duration from 9 to 6 months[43,124], PZA is anticipated to be an irreplaceable component of future first line TB drug regimens[125]. However, the durability of PZA and other therapeutic agents is being challenge by the emergent spread of drug resistant strains of *Mycobacterium tuberculosis*. In order to maintain comparable short course drug regimens it is important to identify suitable alternatives for PZA. To do so, it is necessary to understand the mechanistic basis for susceptibility and resistance of *M. tuberculosis* to PZA and its potential surrogates.

Under standard laboratory growth conditions, PZA lacks measurable activity against *M. tuberculosis* due to the ability of the bacilli to eliminate cytoplasmic POA by an as yet unidentified efflux mechanism[81]. Conditions that promote POA accumulation, such as low pH ($\leq$6.0)[89], anaerobiosis[91], and co-incubation with electrochemical gradient uncouplers[77] or efflux pump inhibitors[81] have been shown to significantly enhance susceptibility of *M. tuberculosis* to PZA. While *M. tuberculosis* can be found within hypoxic compartments during infection[126], the contribution of these factors to *in vivo* PZA susceptibility has yet to be experimentally confirmed.

PZA is a pro-drug that is hydrolyzed to the presumed active form of pyrazinoic acid (POA) by the *M. tuberculosis* pyrazinamidase/nicotinamidase PncA[61]. PncA is an enzyme of the NAD salvage pathway[65,85]. Due to the dispensability of NAD salvage in *M. tuberculosis* metabolism, spontaneous loss of function mutations in the *pncA* gene can arise without a notable fitness cost to the bacilli. As such, *pncA* loss of function mutations show a high correlation with clinical PZA resistance[106,127]. Moreover, a direct association between loss of function mutations in *pncA* and PZA resistance in animal models of infection has been established[116]. While POA is effective *in vitro* against PncA deficient strains of *M. tuberculosis*, it lacks activity *in vivo* presumably due to its high rate of clearance[63].

Several models have recently been proposed to explain the mode of PZA action on *M. tuberculosis*. The first of these models comes from studies involving the PZA structural analog 5-chloropyrazinamide (5-Cl PZA) which was found to be a potent inhibitor of the mycobacterial fatty acid synthase I (FAS-I)[68,73,74]. While *M. tuberculosis* FAS-I activity was found to also be compromised by PZA treatment[68,74,75], *in situ* evidence for this inhibition has been confounded by the inability to over-express FAS-I in *M. tuberculosis*[68]. This model has also been challenged by a report in which inhibition of purified FAS-I by POA was not observed, and FAS-I inhibition in whole cells was suggested to be a downstream consequence of POA-mediated organic acid stress[73]. Further work is critical to resolve direct FAS-I targeting by POA. A second model suggested that POA promotes acidification of the *M. tuberculosis* cytoplasm through a proton shuttling mechanism[77]. In this model, bacilli residing in an acidic environment pump POA anion out to the extracellular environment. A fraction of the excluded POA becomes protonated and re-enters the cell by passive diffusion. Once in the cytoplasm, the proton dissociates from POA and the cycle continues until the cytoplasmic pH equilibrates with that of the extracellular environment. Inconsistent with this model, acid-dependence of PZA activity can be abolished by incubation under alkaline pH[89], over-expression of *pncA*[75] or through preventing POA from cycling in and out of the cell by the addition of efflux pump inhibitors[81]. Moreover, it has been demonstrated that the primary *in vivo* niches for *M. tuberculosis*, phagocyte lysosomes and tubercular granulomas, do not acidify when live bacilli are present[17]. Thus, while acidic culture conditions can promote the cytoplasmic accumulation of POA, low pH can be fully uncoupled from activity of this drug against an essential cellular target. The third model to be proposed suggested that POA inhibits *trans*-translation, a process that many bacteria employ to liberate ribosomes that have stalled on non-stop mRNA transcripts[71]. This model was based in part on an apparent interaction between the ribosomal protein RpsA and POA, and the identification of an *rpsA* polymorphism in a previously described PZA resistant *M. tuberculosis* clinical isolate DHMH 444. Inconsistent with this model, strain DHMH 444 was previously shown to be fully susceptible to POA[117] and susceptible to PZA in a murine model of infection[116]. Moreover, *trans*-translation has been shown to be non-essential for growth under conditions that promote PZA susceptibility, and a strain defective for *trans*-translation was found to be fully susceptible to PZA[118]. Thus, inhibition of *trans*-translation is not likely to explain PZA-mediated growth inhibition of *M. tuberculosis*. The most recent model to be proposed, suggested that PZA inhibits the *M. tuberculosis* aspartate decarboxylase PanD, and thereby inhibits synthesis of the essential metabolic cofactors pantothenate and coenzyme A (Figure 3-1)[66]. This model was based on the identification of *panD* missense mutations in spontaneous PZA resistant *M. tuberculosis* laboratory isolates that did not have loss of function mutations in *pncA*. As FAS-I is pantothenate-dependent and coenzyme A plays a crucial role in carbon and energy metabolism, this model provides a potential explanation for the pleiotropic affects of PZA on *M. tuberculosis*. Yet, additional genetic and biochemical studies are essential to delineate a mechanistic link between PanD and PZA action. While the models described above are not mutually exclusive, many standing questions remain to refine our understanding of PZA mode of action.

Upon evaluating PZA activity against various laboratory strains of *M. tuberculosis*, we found that supplementation of cultures with β-alanine, pantothenate or pantetheine could antagonize the action of PZA and some of its structural analogs. These data are consistent with the previous indication of a link between pantothenate synthesis and PZA action. In this study we found that a *M. tuberculosis* strain deleted for *panC* (encoding pantoate β-alanine ligase; Figure 3-1) and *panD* could be cultivated with pantetheine at a concentration that did not antagonize PZA activity. This finding uncouples pantothenate synthesis PZA action indicating that panothenate-mediated antagonism occurs via a novel mechanism that is independent of PanD. These observations suggest that inhibition of the pantothenate/coenzyme A biosynthetic pathway has the potential to improve PZA potency and restore PZA susceptibility in isolates with pantothenate-linked resistance.

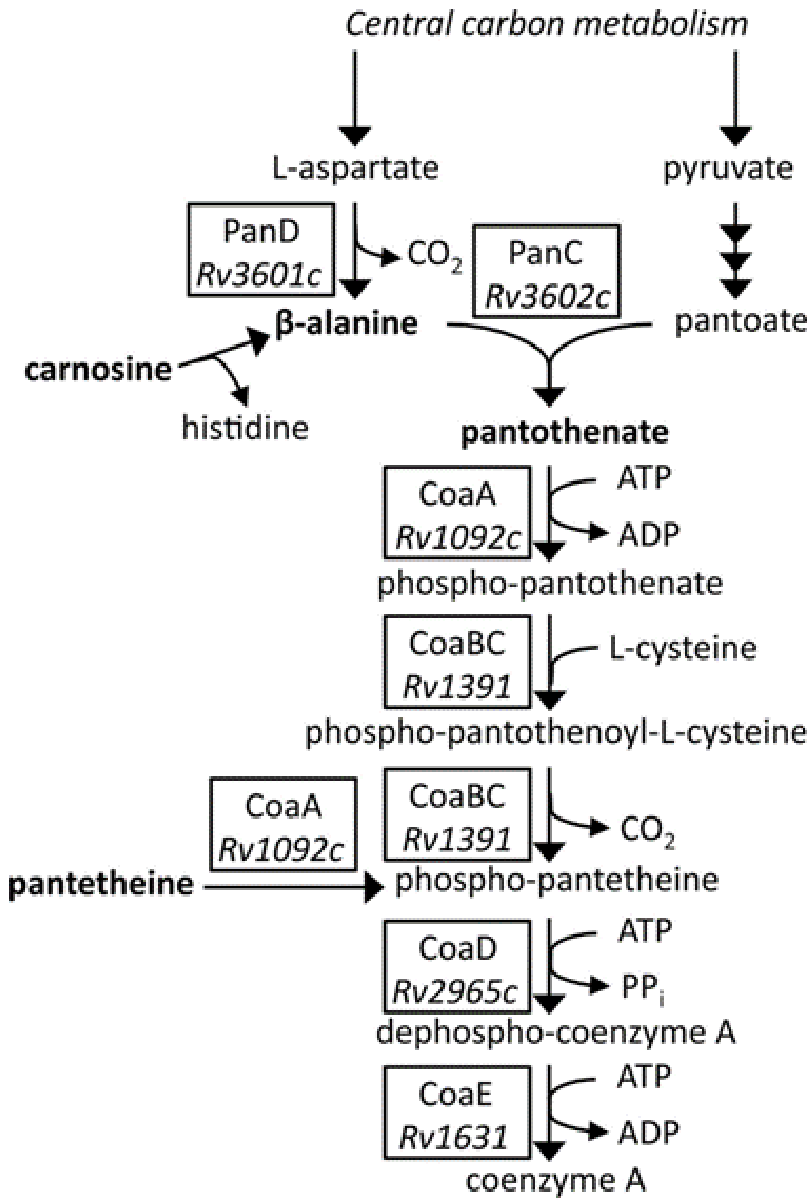

Figure 3-1 Pantothenate/coenzyme A biosynthetic pathway of *M. tuberculosis*. The boxes represent proteins that catalyze the respective reactions depicted by arrows. The series of reactions from pyruvate to pantoate are abbreviated by a triple arrow. The H37Rv genes that encode the proteins are shown in italics. Metabolites that were found to antagonize the antitubercular activity of PZA are shown in boldface.

Materials and Methods

Bacterial strains and growth media. *M. tuberculosis* strains H37Rv, H37Ra, mc^{2}7000 (H37Rv ΔRD1 Δ*panCD*), Erdman and CDC1551 were gifts from W.R. Jacobs, Jr. of Albert Einstein College of Medicine. Strains were grown in Middlebrook 7H9 medium (Difco) supplemented with 10% (vol/vol) oleic acid-albumin-dextrose-catalase (OADC) (Difco), 0.2% (vol/vol) glycerol, and 0.05% (vol/vol) tyloxapol. D,L-Pantothenate (50 µg ml^{-1}) or D-pantethine (7.2 µg ml^{-1}) was added for growth of *M. tuberculosis* strain mc^{2}7000.

Compounds. All chemicals were purchased from Sigma-Aldrich unless otherwise stated. PZA (MP Biomedicals), nicotinamide (Alfa Aesar), *n*-propyl pyrazinoate (*n*PPA; gift from J.T. Welch, SUNY Albany), 5-Cl PZA (gift from J.T. Welch), and isoniazid (INH) were dissolved in dimethyl sulfoxide (DMSO). POA and nicotinic acid (Alfa Aesar) were dissolved in water, the pH was adjusted to 5.8 using NaOH, and solutions were filter sterilized using a 0.2 µm syringe filter. β-Alanine (Alfa Aesar), D,L-pantothenate, D-pantetheine, and L-aspartic acid, carnosine, taurine, 3-aminopropanol, propanoic acid, propylamine, 4-aminobutyric acid, and glycine (Fisher) were dissolved in water and filter sterilized. D-Pantolactone was hydrolyzed to D-pantoate via alkaline saponification[128] then neutralized and filter sterilized.

Antimycobacterial susceptibility determinations. Antimycobacterial susceptibility was determined by measuring optical density of respective cultures at 600 nm (OD_{600}). PZA, POA, nicotinamide and nicotinic acid susceptibility testing was performed using medium adjusted to pH 5.8. For INH, 5-Cl PZA and *n*PPA susceptibility testing, the pH of the growth medium was not adjusted from pH 6.8. At the concentrations used, compounds that were tested for antagonism did not measurably alter the pH of the growth medium. The minimum inhibitory concentration (MIC_{90}) for antimycobacterial compounds was defined as the minimum concentration required for inhibition of at least 90% of growth, relative to the no antimycobacterial control. The minimum antagonistic concentration (MAC_{10}) was defined as the minimum concentration of antagonist required to enable at least 10% the amount of growth in the presence of antimycobacterial compounds, relative to the no antimycobacterial control. For MIC_{90} and MAC_{10} determinations, *M. tuberculosis* strains were first grown to mid-exponential phase in standard growth medium and diluted to an OD_{600} of 0.01 in 5 ml of 7H9 medium in 30 ml square Nalgene bottles. Antimycobacterial compounds and/or antagonists were added to the final concentrations indicated in the text. Cultures were incubated at 37°C with shaking on a rotary platform at 100 rpm for the specified amount of time. All results presented are from a minimum of three independent determinations.

Antagonism growth assays. Growth kinetics of *M. tuberculosis* strains were assessed in the presence of antimycobacterial compounds and select antagonists using the same conditions described above. Exponentially growing cells were diluted to an OD_{600} of 0.01 in supplemented 7H9 containing 200 μg ml^{-1} PZA or 400 μg ml^{-1} POA with or without 1 mM pantothenate, β-alanine, or pantetheine. Cultures were incubated at 37°C with shaking on a rotary platform at 100 rpm. Growth was monitored by following OD_{600} over time.

Results

Metabolites of the pantothenate/coenzyme A biosynthesis pathway antagonize PZA and POA activity in *M. tuberculosis*. While conducting drug susceptibility assays, it was found that the *M. tuberculosis* H37Rv derivative $mc^2$7000 (Δ*panCD* Δ*RD1*) was not susceptible to PZA (Table 3-1). To determine whether this lack of PZA susceptibility was strain or condition specific, the effect of pantothenate supplementation on the PZA susceptibility of different prototrophic laboratory strains of *M. tuberculosis* was assessed (Table 3-1). It was found that the addition of pantothenate to the growth medium increased the PZA MIC_{90} by four fold for strains H37Ra and H37Rv and by greater than eight fold for strains Erdman and CDC1551 (Table 3-1). Thus, the lack of PZA susceptibility in *M. tuberculosis* $mc^2$7000 was due to the presence of exogenous pantothenate in the growth medium, and is likely to occur for any strain of *M. tuberculosis* supplemented with sufficient levels of pantothenate.

To further characterize this effect, the PZA MIC_{90} for *M. tuberculosis* strain H37Ra was determined over a range of pantothenate concentrations. PZA antagonism was found to occur in a dose-dependent manner (Figure 3-2). As normal whole blood concentrations of pantothenate are typically in the low micromolar range[129], it is worth noting that 7 µM pantothenate was sufficient to enable growth of *M. tuberculosis* at a PZA concentration above the proposed resistance breakpoint of 300 µg ml^{-1}[93].

To assess the kinetics of antagonism, growth of *M. tuberculosis* strains H37Ra and H37Rv was monitored during exposure to PZA or POA in medium supplemented with pantothenate or β-alanine. Pantothenate enabled initiation of growth in the presence

Table 3-1 MICs of PZA for various *M. tuberculosis* strains in the absence or presence of exogenously supplied pantothenate

		PZA MIC_{90}[a] ($\mu g\ ml^{-1}$)	
Strain	Relevant characteristics	No pantothenate	200 μM pantothenate
H37Rv	Virulent laboratory strain	200	800
$mc^2$7000	H37Rv Δ*panCD* Δ*RD1*	ND[b]	>800
H37Ra	Spontaneously attenuated derivative of H37Rv	100	400
Erdman	Virulent laboratory strain	100	>800
CDC1551	Virulent laboratory strain	100	>800

[a] MIC_{90}, defined as the minimum concentration that inhibits ≥90% of growth relative to the no-drug control over 3 weeks of incubation in supplemented 7H9 medium, pH 5.8.
[b] ND, not determined.

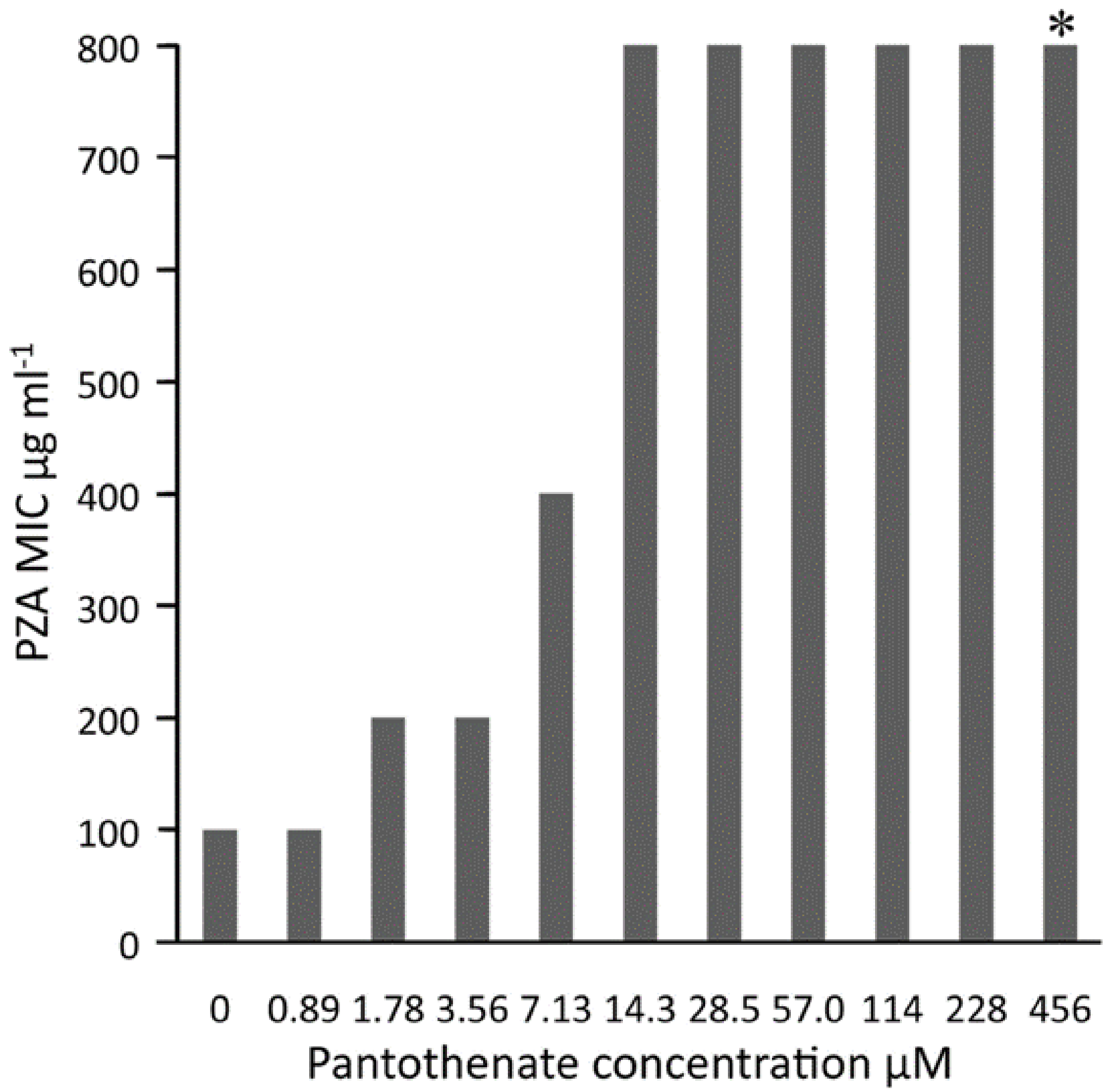

Figure 3-2 Dose response for pantothenate-mediated antagonism of the antitubercular activity of PZA. Pantothenate and PZA were added to cultures of *M. tuberculosis* H37Ra at various concentrations. PZA MICs were determined following 3 weeks of incubation at 37°C. *, PZA MIC was greater than 800 $\mu g\ ml^{-1}$.

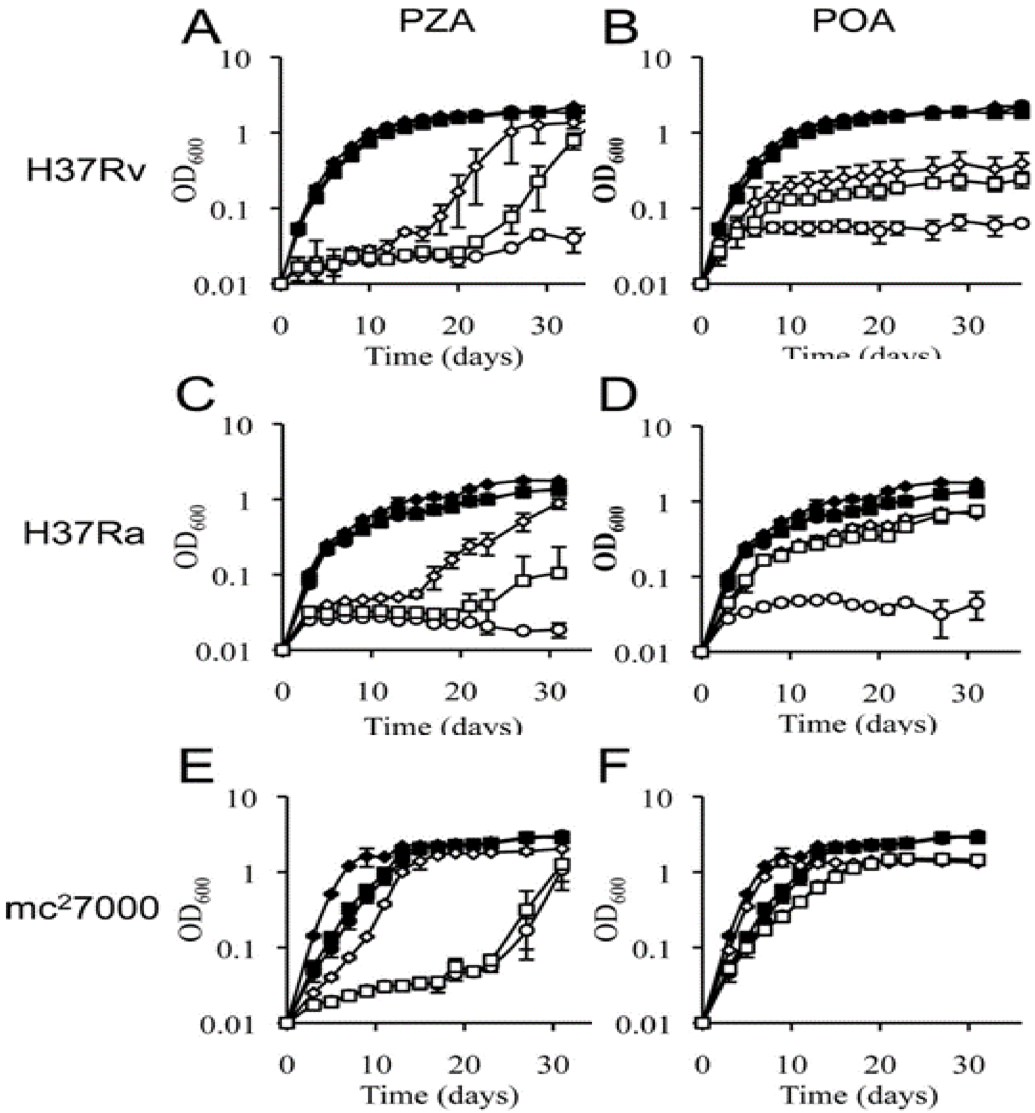

Figure 3-3 Growth kinetics of *M. tuberculosis* strains supplemented with pantothenate and β-alanine during exposure to PZA and POA. The growth of *M. tuberculosis* strains H37Rv (A and B), H37Ra (C and D), and mc²7000 (E and F) in 7H9 medium containing OADC (10%), glycerol (0.2%), and tyloxapol (0.05%) with 1 mM pantothenate (solid diamonds), 1 mM β-alanine (solid squares), or no additional supplementation (solid circles) is shown. (E and F) Strain mc²7000 was additionally supplemented with 7.2 $\mu g\ ml^{-1}$ pantethine. The cultures were treated with either 200 $\mu g\ ml^{-1}$ PZA (A, C, and E) or 400 $\mu g\ ml^{-1}$ POA (B, D, and F) in the presence of 1 mM pantothenate (open diamonds), 1 mM β-alanine (open squares), or no additional supplementation (open circles).

of PZA at an earlier time than β-alanine (Figure 3-3A and 3-3C). Yet, initiation of growth in the presence of pantothenate and PZA was markedly delayed relative to the no drug control (Figure 3-3A and 3C). In contrast, both pantothenate and β-alanine antagonized POA immediately, resulting in growth kinetics similar to the no drug controls (Figure 3-3B and 3D). The starkly different response times for PZA and POA suggest that PZA is likely antagonized following its conversion to POA.

To determine whether pantothenate-related metabolites also antagonize PZA action, other intermediates of the CoA biosynthetic pathway were assessed. Supplementation of *M. tuberculosis* cultures with 1 mM β-alanine, pantothenate or pantetheine lead to a dramatic increase in the MIC_{90} of both PZA and POA (Table 3-2). In addition, carnosine, a dipeptide of β-alanine and histidine, also antagonized PZA and POA activity (Table 3-2). In contrast, aspartate (a metabolic precursor of β-alanine), and pantoate (a co-substrate with β-alanine in the synthesis of pantothenate), did not show measurable antagonistic activity (Table 3-2). Evaluation of the minimum antagonistic concentration (MAC_{10}) for this series of metabolites revealed that pantothenate, β-alanine and pantetheine were the most potent PZA antagonists, while the activity of carnosine was relatively weak (Table 3-3). Aspartate and pantoate did not show measurable antagonistic activity at any of the concentrations that were tested (Table 3-3). These data indicate that β-alanine

Table 3-2 MIC_{90}s of select antimycobacterial compounds in the presence of various metabolites

Compound	Structure	MIC_{90}[a] (μg ml^{-1})					
		No antagonist	Pantothenate	β-Alanine	Pantetheine	Carnosine	Aspartate
PZA	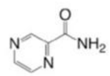	50	400	200	200	200	50
POA	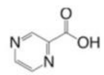	100	>800	800	>800	>800	100
5-Cl PZA	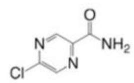	25	>200	ND[b]	ND	ND	ND
Nicotinamide	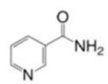	100	200	200	100	200	100
Nicotinic acid	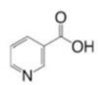	400	400	400	400	400	400
n-Propyl pyrazinoate	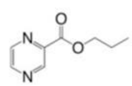	100	>400	ND	ND	ND	ND
INH	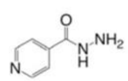	0.0625	0.0625	0.0625	0.0625	0.0625	0.0625

[a] MIC_{90}, defined as the MIC that inhibits >90% of *M. tuberculosis* H37Ra growth relative to the no-drug control over 2 weeks of incubation.
[b] ND, not determined.

Table 3-3Minimum concentrations of metabolites required for antagonism of PZA action against *M. tuberculosis* H37Ra

Antagonist	Structure	MAC_{10}[a] (μM)
β-Alanine	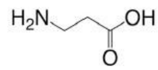	<3.125
Pantoate	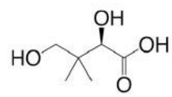	>1,000
Pantothenate	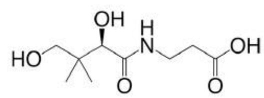	1.78
Pantetheine	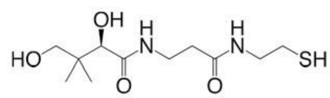	6.25
Aspartate	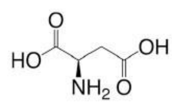	>1,000
Carnosine	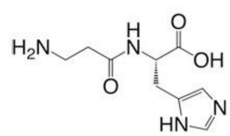	500

[a] MAC_{10}, defined as the minimum concentration of antagonist that permits greater than 10% growth relative to the no-drug control.

Table 3-4 Minimum concentrations of β-alanine structural analogs required to antagonize PZA action against *M. tuberculosis*

Antagonist	Structure	MAC_{10}[a] (μM)
Taurine	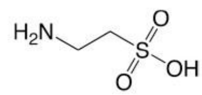	>1,000
3-Aminopropanol		6.25
Propanoic acid	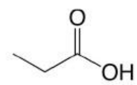	200
Propylamine	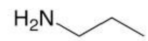	>1,000
4-Aminobutyric acid	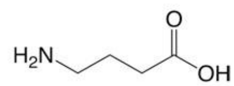	>1,000
Glycine	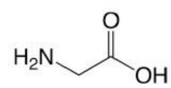	>1,000

[a] MAC_{10}, defined as the minimum concentration of antagonist that permits greater than 10% growth relative to the no-drug control.

Structural analogs of β-alanine antagonize PZA activity. To further assess the structural requirements for this antagonism, we investigated the ability of several β-alanine analogs to antagonize PZA activity in cultures of *M. tuberculosis*. These structural analogs differed from β-alanine by: the absence of the terminal carboxyl group (taurine, 3-aminopropanol and propylamine); the absence of the terminal amino group (propanoic acid); and an altered chain length between the carboxyl group and the amino group (4-aminobutyrate and glycine) (Table 3-4). While most of these analogs did not show any measurable antagonistic activity against PZA, 3-aminopropanol and propanoic acid were found to abolish PZA activity at concentrations of 6.25 and 200 µM, respectively (Table 3-4).

Susceptibility of *M. tuberculosis* to PZA is independent of *panCD*. The ability of β-alanine to antagonize PZA and POA activity is consistent with the speculation that POA inhibits the *M. tuberculosis* aspartate decarboxylase encoded by *panD*[66]. As such, it would follow that any condition that can support growth of a strain deleted for *panD* should antagonize PZA activity. Upon evaluating conditions that permit growth of the pantothenate auxotrophic strain mc^{2}7000, it was found that this strain could be cultured in the absence of pantothenate by supplementation with a sub-antagonistic concentration of pantetheine (Figure 3-3E). Under this growth condition, PZA susceptibility was restored for the first three weeks of incubation, after which growth was observed (Figure 3-3E). This inhibitory effect of PZA for a strain deleted for *panD* indicates that PanD is not the principal target for PZA-mediated inhibition of *M. tuberculosis*.

As POA activity was more potently antagonized by pantothenate/CoA intermediates, 400 μg ml^{-1} POA only showed a modest inhibitory effect for growth of strain $mc^2$7000 in the presence of pantetheine (Figure 3-3F). Similar to that which was observed for other *M. tuberculosis* strains, pantothenate antagonized PZA and POA activity against $mc^2$7000 (Figure 3-3E and 3F). However, in contrast to that which was observed for strains H37Rv and H37Ra, β-alanine failed to antagonize PZA and POA activity for strain $mc^2$7000 (Figure 3-3E and 3F). The essential role for *panCD* in β-alanine mediated antagonism of PZA and POA activity indicates an essential role for pantothenate synthesis in this process.

Metabolites of the pantothenate/CoA biosynthetic pathway antagonize some PZA structural analogs. To determine the specificity of pantothenate-linked antimycobacterial antagonism, other compounds bearing structural similarity to PZA were examined for activity against *M. tuberculosis* during supplementation with metabolites of the pantothenate and CoA biosynthetic pathway. The PZA structural analogs, 5-chloropyrazinamide (5-Cl PZA), nicotinamide, and *n*-propyl pyrazinoate (*n*PPA) were all antagonized by panthothenate supplementation (Table 3-2). Nicotinamide activity was also weakly (2-fold) antagonized by β-alanine and carnosine (Table 3-2). The MIC_{90} of the structurally related compounds isoniazid and nicotinic acid were not altered by any of the metabolites tested (Table 3-2), indicating that antagonism is not general to all anti-tubercular agents.

Discussion

Factors that influence the activity of PZA against *M. tuberculosis* are important considerations for optimizing TB short course therapy. In this study we determined that the anti-mycobacterial activity of PZA is antagonized by the presence of exogenous pantothenate or pantetheine. While PZA activity was also antagonized by metabolites linked to the pantothenate/CoA biosynthetic pathway, the observation that pantoate β-alanine ligase is essential for antagonism by β-alanine indicates that this effect is mediated by pantothenate or a downstream metabolite (Figure 3-1).

Other metabolites that are peripherally associated with the pantothenate/CoA biosynthetic pathway were also found to antagonize PZA activity. Carnosine, a dipeptide of β-alanine and histidine, was identified as a weak antagonist. While carnosine is not directly involved in pantothenate/CoA biosynthesis, it can serve as a source of β-alanine upon hydrolysis of the aminoacyl bond. In mammals, this bond is rapidly hydrolyzed in serum by the M20 zinc dipeptidase carnosinase[130]. In *M. tuberculosis*, *Rv2522c* encodes a carnosinase ortholog (30% identity) whose corresponding activity has yet to be characterized[131]. In addition, 3-aminopropanol, a structural analog of β-alanine lacking the carbonyl group, was also found to antagonize PZA activity. While 3-aminopropanol has no known role in mycobacterial metabolism, *M. tuberculosis* encodes multiple short chain alcohol dehydrogenases and aldehyde dehydrogenases that might convert 3-aminopropanol to β-alanine.

The mechanistic basis for pantothenate-mediated antagonism of PZA action is currently unresolved. Yet, as POA activity is also abolished by exogenously supplied pantothenate, antagonism is not simply due to a failure in the activation of PZA. Based on the previous description of *panD* mis-sense mutations in PZA resistant strains that lack mutations in *pncA*, it has been suggested that PZA might target aspartate decarboxylase[66]. However, in the present study we found that a *M. tuberculosis panD* deletion mutant was still susceptible to PZA when grown with a sub-antagonistic concentration of pantetheine, indicating that PanD is unlikely to be a principal target for PZA. Further, we have also found that pantothenate antagonizes the activity of 5-Cl PZA, a *bone fide* FAS-I inhibitor[68,73,132]. There is currently no precedence for 5-Cl PZA mediated inhibition of pantothenate synthesis. Thus, pantothenate-mediated antagonism occurs via a mechanism that is likely target independent. We anticipate that this antagonism of structurally conserved anti-tubercular compounds relates to these compounds sharing a common localization pathway. Additional studies are required to resolve the mechanistic basis for this phenomenon.

Mammals lack the biosynthetic machinery for *de novo* synthesis of the pantothenate and rely on dietary intake of this essential metabolic cofactor. There is limited data on tissue specific concentrations of pantothenate. Although, with normal levels of consumption (4 to 7 mg per day) human serum pantothenate concentrations are typically on the order of 2 μM[129], the level at which we begin to see antagonism of the antimycobacterial action of PZA in our *in vitro* assays. Despite a lack of evidence for therapeutic efficacy, trials with high dose pantothenate supplementation in treatment for conditions such as cystinosis, acne and hyperlipidemia have been described[133–135]. In one such study, subjects were given oral doses of 70-1,000 mg/kg per day resulting in plasma pantothenate concentrations of greater than 250 µM[133]. It is unknown how this concentration would relate to pantothenate levels within macrophage phagosomes or the lumen of granulomas. Further investigation is necessary to determine whether there is any association between pantothenate intake levels and PZA efficacy. Yet, based on our observations, we speculate that excessive pantothenate supplementation could have a deleterious impact on TB short course therapy.

Acknowledgments

This work was supported by a grant from the NIAID (7UM1 AI068636-07) and institutional startup funds from the University of Minnesota to ADB. ND is supported by an institutional training grant from the NHBLI (2T32HL007741-21). We thank Dr. John T. Welch for providing 5-Cl PZA and *n*PPA, and Dr. William R. Jacobs, Jr. for providing the strains that were used in this study.

Novel pyrazinamide resistance mutations in *Mycobacterium tuberculosis* uncover a dependency on SigE regulation for pyrazinamide activity

Abstract

The emergence of drug resistant *Mycobacterium tuberculosis* strains threatens our capability to successfully treat tuberculosis patients. Resistance to pyrazinamide, a critical component of the first line regimen, occurs via unidentified mutations in up to one third of resistant isolates in the clinic. Using insertional transposon mutagenesis we were able to create a library of novel PZA resistance mutations in virulent *M. tuberculosis* strain H37Rv. Our screen indicated that mutations that altered expression of the sigma factor *sigE* regulon were associated with pyrazinamide resistance. Further characterization of this library of mutants demonstrated resistance to pyrazinamide and its activated form pyrazinoic acid. PZA resistance was confirmed in a H37Rv *ΔsigE* strain and drug susceptibility was restored when *sigE* was provided *in trans*. We now hypothesize that *sigE* induction sensitizes *M. tuberculosis* to pyrazinamide.

Introduction

Mycobacterium tuberculosis, the causative agent of the disease tuberculosis, remains a global health threat despite ongoing efforts to eradicate the disease. Current tuberculosis therapy consists of a four drug regimen administered over the course of a minimum of 6 months of treatment[105]. Successful treatment using the first line therapy is threatened by the emergence of drug resistant strains. Resistance mechanisms are well characterized for 3 of the 4 drugs in the regimen. Pyrazinamide (PZA), considered an irreplaceable component of the first line therapy[125], is the exception with unidentified resistance conferring mutations comprising up to a third of PZA resistant clinical isolates[136].

Long thought of as the key sterilizing agent in the first line regimen PZA has the unique capability to eliminate both growing and non-growing populations in the host[59]. Inclusion of PZA in tuberculosis therapy has allowed a reduction in treatment duration while also lowering relapse rates[105,124]. While the mechanism of action of PZA remains undefined, *in vitro* susceptibility to the drug requires concurrent exposure to stresses such as: acidic pH[137], hypoxia[91], nutrient limitation[107], and heat shock[138]. The mechanistic role these stresses play in inducing PZA susceptibility has not been elucidated although evidence indicates that it is not through altered *pncA* expression[107]. Resistance to PZA occurs primarily through loss of function mutations in the nicotinamidase encoding gene *pncA*, a dispensable gene both *in vitro* and *in vivo*[62]. PncA is responsible for the hydrolysis of the prodrug PZA into the active form pyrazinoic acid (POA), which elicits drug activity[61]. However, up to a third of clinical PZA resistant isolates lack defined mechanisms of resistance.

In this study we used a transposon mutagenized library of H37Rv to select for POA resistant mutants. We isolated and characterized 16 randomly selected resistant mutants from the library. Amongst the 16 POA resistant isolates we found 8 novel resistance conferring mutations. Using a next generation sequencing approach we identified the resistance conferring genomic transposon insertion locations of approximately 2,200 colonies from the POA resistance library. We found over 150 genes, which when mutated, conferred POA resistance. Based on an assessment of the mutations with the highest relative abundance in the library we discovered a role for the SigE reglon in promoting PZA susceptibility. The role of SigE in inducing PZA susceptibility was confirmed in a SigE deletion strain, which was resistant to the drug until SigE was complemented back in. We now hypothesize that SigE induction sensitizes *M. tuberculosis* to PZA through an alteration in the availability of essential metabolic cofactors.

Methods

Bacterial strains and growth media. *M. tuberculosis* strain H37Rv was a gift from W.R. Jacobs, Jr. of the Albert Einstein College of Medicine. The H37RvΔ*sigE* and complemented strain were gifts from T.C. Zahrt at the Medical College of Wisconsin. Strains were grown in Middlebrook 7H9 medium (Difco) supplemented with 10% (vol/vol) oleic acid-albumin-dextrose-catalase (OADC) (Difco), 0.2% (vol/vol) glycerol, and 0.05% (vol/vol) tyloxapol, kanamycin (NEB) was added at 50 µg/mL for cultivation of the complemented *sigE* strain.

Transposon mutagenesis to isolate POA resistant mutants. Strain H37Rv was mutagenized with a *Himar1* mariner transposon, a gift from from William R. Jacobs, Jr. of the Albert Einstein College of Medicine, in the pH 6.8 standard growth medium described above. Approximately $2*10^5$ independent transposon mutagenized bacilli were plated on Middlebrook 7H10 medium supplemented with 10% (vol/vol) OADC (Difco), and 0.2% (vol/vol) glycerol with 50 μg/mL of pyrazinoic acid (POA) (Sigma). Resistant mutants were selected from the plates containing 50 μg/mL POA. The initial isolates were plated on 7H10 medium supplemented with 10% (vol/vol) OADC (Difco), and 0.2% (vol/vol) glycerol either containing 400 μg/mL POA or no drug after their initial isolation to confirm their POA resistance prior to the more detailed drug susceptibility testing.

Antimycobacterial susceptibility testing. The minimum inhibitory concentration of drug that inhibited greater than 90% of the growth observed with drug free controls (MIC_{90}) were determined via measuring the OD_{600} value of cultures after 14 days of treatment. Drug susceptibility testing for PZA and POA in liquid was carried out 7H9 medium supplemented with OADC, glycerol, and tyloxapol (pH 5.8) as indicated above. Isoniazid MIC_{90} determinations were carried out in medium with the same composition at pH 6.8. POA agar MIC_{90} determinations were conducted using 7H10 medium supplemented with OADC and glycerol (pH 6.8) as indicated above. POA was added to the medium post autoclaving, prior to agar solidification, from a 100 mg/mL POA stock (pH 6.8) in water.

Tn-seq library preparation and sequencing. The samples that were sequenced for the resistance library analysis were made using the TruSeq Nano DNA protocol on the Illumina Neoprep system, followed by enrichment of the mariner transposon. gDNA was extracted from approximately 2,200 isolated colonies from the resistance library. Briefly, colonies were scraped into 10 mL of 7H9 complete medium, the mycobacteria were pelleted, and incubated at 80 ^{o}C for 2 hours. Cultures were then pelleted and resuspended and washed in 500 µl of 25 mM Tris pH 7.9, 10 mM EDTA, and 50 mM glucose. The cells were then resuspended in 450 µl of 25 mM Tris pH 7.9, 10 mM EDTA, and 50 mM glucose with 50 µl of 10 mg/ml lysozyme. Samples are then incubated at 37 ^{o}C for 16 hours. After the incubation is complete 100 µl of 10% SDS and 50 µl of 10 mg/ml proteinase K are added and then the mixture is incubated at 55 ^{o}C for 30 min. 200 µl of 5M NaCl and 160 µl of CTAB saline solution (0.7M NaCl, 0.275M hexadecyl-trimethylammonium bromide, CTAB) were then added and the samples are incubated at 65˚C for 10 min. DNA was extracted using multiple chloroform:isoamyl alcohol treatments. The DNA was then precipitated with isopropanol and washed with 70% EtOH prior to its resuspension in EB buffer (Qiagen).

For splinkerette library construction, DNA was digested with BamHI or BstYI Transposon junctions were amplified by using a transposon specific primer Mariner_1R_TnSeq_noMm (TCGTCGGCAGCGTCAGATGTGTATAAGAGACAGCCGGGGACTTATCAGCCAACC) and and the splinkerette primers Nextera_Splink#1 (GTCTCGTGGGCTCGGAGATGTGTATAAGAGACAGCGAAGAGTAACCGTTGCTAGGAGAGACC) or Nextera_Splink#2 (GTCTCGTGGGCTCGGAGATGTGTATAAGAGACAGGTGGCTGAATGAGACTGGTGTCGAC). Splinkerete primers contain a hairpin loop and anneal to the restriction digested ends of the DNA. Transposon junctions were amplified by using a transposon specific primer Mariner_1R_TnSeq_noMm and P7 primers with HotStarTaq Master Mix Kit (Qiagen) with the following PCR condition (94 °C for 3 min, 30 cycles of 98 °C for 20 seconds, 65 °C for 15 seconds, and 72 °C for 2 min, 72 °C for 7 minutes, 4 °C hold).

DNA fragmentation and Illumina P7 adaptor (CAA GCA GAA GAC GGC ATA CGA GAT) ligation were performed in NeoPrep Library Prep System (Illumina). Transposon junctions were amplified by using a transposon specific primer Mariner_1R_TnSeq_noMm and P7 primers with HotStarTaq Master Mix Kit (Qiagen) with the following PCR condition (94 °C for 3 min, 30 cycles of 94 °C for 30 seconds, 65 °C for 30 seconds, and 72 °C for 60 seconds, 72 °C for 10 minutes).
The Mariner enriched samples were diluted 1:100 and indexed for 10 cycles to add unique barcodes and the necessary P5 and P7 flow sites for Illumina sequencing (94 °C for 3 min, 94 °C for 30 seconds, 55C for 30 seconds, 72 C for 30 seconds, Repeat denature, anneal, elongate 9 more times, 72C for 10 minutes)

Sequence analysis. Sequence reads were trimmed using CutAdapt[139]. We first trimmed sequence reads for transposon and adaptor sequences (CCGGGGACTTATCAGCCAACCTGT) that were ligated to 5'ends. We also discarded all the sequence reads that did not contain adaptor sequence in the 5' trimming process. After the 5' trimming process, all the sequence reads begin with TA. We then trimmed sequence reads for adaptor sequences ligated to the 3’end (GATCCCACTAGTGTCGACACCAGTCTC). After the trimming, we discarded the sequence reads that were shorter than 18 bp. We used the CutAdapt default error rate of 0.1 for all trimming processes.

The trimmed sequence reads were mapped (allowing 1 bp mismatch) to the *M. tuberculosis* H37Rv genome (GenBank: AL123456.3) using Bowtie[140]. The genome mapped sequence reads were printed in SAM format and counted sequence reads per each TA dinucleotides site in the *M. tuberculosis* H37Rv genome using SAMreader_TA script[141].

Pooling strategy for plate arrayed transposon mutant library identification. A pooling strategy was used to identify and isolate the resistant mutants using next generation sequencing. This strategy is similar to previously used methods[142] except that rows and columns from every plate were pooled as were quadrants from each 96 well plate. gDNA isolation and sequencing was the same as described above for the splinkerette sequencing except 5 units of BfuCI were incubated at 37 ^{o}C for 2 hours with 80 ^{o}C inactivation for 20 minutes instead of BamH1 to permit smaller digested fragments. A 1:50 dilution of the mariner enrichment was used for indexing.

Results

Endeavoring to gain a better understanding of PZA susceptibility we sought to identify PZA resistance conferring mutations in the virulent *M. tuberculosis* strain H37Rv using a *Himar1* mariner based transposon library to select for PZA resistance. Knowing that selection on PZA would provide a preponderance of *pncA* mutations, mutants were instead selected using an inhibitory concentration of POA. This selection produced POA resistant colonies at a frequency of approximately 0.44% while spontaneous resistance to PZA and POA has been reported at approximately 0.001%[79,143]. Sixteen colonies were selected for follow up analysis. After eliminating siblings, nine unique transposon insertion sites were identified comprising of one mutation in *panD* and eight genes that had never been associated with PZA resistance previously (Table 3-5).

To assess the magnitude of resistance, the minimum inhibitory concentration (MIC_{90}) in liquid medium was determined for each strain for both POA and PZA (Table 3-5). The isolates displayed varying degrees of susceptibility to POA and PZA compared to *M. tuberculosis* strain H37Rv ranging from 2 to >16 fold, and 2 fold, respectively (Table 3-5). Confirming the specificity of the resistance to PZA, no difference in INH susceptibility was found in the mutants compared to the parental strain (Table 3-5). Resistance to POA on agar medium was similar to that of liquid medium for all of the isolates except the insertion in *Rv0211* (*pckA*), which had ≥32 fold resistance compared to H37Rv on agar while only 2-4 fold increased resistance in liquid medium. The basis for the disparate POA susceptibility for *Rv0211* mutant strains is currently unknown.

Having confirmed multiple non-redundant novel mutations conferring POA resistance within the initial isolates, we next sought to use a Tn-seq based approach to examine the remainder of the library. Genomic DNA was harvested from a pool of the *M. tuberculosis* POA resistant library and submitted for Illumina sequencing. In total, we identified 124 genes and 47 intergenic regions that were associated with POA resistance in our analysis. Relative abundance for insertions into each TA site was tallied separately for each gene and intergenic region and plotted based on genomic position and percentage of TA sites hit (Fig. 3-4A and 4B). Additionally, each resistance conferring mutation was assigned to a functional group based upon the location of the insertion. The majority of mutations conferring POA resistance were found in the functional categories of: cell wall and cell processes, intermediary metabolism and respiration, and conserved hypotheticals (Fig. 3-4C). Resistance arising from metabolic alterations has previously been documented. Pantothenate, a precursor of coenzyme A (CoA), was found to antagonize PZA and POA anti-tubercular activity[87].

We next clustered the most highly abundant resistance conferring insertion sites to determine if a particular function was targeted for POA resistance. Insertions in the gene encoding for the stress responsive sigma factor, SigE, and in the intergenic region upstream of ClpC1, a protease involved in the activation of SigE[144], comprised two of the locations marked by a high relative abundance in the library (Table 3-6). Mutations affecting ClpC1 have been recently described to confer PZA resistance[143]. SigE is a transcription factor involved in cellular response to multiple stresses including acidic pH, hypoxia, nutrient limitation, heat shock, and oxidative damage[145]. While SigE has been

Table 3-5: Phenotypic characterization of novel pyrazinamide resistance mutations

Strain	Liquid: POA MIC_{90}[a] (µg/mL)	Liquid: PZA MIC_{90}[a] (µg/mL)	Liquid: INH MIC_{90}[a] (µg/mL)	Agar: POA MIC[b] (µg/mL)	Function
H37Rv	200	50	0.0625	≤100	NA
H37Rv *Rv0211*::Tn	400-800	100	≤0.0625	3200	Phosphoenolpyruvate carboxykinase *pckA*
H37Rv *Rv0522*::Tn	800	100	≤0.0625	800	GABA permease *gabP*
H37Rv *Rv2705c*::Tn	400-800	100	≤0.0625	400	Hypothetical protein
H37Rv *Rv2706c*::Tn.1	400	100	≤0.0625	200	Hypothetical protein
H37Rv *Rv2706c*::Tn .2	800	100	≤0.0625	400	Hypothetical protein
H37Rv *Rv3256c*::Tn	800	50-100	≤0.0625	400	Hypothetical protein
H37Rv *Rv3601c*::Tn	>1600	100	≤0.0625	800	Pantothenate kinase *panD*
H37Rv *Rv3727*::Tn	1600	100	≤0.0625	800	Hypothetical protein
H37Rv *Rv3916c*::Tn	800	100	≤0.0625	400	Hypothetical protein
H37Rv *MTB000070::*Tn	400-800	50	ND	ND	Upstream of ATP dependent protease *clpC1*
H37Rv Δ*sigE*	≥800	400	ND	ND	NA
H37Rv Δ*sigE* pMV306-*sigE*	400	50-100	ND	ND	NA

[a]MIC_{90} is defined as the lowest amount of drug that inhibited greater than 90% of the growth when compared to drug free cultures. Liquid MICs were conducted in 7H9+OADC+glycerol+tyloxapol for 14 days. All liquid cultures were incubated shaking at 37°C with the indicated amount of drug at pH 6.8 for INH and pH 5.8 for PZA and POA .

[b]MIC is defined as the lowest amount of drug that visually inhibited growth when compared to drug free cultures. Plate MICs were conducted on pH 6.8 7H10+OADC+glycerol plates for 21 days. Plates were incubated at 37°C.

A. B.

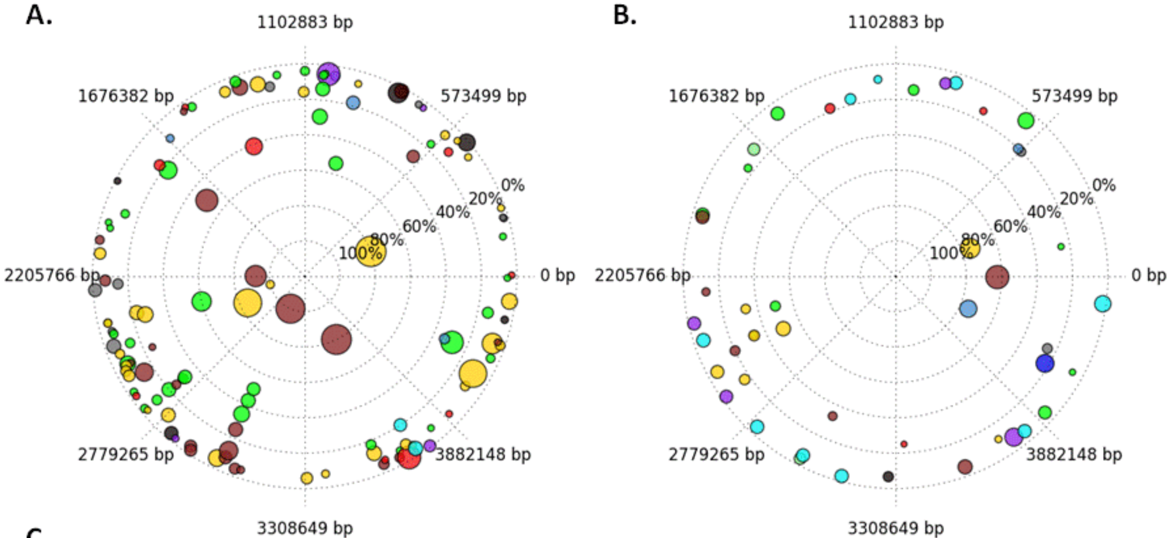

C.

Functional categories	Intergenic: Regions with insertions	Intergenic: % of total insertions	Intragenic: Genes with insertions	Intragenic: % of total insertions	Total: % of total insertions
Virulence, detoxification, adaption	2	1%	7	4%	5%
Lipid metabolism	1	1%	5	3%	4%
Information pathways	3	2%	10	6%	8%
Cell wall and cell processes	9	5%	35	20%	26%
Stable RNAs	1	1%	0	0%	1%
Insertion seqs and phages	9	5%	2	1%	6%
PE/PPE	4	2%	4	2%	5%
Intermediary metabolism and respiration	8	5%	34	20%	25%
Unknown	2	1%	0	0%	1%
Regulatory proteins	2	1%	4	2%	4%
Conserved hypotheticals	6	4%	23	13%	17%
Total	47	27%	124	73%	100%

Figure 3-4: POA resistance mutations via Tn-seq. (A+B)The distance from the point to the center of the plot indicates the frequency of TA sites detected with transposon insertions per gene where 100% represents the detection of all available TA sites. The radius of the circle of each data point represents the total reads associated with all of the insertions in the corresponding gene plotted on a log scale. The color of each point corresponds to the functional category that is suspected of being affected by insertions at that location. The genomic position is indicated on the outermost edge of the circle. (A) Data points from intragenic regions. (B) Data points from intergenic regions. (C) Summary of the frequency of each affected functional category covering all insertions.

Table 3-6: Unique insertions in the locations of highest relative abundance

Locus	Cellular Function	Unique Insertions
pckA	PEP carboxykinase, 1st step of gluconeogenesis	29
aceE	pyruvate dehydrogenase, last step of glycolysis	52
sigE	stress-related sigma factor, transcription	16
clpC1	protease involved in activation of SigE	4
phoT, pstS3, pstC2, pstA1	low phosphate response	28
pafA, prcB , pup, dop, mpa	mycobacterial proteosome	70
cysA, cysW, cysT, subI	sulfur utilization	27
panD	pantothenate/coenzyme A biosynthesis	3

determined to be essential *in vivo*, it is non-essential for *in vitro* growth in the absence of environmental stress[146]. As many of the stresses that activate a SigE response have been demonstrated to increase susceptibility to PZA, we sought to further characterize the relationship between SigE and PZA susceptibility. As we did not have a *clpC1:*Tn mutant in our initial isolates we enacted a pooling strategy combined with next generation sequencing to isolate the mutant from our resistance library. To demonstrate the role of *sigE* in PZA susceptibility, the following strains were tested for susceptibility to PZA and POA: Δ*sigE*, Δ*sigE* pMV306**::***sigE***,** and *clpC1*::Tn mutants.

As *clpC1* is essential in *M. tuberculosis*, the transposon in our *clpC1*::Tn mutant was inserted upstream of the *clpC1* locus. The Δ*sigE* strain was resistant to both POA and PZA, while the *clpC1*::Tn mutant was only resistant to POA (Table 3-5). Susceptibility to both POA and PZA were restored to the Δ*sigE* mutant through complementation (Table 3-5).

Discussion

Through identification of resistance promoting mutations impacting the *sigE* regulon, we have uncovered an unexpected relationship between cellular stress response and PZA susceptibility. The stresses required for PZA susceptibility, namely: acidic pH, hypoxia, nutrient limitation, and heat shock, are the same stresses that induce the SigE regulon. Therefore, it follows that the *sigE* regulon plays a role in sensitizing the cell to

PZA. While the mechanism linking *sigE* induction to PZA susceptibility is not yet clear, one possibility is that *sigE* induction may impact the levels of free Coenzyme A (CoA), leading to PZA susceptibility. SigE has been previously demonstrated to impact regulation of phosphoenolpyruvate carboxykinase, *pckA,* and pyruvate dehydrogenase, *aceE,* in *M. tuberculosis*[147]. Both of these mutations were also highly represented in our Tn-seq analysis (Table 3-6). Additionally, excluding *pstA1* and *prcB* every other gene listed in table 3-6 is differentially expressed in a Δ*sigE* strain suggesting the genes are at least partially regulated by the SigE regulon[148]. These data, taken with the previous finding that POA treatment decreases intracellular abundance of CoA[79], suggest that perturbations in CoA levels drive *M. tuberculosis* susceptibility to PZA and POA. We propose that external stress leads to an induction of the *sigE* regulon leading to a decrease in free CoA levels. Once free CoA levels are depleted, treatment with POA leads to growth inhibition and cell death (Figure 3-5). This model is supported by the high prevalence of *pckA* and *aceE* mutants in our transposon library. Mutations in *pckA* and *aceE* may promote increased levels of free CoA through perturbations of acetyl-CoA turnover, thus preventing POA mediated killing. Further support for this model is the observation that exogenous pantothenate can antagonize anti-tubercular PZA and POA action, likely through protection of free CoA levels[79,87]. These observations also suggest that CoA levels may determine the bactericidal effect of PZA and POA treatment. In conditions lacking a cellular stress, PZA and POA are needed at very high concentrations to exert a strong enough effect on intracellular CoA and impact growth. However, during stress conditions, intracellular CoA levels are already lowered due to the stress response and thus more susceptible to perturbations by PZA or POA.

Despite over 60 years of clinical use, the mechanism of action, and up to one third of resistance conferring mutations, remain undefined for PZA. Using next generation sequencing approaches have allowed for the identification of novel PZA resistant mutants. Generation of *in vitro* resistance libraries allow anticipation of the evolution of clinical resistant strains even if they have yet to be detected. Furthermore, additional characterization of these strains might open the door to solving the elusive mechanism of action of PZA through the newly observed connections between SigE induction, CoA level modulation, and PZA susceptibility.

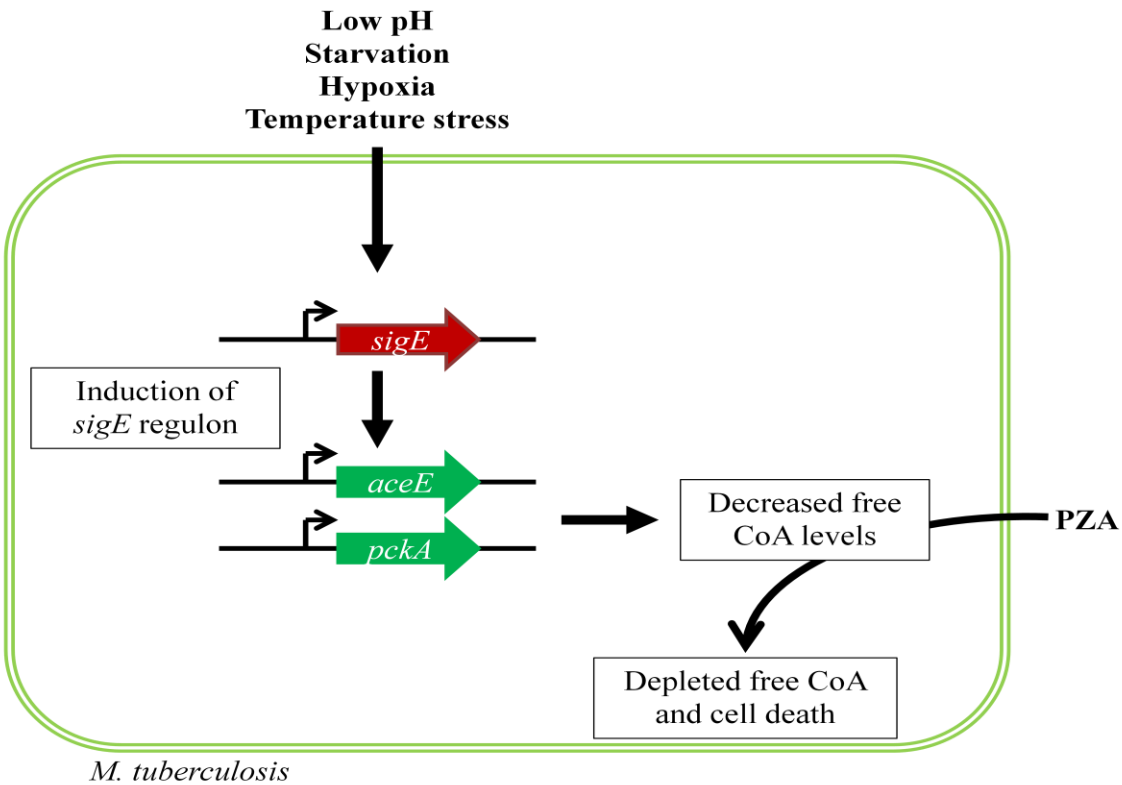

Figure 3-5 Model for impact of PZA on free CoA. SigE induction, in response to various environmental stresses, increases the expression of *aceE* and *pckA* leading to reduced levels of free CoA. As a product of its mechanism of action PZA also reduces CoA. Induction of the SigE regulon concurrently with PZA treatment reduces free CoA levels to a metabolic point of no return initiating cellular death.

Chapter 4

Pyrazinamide treatment synergizes with oxidative stress

Disparate *in vivo* and *in vitro* activities of PZA have led to the suggestion that there may be a host-derived component that is required for PZA activity against *M, tuberculosis*. Early studies in our laboratory indicated there might be a correlation between increased PZA susceptibility and exposure to reactive oxygen species. Pursuing this as a possible clue into the mechanism of action of the drug we tested the H_2O_2 susceptibility of PZA treated *M. tuberculosis* cultures finding that the two synergized with each other. The synergy was determined to enhance both the inhibitory as well as the bactericidal capabilities of each compound. Our data suggest that the synergy was mediated through an increase in the rate of hydroxyl radical production from H_2O_2 by complexes of POA and iron. Consistent with the model, PZA and POA treated cultures showed enhanced oxidative damage upon exposure to H_2O_2. Based on this study we hypothesize that PZA enhances the killing capacity of the host induced oxidative burst *in vivo*. This paper is being prepared for submission and I am the first author. For this paper I have done the majority of the work and I am responsible for writing the paper. Ranee Aflakpui, Brandon Rosen, and Dr Elise Lamont have also contributed to this manuscript.

Pyrazinamide potentiates oxidative stress in

***Mycobacterium tuberculosis* by accelerating the Fenton reaction**

Abstract

The mechanistic basis for the antimicrobial activity of pyrazinamide (PZA) against *Mycobacterium tuberculosis* remains unknown despite its use in tuberculosis therapy for over 60 years. PZA activity requires the conversion into pyrazinoic acid (POA) by the mycobacterial encoded amidase PncA. The majority of PZA resistant clinical isolates of *M. tuberculosis* are associated with loss-of-function mutations in *pncA*. Previous studies have indicated that POA interacts with Fe^{2+}, yet the role this plays in the antitubercular activity of the drug has never been reported. Using isothermal titration calorimetry, a technique for evaluating the thermodynamic parameters of ligand:ligand interactions, we determined that POA, and not PZA, was capable of binding different divalent transition metals including Fe^{2+}. However, neither PZA nor POA was found to interact with Fe^{3+}. Chemical synthesis studies have previously reported that POA and iron complexes are capable of promoting the oxidation of hydrocarbons in the presence of H_2O_2. We therefore hypothesized that the antitubercular activity of POA involves enhancing susceptibility to oxidative stress through accelerating the production of hydroxyl radicals from H_2O_2. Using an assay to measure the formation of hydroxyl radicals from H_2O_2 we found that inclusion of POA accelerated the formation of this species more rapidly than Fe^{2+} alone. Substituting other divalent metal ions for Fe^{2+} we found that POA-Cu^{2+} complexes were also able to accelerate the production of hydroxyl

radicals from H_2O_2. The increased production of hydroxyl radicals from the addition of POA resulted in elevated levels of protein carbonylation in a cell free assay and in whole cells using PZA. Based on these results we evaluated potential synergy between PZA and known oxidative stressors in *M. tuberculosis*. In accordance with our previous results we found that *M. tuberculosis* cells were hyper-susceptible to H_2O_2 during PZA treatment, yet found little to no synergy with the compounds menadione and clofazimine which are associated with heightened cellular production of superoxide. To our knowledge this work is the first to demonstrate that PZA treatment potentiates oxidative stress susceptibility in *M. tuberculosis*. As *M. tuberculosis* resides within phagosomal compartments within macrophages we hypothesize that PZA synergizes with the host induced oxidative burst as part of its antimicrobial activity. Elucidating the mechanistic basis for PZA action will enable identification of next generation agents that have superior activity against *M. tuberculosis*.

Introduction

Pyrazinamide (PZA) is a critical component of the first line therapy to treat *Mycobacterium tuberculosis* infections due to its combinatorial role in reducing treatment duration while decreasing disease relapse rates [43,124]. Given its unique ability to sterilize tubercle bacilli, PZA is considered as an irreplaceable drug in first and second line regimens and a likely component of any future regimens [125]. Although PZA has been employed for over 65 years in clinical application, the mechanism by which PZA mediates its antimycobacterial activity remains elusive.

Current dogma classifies PZA as a bacteriostatic agent based upon its inability to kill *M. tuberculosis* cells during *in vitro* exposure. However, early in tuberculosis (TB) drug development, PZA was prescribed as a monotherapy to TB patients due to a paucity of effective antitubercular options [59]. Approximately 56% of PZA responsive patients had no detectable bacilli in their sputum following this therapy, while 22% of patients achieved mycobacterial sterilization [59]. The disparate activity of PZA during *in vitro* and *in vivo* exposure implicates a possible host derived component that is required for drug efficacy in TB patients. PZA activity is diminished in murine models harboring compromised immune systems, such as Kramnik [149,150] and nude [151], which further supports the linkage between the drug and the immune response.

Murine models of TB recapitulate many hallmarks associated with *M. tuberculosis* infections in humans, including the ability of an aerosolized infectious dose to establish residence inside alveolar macrophages and dependence on a T_h1 driven T-cell response for immunological control. Once replicating bacilli are contained, macrophage and neutrophil dominated granulomas are formed and the stage is set for a long-term latent infection. However, PZA induced mycobacterial clearance is notably diminished in the murine model compared to TB patients[59,152]. Discrepancies between PZA function in mice and humans is likely attributable to differing host responses.

Production of reactive nitrogen species (RNS) is thought to be the dominant factor controlling *M. tuberculosis* infections in mice [35]. Nitric oxide (NO) is the primary RNS generated during the host response and is carefully regulated by cytokines [25,37]. NO is enzymatically generated by the inducible NO synthase (iNOS) through a two-step reaction that oxidizes L-arginine and culminates in NO and L-citrulline production [36]. Mice deficient in iNOS activity show an inability to control *M. tuberculosis* infection, resulting in dramatically acute mortality rates [35]. Loss of iNOS activity in *M. tuberculosis* infected human alveolar macrophages does not reduce their killing capacity bringing into question the relevance of RNS during the human resposne[38].

The production of reactive oxygen species (ROS) is the primary control mechanism for *M. tuberculosis* infections in human phagocytes. Superoxide is generated within the phagosome through the transfer of electrons from cytosolic NADPH to molecular oxygen mediated by the multi protein complex NADPH phagocyte oxidase. Inside the phagosomal environment superoxide quickly dismutates into the more stable hydrogen peroxide (H_2O_2), which can further react with metal ions to produce highly reactive hydroxyl radicals. Hydroxyl radicals induce cellular death through damaging proteins, DNA, and lipids. Mutations in the ROS producing NADPH phagocyte oxidase complex are associated with increased susceptibility to mycobacteria in humans [39,40] but not in mice [153].

PZA associated mycobacterial clearance is achieved during the ROS dominated immune response in humans but to a far lesser degree then in the RNS dependent response in mice. The sterilization discrepancy between the two hosts could be attributable to a modulation of ROS activity by PZA. A chemical reaction between pyrazinoic acid (POA), the enzymatically activated form of PZA, and ROS has previously been observed[154]. Industrial chemical synthesis studies demonstrated the oxidation of hydrocarbons in solutions containing H_2O_2 in the presence of POA and iron [154]. While the chemical mechanism is unknown it was predicted to involve the direct formation of hydroxyl radicals from the interaction of POA-iron with H_2O_2 [155]. The link between this observation and the mechanism of action of POA in a biological system has not been examined.

To date, the mode of action of PZA remains unresolved, as does the mechanistic basis for a functional immune response for its activity. PZA may directly modulate the host immune response to enable mycobacterial clearance. Based upon increased susceptibility to PZA in the ROS dominated human response and chemical evidence for a reaction between POA, iron, and H_2O_2, it is likely that POA induces increased mycobacterial oxidative stress through direct modulation of host derived ROS.

Methods

Bacterial strains and growth media. *M tuberculosis* strains H37Rv, and H37Ra were gifts from W.R. Jacobs of the Albert Einstein College of Medicine as where the *M. bovis* strains BCG-*pncA* and BCG. Strains were cultured in 7H9 medium (Difco) with 0.2% (vol/vol) glycerol, 0.05% (vol/vol) tyloxapol, and either 10% (vol/vol) oleic acid-albumin-dextrose-catalase (OADC) or 10% albumin-dextrose-sodium choloride (ADS) as indicated.

Isothermal titration calorimetry (ITC) assays. Experiments involving ITC were conducted on the MicroCal VP-ITC at 25.0 ^{o}C. As ITC is a very sensitive technique it was necessary to carry out these studies in a buffer that would have minimal interactions with the ligands. The Good's buffer MES was chosen due to its biochemical inertness and its pK_a near the acidic pH that is associated with *in vitro* PZA susceptibility. POA was dissolved in 500 mM MES buffer (pH 6.0). The pH of the POA buffer solution was adjusted to pH 6.0 to account for any pH change due to POA. The divalent ions were dissolved in the same buffer immediately prior to the first injection. POA was loaded into the syringe at 10 mM while the divalent ions were at 0.33 mM in the cell. Each experiment consisted of 28 injections of 10 μl over a 2 second duration into 1449.7 μl of ligand within the cell. The solution mixtures were stirred at 300 rpm and the interval between injections was set at 500 seconds. Origin 7 software (Origin®) was used to collect and analyze the data.

Hydroxyl radical production assay. Hydroxyl radicals were measured in cell free assays through the use of coumarin-3-carboxylic acid (3-CCA) as previously described [156]. Assays were conducted with 0.2 mM POA, dissolved in 500 mM MES buffer with the subsequent pH adjusted to pH 6.0, and 0.1 mM of the divalent ions. 5 mM 3-CCA was used with 5 mM H_2O_2. Assays were carried out in 500 mM MES buffer pH 6.0 and measured on a 96 well plate reader at an emission of 450 nm with a 395 nm excitation.

Protein carbonylation assays. The protein used in the assays was either bovine serum albumin (BSA), as in the cell free assays, or was harvested from H37Ra cultures. The cell free assays contained 200 µg/mL BSA and were carried out in 10 mM MES (pH 5) buffer at 37 ^{o}C. POA and Fe^{2+} were added where indicated at 2 mM and 1mM respectfully. Protein was harvested at the indicated timepoints after the addition of 25 mM H_2O_2.

The H37Ra cultures were pregrown in 7H9 complete medium with ADS (pH 6.8), washed once with 7H9 complete medium with dextrose-sodium choloride (pH 5.8), and were then resuspended in 7H9 complete medium with DS (pH 5.8) prior to the addition of PZA. 125 mL of an OD_{600} 0.05 H37Ra culture were used for each sample. Cultures receiving drug treatment were pretreated with PZA at 200 µg/mL for 72 hours prior to the addition of 5 mM H_2O_2 for 24 hours. Cultures were then pelleted and resuspended 2 mL of 7H9 complete medium with dextrose-sodium choloride (pH 5.8) Cultures were then lysed via bead beating to extract the protein.

Measurement of carbonylation was carried out via the spectrophotometric method as described in Wehr, N. B. & Levine 2013[157] in triplicate for each of the experiments. In brief lysates were first treated with 1% streptomycin sulfate for 30 min on ice followed by a 30 min spin at 13.2 krpm at 4 ^{o}C to pellet the DNA. The supernatants were transferred and treated with 2,4 dinitrophenylhydrazine (DNPH) for 10 min prior to the precipitation of the protein using 10% trichloroacetic acid. The protein pellets were then washed 3x with 1 mL of ethanol-ethyl acetate followed by low speed pelleting. The final protein suspension was made in 800 µL of 6.0 M guanidine HCl, 0.5 M potassium phosphate (pH 2.5). Carbonyl content was then determined using the absorbance at 395 nm on a spectrophotometer in quartz cuvettes.

MIC and FIC determination. Drug susceptibility was determined for *M. tuberculosis* cultures by measuring the optical densities of cultures at 600 nm (OD_{600}). MIC_{90} assays were conducted by determining the minimum amount of drug that was required to inhibit 90% of the growth in treated cultures when compared to untreated controls. POA stocks were made in water and the pH was adjusted with NaOH to match the pH of the medium prior to its addition. Synergies between different combinations of antimicrobials were determined by conducting fractional inhibitory concentration (FIC) experiments. The FIC experiments were carried out by setting up checkerboard assays with varying 2 fold concentrations of each antimycobacterial compound examined. Inhibition was scored in the FIC experiments based on the lowest amount of antimicrobial that was required to inhibit 90% of the growth in untreated cultures during concurrent exposure to a constant concentration of the other antimicrobial beind tested. The fractional inhibitory concentration index (FICI) was determined by calculating the sum of the measured FIC values for each compound at each point and then reporting the lowest value determined. All MIC and FIC assays were conducted in 7H9 complete medium with ADS (pH 5.8) at 37 ^{o}C on a 100 rpm rotary shaker in triplicate.

Survival assays. H37Ra cultures were pretreated with either PZA at 200 µg/mL or POA at 400 µg/mL for 72 hours prior to the addition of varying concentrations of H_2O_2 for 24 hours. The incubations were carried out in 7H9 complete medium with ADS (pH 5.8) at 37 ^{o}C on a 100 rpm rotary shaker in triplicate. Post completion of the H_2O_2 incubation cultures were 10 fold serially diluted and spotted on 7H10 complete medium with OADC and incubated at 37 ^oC until colonies were visible. Each experiment was carried out in triplicate.

Results

POA, not PZA, is an ferrous iron chelator

During the phagosomal oxidative burst hydroxyl radicals are generated from the interaction of H_2O_2 with divalent metals through the Fenton reaction. In the Fenton reaction ferrous iron (Fe^{2+}) is oxidized by H_2O_2 leading to the formation of ferric iron (Fe^{3+}) and a hydroxyl radical. Fe^{2+} is then regenerated through the reduction of Fe^{3+} by H_2O_2. POA has previously been suggested to promote the Fenton reaction though formation of complexes with Fe^{2+} [155]. Isothermal titration calorimetry (ITC) was used to assess the chelating capabilities of PZA and POA. ITC can detect the binding thermodynamics between any two ligands based upon the small temperature change that is associated with endothermic or exothermic interactions. No binding was detected when POA was injected into MES buffer alone indicating there were no interactions between the drug and the buffer (Figure 4-1A). There was also no binding detected when POA was injected into solutions of Fe^{3+} (Figure 4-1B). The injection of POA into solutions of Fe^{2+} demonstrated that POA did indeed bind Fe^{2+} with a K*d* of 230 μM at a stoichiometry of 2:1 (Figure 4-1C). PZA did not bind Fe^{2+}, indicating that Fe^{2+} binding is specific for POA (Figure 4-1D).

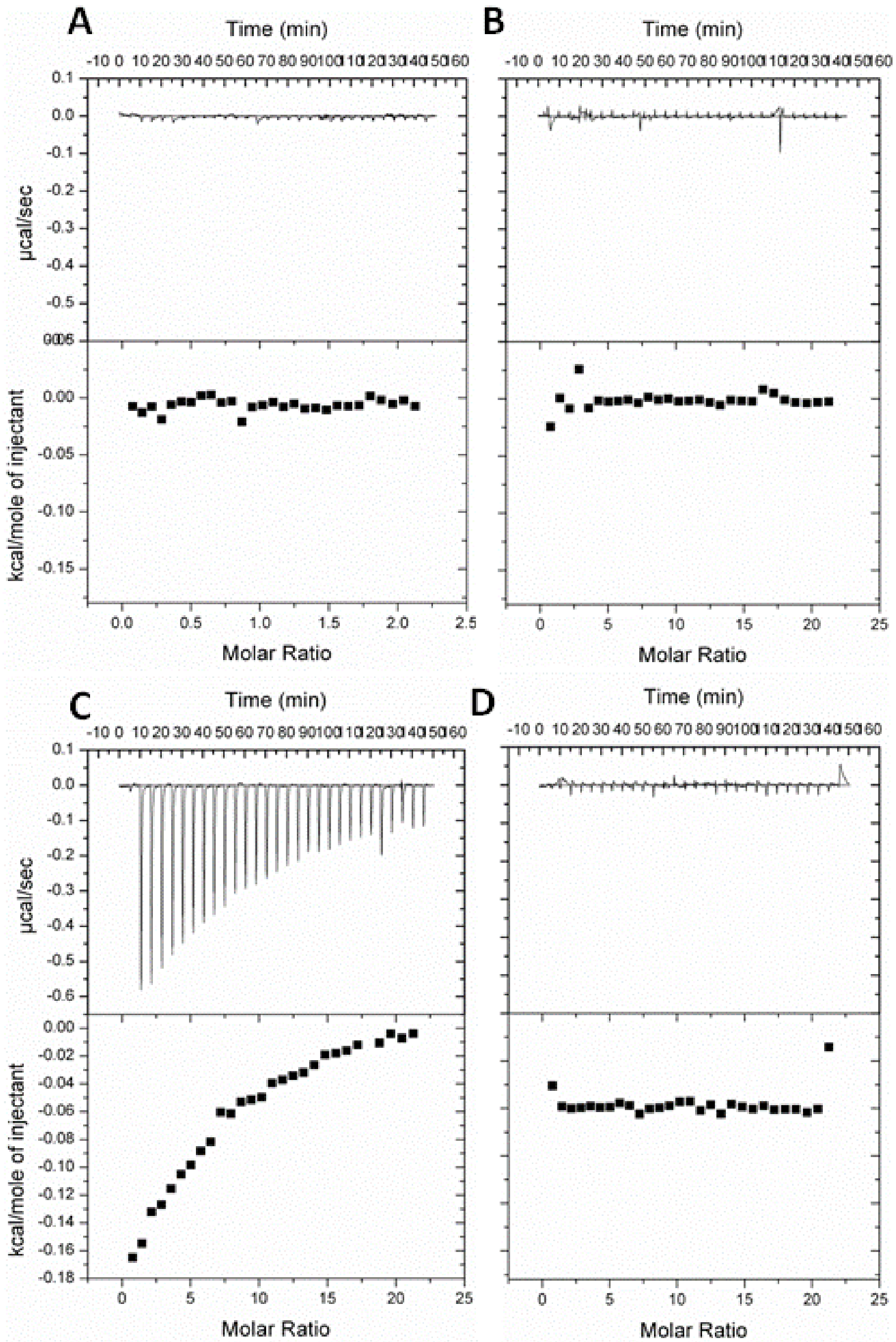

Figure 4-1. POA, and not PZA, interacts with Fe^{2+}. Isothermal titration calorimetry, a technique that measures the change in free energy upon interaction of two ligands, was used to assess binding between iron and POA/PZA . Experiments were carried out in pH 6 MES buffer with 30 injections per experiment. (A) POA and MES buffer. (B) POA and ferric iron. (C) POA and ferrous iron. (D) PZA and ferrous iron.

We next sought to determine if POA could chelate any other metals. Using ITC, we selected an assortment of biologically relevant divalent ions for potential binding partners for POA. POA was found to bind to the following listed by decreasing affinity: Cu^{2+}, Ni^{2+}, Fe^{2+}, Zn^{2+}, and Co^{2+} (Table 4-1). Interestingly, POA did not have any detectable binding to Mg^{2+} or Ca^{2+} nor the divalent transition metal Mn^{2+} (Table 4-1). Together these data indicate that POA is able to bind multiple biologically relevant metals but is not able to bind all divalent ions.

POA accelerates hydroxyl radical production through the Fenton reaction

Having characterized the affinity of POA for various divalent metals, we asked if the presence of POA would alter hydroxyl radical production through the Fenton reaction. We implemented a cell-free assay to measure hydroxyl radical formation using 3-CCA. The rate of hydroxyl radical production was enhanced approximately two-fold due to the addition of POA compared to the POA-free control (Figure 4-2). The inclusion of alternative divalent ions *in lieu* of Fe^{2+} did not reproduce this effect (Table 4-2). In summary, data suggests that POA-ferrous iron complexes enhance the production of hydroxyl radicals from H_2O_2.

POA-iron complexes interact with H_2O_2 to mediate increased oxidative damage to proteins

A POA mediated increase in hydroxyl radical formation would be expected to lead to enhanced cell associated oxidative damage. One such product of cellular oxidative

Table 4-1: Dissociation constants for POA with various divalent metal ions

Metal	K*d** (μM)
Cu^{2+}	46
Ni^{2+}	120
Fe^{2+}	230
Zn^{2+}	250
Co^{2+}	400
Mg^{2+}	ND[a]
Ca^{2+}	ND[a]
Mn^{2+}	ND[a]

*K_d, dissociation constants were determined in MES buffer pH 6.0 by using an VP-ITC isothermal titration microcalorimeter and calculated with MicroCal Origin software.

[a] Not determined, beyond the limit of detection

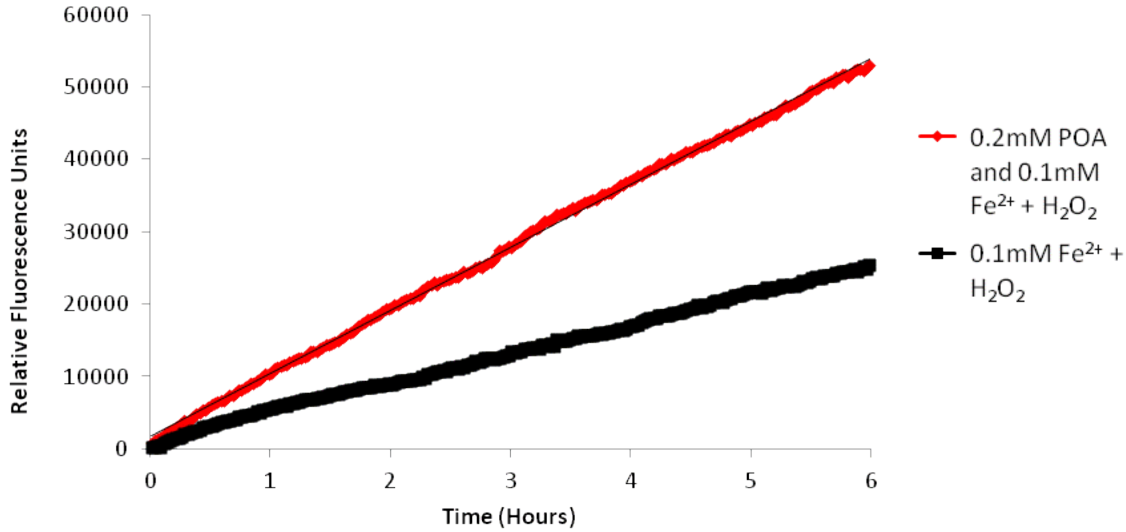

Figure 4-2. POA accelerates the formation of hydroxyl radicals from Fe^{2+} and H_2O_2. Coumarin-3-carboxylic acid was used to measure the rate of hydroxyl radical formation from the addition of POA to Fe^{2+} and H_2O_2. Hydroxyl radicals are quantified via the characteristic emission profile of 7-hydroxycoumarin-3-carboxylic acid.

Table 4-2. The rate of hydroxyl radical formation from hydrogen peroxide is enhanced by complexes of POA and either iron or copper.

Metal	Fold change in rate of hydroxyl radical formation (POA/No POA)	*p*-value
Fe^{2+}	1.75	2.80E-04
Cu^{2+}	1.19	3.38E-07
Ni^{2+}	0.37	4.30E-03
Zn^{2+}	No significant change	
Co^{2+}	No significant change	
Mg^{2+}	No significant change	
Ca^{2+}	No significant change	
Mn^{2+}	No significant change	

damage is protein carbonylation, which occurs when side chains of proteins become carbonylated upon exposure to ROS. Through loss of biochemical function, carbonylated proteins can initiate deleterious events that disrupt essential biological processes in the cell. Carbonyl groups can be derivatized with DNPH and then quantified by measuring the amount of DNPH in a given protein sample spectrophotometrically. Levels of protein carbonylation were used to assess the impact of POA on H_2O_2 associated oxidative damage. Cell-free experiments used bovine serum albumin (BSA) as a source of protein. Within 30 minutes after the addition of H_2O_2 BSA associated carbonylation was increased by approximately 4-fold compared to baseline. The increase of BSA carbonylation was due to the addition of POA in solutions containing iron and H_2O_2 (Figure 4-3A).

In order to measure carbonylation from whole cells, cultures of *M. tuberculosis* H37Ra were treated with PZA prior to H_2O_2 challenge. Cultures were lysed and protein was extracted. Carbonylation was enhanced by the addition of PZA (Figure 4-3B) to the cultures irrespective of exogenous ROS. The combinatorial effect of H_2O_2 and PZA yielded greatly increased carbonylation when compared to any of the single treatment controls (Figure 4-3B).

PZA synergizes with H_2O_2 through a POA dependent mechanism to inhibit *M. tuberculosis*

The host induced oxidative burst is hypothesized to yield high concentrations of ROS over the course of only 25-30 min after phagocytosis of an invading bacterium[158].

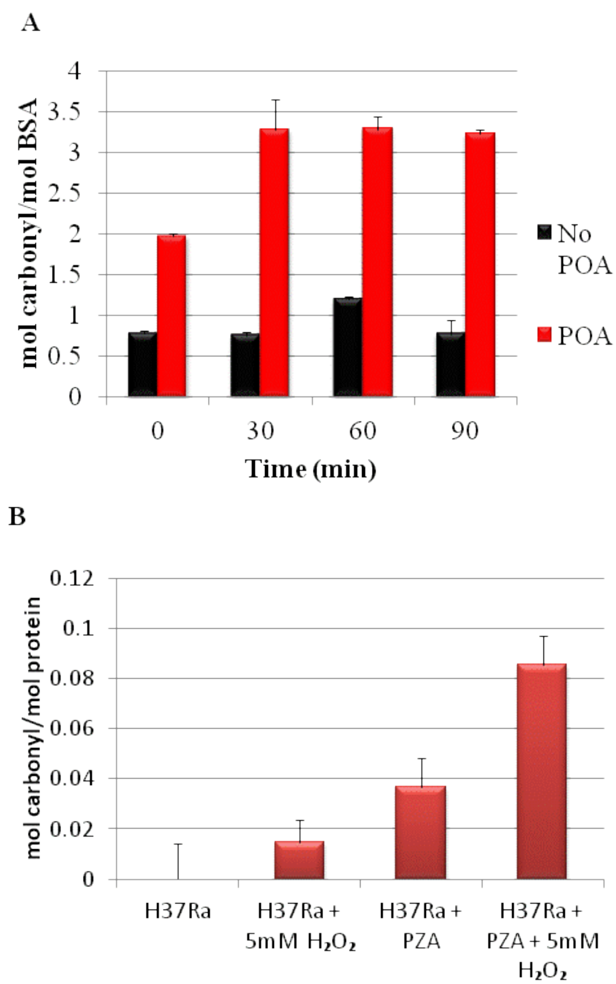

Figure 4-3. Protein associated oxidative damage is enhanced during PZA treatment. Protein carbonylation was measured after exposure to POA in cell free assays using BSA, or PZA treated H37Ra cultures. Carbonyl groups were derivatized with 2,4-dinitrophenylhydrazine and the molar ratio of carbonyl groups to protein was determined. (A) Cell free time course using BSA as a representative protein. (B) PZA treated H37Ra cultures.

While the NADPH oxidase complex produces superoxide, its instability renders H_2O_2 as the dominant antibacterial ROS. Therefore, PZA synergy with host derived ROS is likely due to association with H_2O_2. In order to determine if PZA synergizes with H_2O_2 to kill *M. tuberculosis*, FIC experiments using PZA pretreatment followed by H_2O_2 exposure were conducted in both H37Rv and H37Ra. *M. tuberculosis* strain H37Ra was hyper-susceptible to H_2O_2 post PZA exposure (Figure 4-4A). PZA and H_2O_2 were also synergistic against the fully virulent strain *M. tuberculosis* H37Rv (Figure 4-4B). The FICI, a measure of the degree of synergy between two compounds with synergy being defined as an FICI <0.5[159], was 0.0625 for H37Ra and 0.185 for H37Rv, indicating PZA and H_2O_2 were highly synergistic against both strains. The simultaneous addition of PZA with H_2O_2 yielded reduced the degree of synergy against H37Rv (FICI =0.5) compared to PZA pre-exposure, which demonstrates a necessity for sufficient drug exposure time, likely relating to the need for POA conversion (Figure 4-4C).

Given that the addition of POA was associated with increased oxidative damage and its conversion is strictly required for drug efficacy, we hypothesized that POA rather than PZA was directly involved in synergy with H_2O_2. The *M. bovis* attenuated vaccine strain Bacillus Calmette–Guérin (BCG) was used to examine the requirement for POA for synergy with H_2O_2. Like all *M. bovis* strains, BCG is naturally resistant to PZA due to

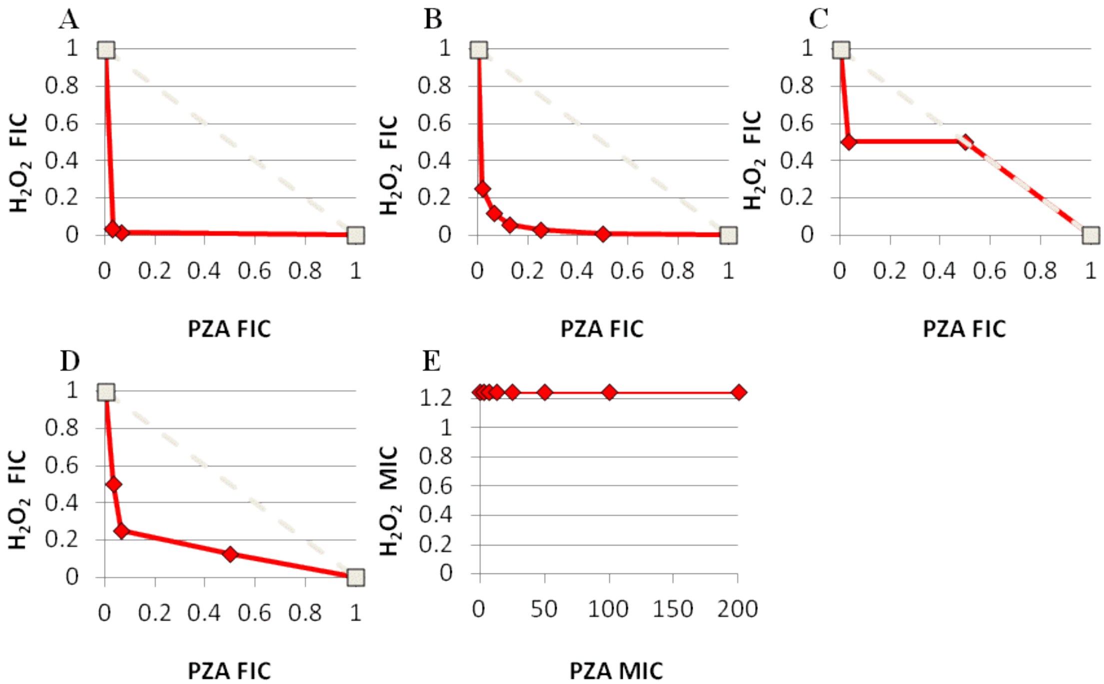

Figure 4-4: PZA treatment synergizes with H_2O_2 through a POA mediated mechanism. FIC plots were generated from the treatment of (A) H37Ra, and (B) H37Rv with PZA 72 hours prior to being challenged with H_2O_2 in pH 5.8 7H9+ADS+Gly+tylox. (C) FIC plot was generated from the treatment of H37Rv with PZA immediately prior to being challenged with H_2O_2 in pH 5.8 7H9+ADS+Gly+tylox. (D) FIC plot was generated from the treatment of BCG-*pncA* with PZA 72 hours prior to being challenged with H_2O_2 in pH 5.8 7H9+ADS+Gly+tylox. (E)) MIC plot was generated from the treatment of BCG with PZA 72 hours prior to being challenged with H_2O_2 in pH 5.8 7H9+ADS+Gly+tylox. A representative of multiple experiments for each condition is shown and the gray dotted line represents the line of additivity.

a loss of function mutation in *pncA*, which encodes the nicotinamidase responsible for converting PZA to POA. Ectopic expression of *pncA* in BCG permits POA conversion promoting PZA susceptibility in this strain [75]. FIC experiments were carried out in wild type BCG and BCG-*pncA* to examine the requirement for POA conversion for synergy with H_2O_2. Similar to H37Ra and H37Rv, PZA synergized with H_2O_2 against BCG-*pncA* strain (FICI =0.3125) (Figure 4-4D). Pre-incubation of wild type BCG with PZA did not alter susceptibility of the bacilli to H_2O_2. These data indicate that POA conversion is required for synergy with H_2O_2 (Figure 4-4E).

PZA treatment synergizes with H_2O_2 to kill *M. tuberculosis*

Despite PZA associated bacterial clearance *in vivo*, concentrations as high as 10X the MIC fail to eliminate *M. tuberculosis* *in vitro* [107]. Therefore, we asked if the bactericidal activity of PZA in the host is due to its synergy with H_2O_2. Using a whole cell experiment, we exposed mid-log phase *M. tuberculosis* cultures to PZA, H_2O_2, and clofazimine and menadione. Both clofazimine and menadione are reported to induce superoxide in *M. tuberculosis* through interacting with mycobacterial respiration[160,161]. H37Ra cultures were either pretreated with PZA (2-4x the MIC) or vehicle control for 3 days, subsequently exposed to varying concentrations of ROS generators for 24 hrs, and plated on 7H10 agar to determine the titer of viable colony forming units. No change in bactericidal activity was observed with the combination of menadione and PZA (Figure

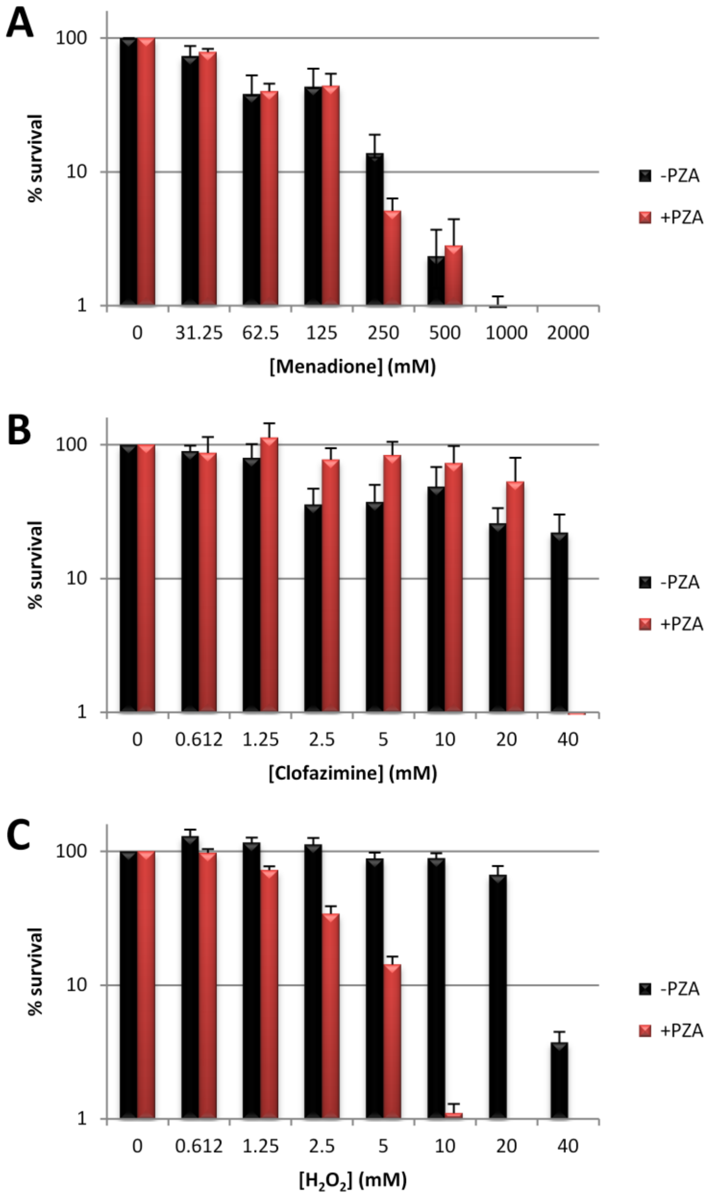

Figure 4-5: PZA synergizes with H_2O_2 to kill *M. tuberculosis*. The %survival of H37Ra was determined for 1.6mM PZA pretreated H37Ra cells after exposure to sources of ROS for 24hours. Cultures were then plated and incubated at $37^{o}C$ for CFU determination. (A) <emadione. (B) Clofazimine. (C) H_2O_2.

4-5A). The addition of clofazimine to PZA treated cells enhanced killing marginally but only at the highest concentration tested (Figure 4-5B). Consistent with our previous results, the bactericidal effect of H_2O_2 was enhanced by approximately 8 fold when the cultures were pretreated with PZA (Figure 4-5C).

Discussion

Our study indicates that the mechanistic basis for PZA activity is through modulation of ROS by complexes formed with metals (Figure 4-6). We show that POA-Fe^{2+} complexes increased hydroxyl radical formation and enhanced cellular oxidative damage. Sub-inhibitory levels of ROS were capable of bactericidial activity against *M. tuberculosis* when combined with PZA. PZA treatment is therefore likely more effective in humans than in mice due to the requirement for a ROS driven immune response.

While POA enhances hydroxyl radical formation, it does not generate H_2O_2. H_2O_2 is produced by early host responses against *M. tuberculosis* within the phagosome. A robust immune system would therefore be required to potentiate POA activity. A dysfunctional or weak host induced oxidative burst would render POA less effective due to the absence of an exogenous H_2O_2 source. This is likely the basis for reduced PZA activity in immune-compromised hosts.

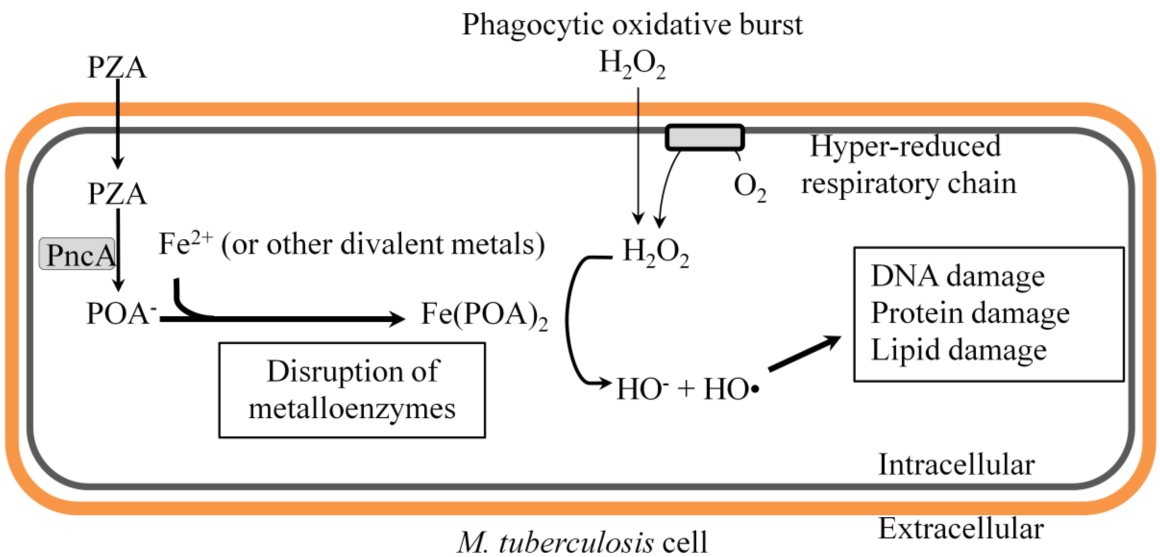

Figure 4-6: Model for PZA modulation of host derived ROS. PZA passively diffuses into the cell and is converted into POA by PncA. POA chelates divalent iron from metalloenzymes, or other sources, and forms complexes of two POA per one ferrous iron. The POA-iron complexes react with host and endogenous derived H_2O_2 to increase hydroxyl radical production leading to increased cellular associated oxidative damage.

A dependence on exogenous ROS may also be the basis for the disparate *in vitro* and *in vivo* activities of PZA. Although PZA fails to sterilize *M. tuberculosis* under standard *in vitro* culture conditions, bacteriostatic activity is observed during concurrent exposure to an acidic pH. Acid shock has previously been linked to enhanced susceptibility to H_2O_2 in *M. tuberculosis* [162]; however, recent evidence indicates that acid pH is dispensabe for POA susceptibility [107]. Thus, the activity of PZA is pH independent. Acid sensitive mutants of *M. tuberculosis* have been associated with increased oxidative stress susceptibility[163] implicating a potential role for acid shock in potentiating PZA rather than a direct role in its mechanism of action.

POA may interact with metabolically derived endogenous ROS in vitro; however, ROS concentration may not be sufficient to synergize with POA. This hypothesis is supported by our observations that PZA treated cells experience heightened oxidative damage in the absence of exogenous H_2O_2. *M. tuberculosis* has previously been characterized as being hypersensitive to perturbations in its endogenous ROS compared to other mycobacteria [164]. It follows that POA mediated increases in endogenous ROS may be the basis for the bacteriostatic activity of the drug *in vitro*.

Although protein carbonylation was used to assess oxidative damage, we expect that an increase in hydroxyl radical formation would impact other bacterial components and processes that are vital to the cell. POA mediated increases in hydroxyl radical production can be anticipated to lead to oxidative damage to lipids and DNA in addition to the observed protein damage. Given the sensitivity *M. tuberculosis* has to compounds targeting the cellular envelope, it is possible that lipid peroxidation may be a key driving force in the observed bactericidal activity of PZA and ROS. Importantly, lipid peroxidation could be the basis for pantothenate mediated antagonism of PZA.

Iron availability may also play a key role in the anti-mycobacterial activity of POA. When compared to the siderophore based iron acquisition systems employed by *M. tuberculosis* with a K_d in the 10^{-49} M range [165] POA is a fairly weak iron chelator with a K_d of 2.3×10^{-5} M. It is therefore unlikely that POA would have any disruptive effect on iron acquisition of *M. tuberculosis* when it is residing in the extracellular environment. However intrabacterially, where *M. tuberculosis* siderophores are absent, POA may be capable of disrupting metal homeostasis and metallo-enzyme function and synthesis. Iron availability likely impacts the hydroxyl radical production potential of POA in the presence of H_2O_2. This is evidenced by the scale difference between our BSA and whole cell carbonylation assays in which exogenous iron was provided or withheld, respectively. Increased *in vitro* iron concentrations have also been previously associated with enhanced PZA activity [166], further linking the abundance of iron to drug activity.

In the continual pursuit of improved anti-mycobacterial therapies, this study suggests a new route for potentiating PZA activity *in vivo* in light of the newly discovered mechanism of action. Such compounds would include those that enhance phagosomal oxidative stress as well as disrupt mycobacterial metal homeostasis. Additionally, targeting the capability of *M. tuberculosis* to manage oxidative stress is expected to enhance PZA treatment. Mutations in the *M. tuberculosis* catalase are the main mycobacterial resistance mechanism to isoniazid; however, these same mutations are expected to render cells susceptible to PZA. This may explain why PZA and isoniazid are complimentary components of short-course therapy.

Based on this study we hypothesize that PZA works synergistically with the host induced oxidative burst to potentiate its activity in vivo. Enhancement of oxidative stress and metal disruption represents a new avenue for rationale anti-TB drug design.

Chapter 5

Conclusions

The work presented in this thesis expands on our understanding of the "black box" that is pyrazinamide (PZA). Although multiple models for the mechanism of action of PZA against *M. tuberculosis* had been previously proposed they lacked sufficient confirmatory evidence. In this thesis we addressed the previously proposed models, and, upon finding them unsupported, we generated a new model based upon our findings. The studies contained within this thesis shed light on some of the mysteries of PZA including: the mycobacterial resistance mechanisms to the drug, the influence of metabolism on the drug's activity, and the reason for the disparate *in vitro* and *in vivo* activities of the drug. This work could have implications for the clinical treatment of tuberculosis (TB) as well as informing future drug discovery efforts.

We assessed the validity of the previously proposed models for PZA activity in Chapter 2. We first addressed the model that proposed POA functioned as a proton ionophore. Previous studies established that overexpression of *pncA* eliminates the acidic requirement for PZA activity[75], however, we expanded on that finding by demonstrating that POA activity against the cell is independent of extracellular pH[107]. Additionally, mycobacterial intracellular pH is not markedly decreased after POA treatment as it is upon exposure to characterized proton ionophores[107]. While the role of an acidic extracellular environment appears to promote POA accumulation[167] the mechanism of action of PZA can be uncoupled from a dependency on pH.

In Chapter 2 we also addressed the model that proposed POA targets the ribosomal rescue mechanism of *trans*-translation. The proponents of this model demonstrated direct binding between POA and RpsA and that mutations in *rpsA* conferred PZA resistance[71]. However, our subsequent study detected no binding between POA and RpsA and drug susceptibility was unaltered in isogenic laboratory strains containing the reported *rpsA* mutations. Additionally, POA was found to have no affect on an *in vitro trans*-translation assay with purified mycobacterial ribosomes. Strain DHMH444, containing the *rpsA* mutation, is fully susceptible to POA *in vitro*[168] and to PZA within a murine model[116] implicating the strains previously characterized reduction in *pncA* expression as the likely cause for its slight PZA resistance[168]. Taken together the data indicates the mechanism of action of PZA/POA is also independent of *trans*-translation.

In chapter 3 we addressed a previously proposed model for the mechanism of action of PZA while also characterizing PZA antagonism by a metabolite of the CoA biosynthesis pathway. We discovered that pantothenate, and some of its metabolic precursors including β-alanine, antagonized the activity of both PZA and POA. β-alanine is synthesized by PanD through the decarboxylation of L-aspartate for the production of pantothenate. Mutations in *panD* had been previously associated with PZA resistance[87] leading to the model that suggested PanD as the molecular target of POA[72]. However, PZA susceptibility was maintained in the pantothenate auxotrophic strain mc^{2}7000 which lacks *panD* indicating the target of the drug is independent of the enzymatic activity of PanD[87]. β-alanine failed to inhibit PZA activity in mc^{2}7000 which also lacks the pantoate β-alanine ligase PanC that is required for the formation of pantothenate, implicating pantothenate or a further downstream metabolite as the important factor for antagonism[87].

In Chapter 3 we demonstrated that multiple metabolic precursors of CoA biosynthesis antagonize PZA suggesting the cofactor may be linked to altering susceptibility to the drug. CoA functions as a ubiquitous cofactor throughout the cell and serves a crucial role in carbon and energy metabolism. CoA production is essential in *M. tuberculosis* and perturbations in its production have previously been targeted for possible therapeutic strategies[169,170]. POA treatment leads to a reduction in pantothenate and CoA level in BCG, an effect ameliorated by the addition of exogenous pantothenate[79]. Additionally, POA resistant strains bearing *panD* mutations do not show a decrease in CoA after drug treatment[79]. Considering *panD* is dispensable for PZA activity then its function in conferring resistance could be through increasing the production of CoA. However, *in lieu* of drug treatment CoA and panthothenate levels in the *panD* mutants are not markedly different than wild type[79]. Perhaps the resistance to POA in these mutants is through the dysregulation of *panD* expression instead of altering the activity of the enzyme. This possible explanation for the observed resistance is supported by the finding that even overexpression of wildtype *panD* confers resistance in an otherwise susceptible strain[72].

In the second portion of Chapter 3 we described the characterization of novel PZA resistance mutations in *M. tuberculosis*. We used a library of transposon mutagenized H37Rv to select for resistance to POA instead of PZA to eliminate the selective advantage of *pncA* mutations. A large resistance library was obtained through this mutagenesis method which required a Tn-seq based approach to map all of the resistance conferring mutations. This analysis identified mutations in intra- and intergenic regions of the genome that had never previously been associated with POA resistance. An assessment of the functional significance of each mutation found the insertions were primarily in genes and intergenic regions associated with cell wall and cell processes, intermediary metabolism and respiration, and conserved hypotheticals.

When ranking the resistance library by relative abundance insertions in *sigE* and in the intergeneic region upstream of *clpC1* map as two of the most frequent insertion locations. *sigE* encodes the extracytoplasmic function family sigma factor E and represents the only transcription factor detected in the selection for POA resistance. *clpC1* encodes an ATP-dependent cytoplasmic protease which is required for SigE activation through its degradation of anti-sigma factor RseA[144,145]. The resistance phenotype associated with a *sigE* disruption was confirmed in an H37Rv Δ*sigE* strain and the near wild type susceptibility to PZA and POA was restored when *sigE* was complemented back in. A majority of the other locations with the highest relative abundance in the library were previously associated with differential expression in a Δ*sigE* mutant[148].

The high relative abundance of mutations associated with activation of SigE and its regulon suggests the induction of the sigma factor may be required for POA activity. The requirement for SigE induction is likely independent of any effect on *pncA* due to the observed resistance to POA in the Δ*sigE* mutant. In *M. tuberculosis* the SigE regulon is induced in response to the extracellular stressors low pH, nutrient limitation, hypoxia, and reactive oxygen species[145]. *M. tuberculosis* is conditionally susceptible to PZA *in* *vitro* through its dependence upon conditions that promote extracytoplasmic stress. The conditions required for *in vitro* PZA activity are: acidic pH[60], nutrient limitation[107], hypoxia[91], and oxidative stress (Chapter 4). The assumption in the field was that PZA required concurrent exogenous stress because the drug was only effective against non-growing cells. We now hypothesize that extracytoplasmic stress is required for the induction of the SigE regulon, which increases susceptibility to PZA through an as-of-yet-unidentified mechanism (Figure 5-1).

PZA is more effective against *M. tuberculosis* in human phagocytes where ROS is the dominant host produced radical than in the RNS dependent response in mice. If PZA enhanced the activity of ROS it could explain the dependence on a functional immune response for the drug's activity. Following up on the observation in industrial chemical synthesis studies that found hydrocarbons can be oxidized by H_2O_2 when in the presence of POA and iron[154] we examined the interaction of PZA with oxidative stress in Chapter 4.

The chemical synthesis studies indicated potential binding between POA and iron, an interaction which was supported via previous studies[155]. Classifying the chelating capabilities of POA using isothermal titration calorimetry demonstrated that POA was able to bind multiple divalent metals including: Cu^{2+}, Ni^{2+}, Fe^{2+}, Zn^{2+}, and Mn^{2+}. While capable of binding Fe^{2+} there was no detectable interaction between POA and Fe^{3+} indicating specificity for divalent iron.

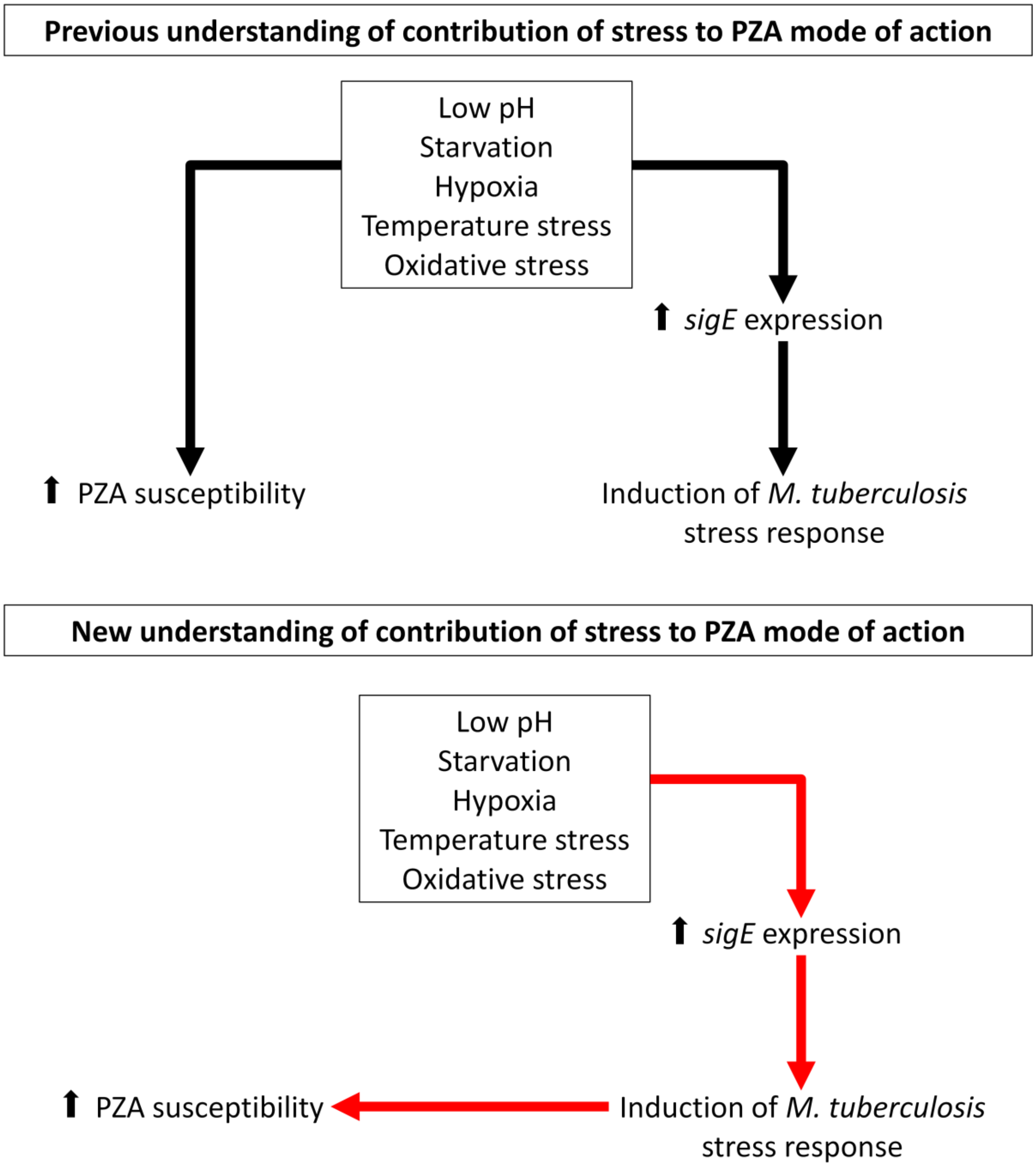

Figure 5-1: Model of stress induction for PZA susceptibility. *M. tuberculosis* requires concurrent exposure to stress for *in vitro* susceptibility to PZA. The stress was assumed to be required to weaken the cell to promote PZA activity. Our data indicates that the stresses required for PZA susceptibility; namely acidic pH, nutrient limitation, hypoxia, temperature, and oxidative stresses, are the same stresses that induce the SigE regulon. We now hypothesize that SigE induction sensitizes *M. tuberculosis* to PZA and that the stresses thought to be required for weakening the cell for PZA activity are instead required for SigE induction.

Unlike POA, PZA was not found to interact with Fe^{2+}. The addition of POA to the reaction between Fe^{2+} and H_2O_2 was found to lead to enhanced inhibitory and killing power against *M. tuberculosis* when compared to the same reaction in the absence of POA. POA-Fe^{2+} complexes in cell free and PZA in whole cell assays were found to significantly increase protein associated oxidative damage in the presence of H_2O_2.

POA-Fe^{2+} complexes synergize with H_2O_2 against *M. tuberculosis* through either impeding the cells capability to manage oxidative stress or by directly altering the production of damaging radicals. Considering the cell free assays with exogenously added BSA indicated enhanced protein carbonylation the later possibility seemed more likely, although a combinatorial effect may occur within whole cells. The synergy between POA and H_2O_2 was thought to occur through an acceleration of the Fenton reaction. In the Fenton reaction Fe^{2+} is oxidized by H_2O_2 which leads to the formation of Fe^{3+} and a hydroxyl radical. $Fe^{2+}$is then regenerated through the reduction of Fe^{3+} by H_2O_2. An assay was implemented to measure the production of hydroxyl radicals from the interaction of Fe^{2+} and H_2O_2. The addition of POA to the ferrous reaction was associated with an approximately 2 fold increase in the production of hydroxyl radicals. The chemical mechanism behind this increase in hydroxyl radical production remains unknown but it may involve the stabilization of the Fe^{2+} ion. We now hypothesize that the host environment is critical for PZA activity *in vivo* due to the drugs enhancement of the host induced oxidative burst.

In addition to enhancing the host induced oxidative burst the host environment may play a role in promoting PZA susceptibility through the induction of the SigE regulon. Many of the same stresses required for *in vitro* PZA susceptibility are also encountered by *M. tuberculosis* in the phagosome. Based upon the requirement for extracytoplasmic stress for *in vitro* susceptibility we hypothesize that *in vivo* activity of PZA would require a robust immune response to induce drug susceptibility. This hypothesis is supported by the observation that PZA activity is diminished in murine models that have a compromised immune response including both Kramnik[149,150] and nude[151] mice. It is not currently clear if all of the phagosomal derived stress is required for inducing PZA susceptibility. Further experiments are required to tease apart the interactions between the different sources of stress and PZA activity within phagocytes.

CoA availability is a unifying theme that resonates with the varied conditions and mutations that are associated with altered PZA susceptibility and efficacy. CoA levels are diminished after PZA treatment in susceptible cells but not in cells that are resistant to the drug. Exogenous pantothenate drives CoA production and circumvents the reduction in CoA that is associated with PZA treatment. Conditions that are associated with lower CoA production, like hypoxia and nutrient limitation, are also associated with increased PZA susceptibility. SigE modulates the expression of phosphoenolpyruvate carboxylase (*pckA*) and pyruvate dehydrogenase (*aceE*) to induce acetyl-CoA production reducing available free CoA. Disruption of SigE should increase available free CoA which could be the basis for PZA resistance in a SigE mutant. Free CoA levels can be furthered depleted through the increase in oxidative radicals that are associated with the interaction of POA with H_2O_2. CoA availability has previously been linked to oxidative stress sensitivity through its role in the synthesis of the antioxidant mycothiol[171]. Pantothenate supplementation drives glutathione production in Eukaryotes, who use glutathione instead of mycothiol, aiding in reducing cellular oxidative damage[172,173]. Increased hydroxyl radical production due to the synergy between POA and H_2O_2 may directly interfere with CoA or it may reduce available CoA through its use in mycothiol synthesis. Loss of CoA availability may push the cell beyond a metabolic point of no return. CoA depletion should occur regardless of the growth phase of the bacteria yet would be expected to be more pronounced in persistent cells that are already operating at a lower metabolic rate which could explain the increased efficacy of PZA against stationary bacilli. We hypothesize that PZA treatment synergizes with oxidative stress to reduce the levels of free CoA (Figure 5-2).

More experiments are required to fully elucidate the impact PZA treatment may have on CoA production and SigE expression. Conditions that promote PZA resistance, pantothenate based antagonism and the various metabolic interactions indicated by the Tn-seq, may also impact SigE expression. If SigE expression increases susceptibility to PZA then a *sigE* overexpression mutant may become susceptible to PZA at conditions where the drug is usually ineffective, like neutral pH, further supporting the SigE model. The interplay between SigE expression and the increased oxidative stress observation can be elucidated by conducting PZA and H_2O_2 FICs in the *sigE* mutant strains and in the Tn resistant strains. The importance of ROS for PZA action *in vivo* can be determined by administering PZA to *M. tuberculosis* infected NADPH oxidase mutant mice. The model

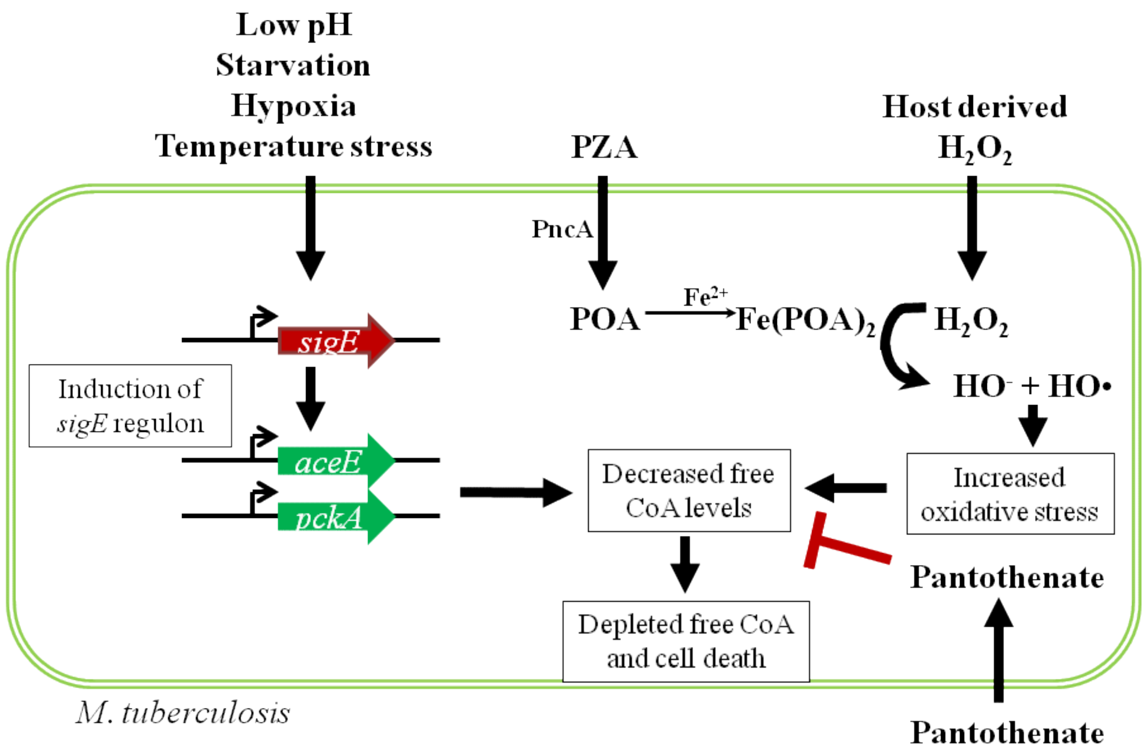

Figure 5-2: Model for PZA mechanism of action. Increased hydroxyl radical production from the interaction of POA-iron with H_2O_2 leads to a reduction in the levels of CoA. The induction of the SigE regulon also decreases free CoA through its utilization in central metabolism. Depletion of free CoA causes a metabolic point of no return inducing cellular death in *M. tuberculosis*. Pantothenate supplementation antagonizes PZA through increasing the production of CoA.

predicts that PZA action would be abolished in mice incapable of generating the host induced oxidative burst.

In conclusion, we have uncovered multiple clues into the mechanism of action of PZA. Our current working model predicts PZA decreases mycobacterial CoA through increasing intracellular oxidative stress. This model explains the disparate *in vivo* and *in vitro* susceptibilities of PZA and why the drug is more effective against cells that are not actively replicating. In addition, based on the Tn insertion mutants we found we can predict what the identity of the remaining clinical PZA resistance strains are, potentially increasing the capability to genetically determine PZA susceptibility in the clinic. This study can guide future drug discovery efforts in creating compounds that can maintain the same mechanism of action as PZA but can circumvent the established resistance mechanisms.

Bibliography

1. Floyd, K. Global tuberculosis report 2016. *WHO Rep.* (2016).
2. Barkan, D., Hedhli, D., Yan, H. G., Huygen, K. & Glickman, M. S. *Mycobacterium tuberculosis* lacking all mycolic acid cyclopropanation is viable but highly attenuated and hyperinflammatory in mice. *Infect. Immun.* **80,** 1958–1968 (2012).
3. Stahl, D. A. & Urbance, J. W. The division between fast- and slow-growing species corresponds to natural relationships among the mycobacteria. *J. Bacteriol.* **172,** 116–124 (1990).
4. Saini, D. *et al.* Ultra-low dose of *Mycobacterium tuberculosis* aerosol creates partial infection in mice. *Tuberculosis* **92,** 160–165 (2013).
5. Lillebaek, T., Dirksen, A., Baess, I., Strunge, B. & Thomsen, V. Ø. Molecular Evidence of Endogenous Reactivation of *Mycobacterium tuberculosis* after 33 Years of Latent Infection. *J. Infect. Dis.* 401–404 (2002).
6. Peter A. Selwyn, M.D., M.P.H., Diana Hartel, M.P.H., Victor A. Lewis, M.D., Ellie E. Schoenbaum, M.D., Sten H. Vermund, M.D., Robert S. Klein, M.D., Angela T. Walker, M.D., and Gerald H. Friedland, M. D. A prospective study of the risk of tuberculosis among intravenous drug users with human immunodeficiency virus infection. *N. Engl. J. Med.* **314,** 745–748 (1986).
7. Coscolla, M. *et al.* Novel *Mycobacterium tuberculosis* complex isolate from a wild chimpanzee. *Emerg. Infect. Dis.* **19,** 969–976 (2013).

8. de Jong, B. C. *et al.* Progression to active tuberculosis, but not transmission, varies by *Mycobacterium tuberculosis* lineage in The Gambia. *J. Infect. Dis.* **198,** 1037–43 (2008).

9. de Jong, Bouke C; Hill, Philip C; Brookes, Roger H; Otu, Jacob K; Peterson, Kevin L; Small, Peter M; Adegbola, R. A. *Mycobacterium africanum*: a new opportunistic pathogen in HIV infection? *Aids* 1714–1715 (2005).

10. Stead, W. W. *et al.* When did *Mycobacterium tuberculosis* infection first occur in the new world? An important question with public health implications. *Am. J. Respir. Crit. Care Med.* **151,** 1267–1268 (1995).

11. Sreevatsan, S. *et al.* Restricted structural gene polymorphism in the *Mycobacterium tuberculosis* complex indicates evolutionarily recent global dissemination. *Proc. Natl. Acad. Sci. U. S. A.* **94,** 9869–9874 (1997).

12. Brosch, R. *et al.* A new evolutionary scenario for the *Mycobacterium tuberculosis* complex. *Proc. Natl. Acad. Sci.* **99,** 3684–3689 (2002).

13. Ravenel, M. P. Tuberculosis of bovine origin. *Am. J. Public Health* **23,** 316–318 (1933).

14. LoBue, P. A., Betacourt, W., Peter, C. & Mosert, K. S. Epidemiology of *Mycobacterium bovis* disease in San Diego County, 1994-2000. *Int. J. Tuberc. Lung Dis.* **7,** 180–185 (2003).

15. Evans, J. T. *et al.* Cluster of human tuberculosis caused by *Mycobacterium bovis*: evidence for person-to-person transmission in the UK. *Lancet* **369,** 1270–1276 (2007).

16. MacGurn, J. a & Cox, J. S. A genetic screen for *Mycobacterium tuberculosis* mutants defective for phagosome maturation arrest identifies components of the ESX-1 secretion system. *Infect. Immun.* **75,** 2668–78 (2007).

17. Crowle, A. J., Dahl, R., Ross, E. & May, M. H. Evidence that vesicles containing living, virulent *Mycobacterium tuberculosis* or *Mycobacterium avium* in cultured human macrophages are not acidic. *Infect. Immun.* **59,** 1823–1831 (1991).

18. Wallgren, A. The time-table of tuberculosis. *Tubercle* **29,** 245–251 (1948).

19. Wolf, A. J. *et al.* Initiation of the adaptive immune response to *Mycobacterium tuberculosis* depends on antigen production in the local lymph node, not the lungs. *J. Exp. Med.* **205,** 105–15 (2008).

20. Fulton, S. a *et al.* Inhibition of major histocompatibility complex II expression and antigen processing in murine alveolar macrophages by *Mycobacterium bovis* BCG and the 19-kilodalton mycobacterial lipoprotein. *Infect. Immun.* **72,** 2101–2110 (2004).

21. Chackerian, A. a, Alt, J. M., Perera, T. V, Dascher, C. C. & Behar, S. M. Dissemination of *Mycobacterium tuberculosis* is influenced by host factors and precedes the initiation of t-cell immunity. *Infect. Immun.* **70,** 4501–4509 (2002).

22. Blomgran, R. & Ernst, J. D. Lung neutrophils facilitate activation of naive antigen-specific CD4+ T cells during *Mycobacterium tuberculosis* infection. *J. Immunol.* **186,** 7110–9 (2011).

23. Fremond, C. M. *et al.* IL-1 receptor-mediated signal is an essential component of MyD88-dependent innate response to *Mycobacterium tuberculosis* infection. *J.*

Immunol. **179,** 1178–89 (2007).

24. Nathan, B. Y. C. F., Murray, H. W., Wlebe, I. E. & Rubin, B. Y. Identification of interferon-gamma as the lymphokine that activates human macrophage oxidative metabolism and antimicrobial activity. *J. Exp. Med.* **158,** 670–689 (1983).

25. Lee, S. C., Dickson, D. W., Liu, W. & Brosnan, C. F. Induction of nitric oxide synthase activity in human astrocytes by interleukin-1β and interferon-γ. *J. Neuroimmunol.* **46,** 19–24 (1993).

26. Yazdanpanah, B. *et al.* Riboflavin kinase couples TNF receptor 1 to NADPH oxidase. *Nature* **460,** 1159–1163 (2009).

27. Kusner, B. D. J., Hall, C. E. & Schlesinger, L. S. Killing of virulent *Mycobacterium tuberculosis* by reactive nitrogen intermediates produced by activated murine macrophages. *J. Exp. Med.* **184,** 1111–1122 (1996).

28. Cooper, B. A. M. *et al.* Disseminated tuberculosis in interferon-γ gene-disrupted mice. *J. Exp. Med.* **178,** 2243–2247 (1993).

29. Flynn, J. L. *et al.* An essential role for interferon γ in resistance to *Mycobacterium tuberculosis* infection. *J. Exp. Med.* **178,** 2249–2254 (1993).

30. Flynn, J. L. *et al.* Tumor necrosis factor-α is required in the protective immune response against *Mycobacterium tuberculosis* in mice. *Immunity* **2,** 561–572 (1995).

31. Gonzalez-juarrero, M. *et al.* Temporal and Spatial Arrangement of Lymphocytes within Lung Granulomas Induced by Aerosol Infection with *Mycobacterium tuberculosis* Temporal and Spatial Arrangement of Lymphocytes within Lung

Granulomas Induced by Aerosol Infection with Mycobacteri. *Infect. Immun.* **69,** 1722–1728 (2001).

32. Fayyazi, A. *et al.* Apoptosis of macrophages and T cells in tuberculosis associated caseous necrosis. *J. Pathol.* **191,** 417–425 (2000).

33. Swaim, L. E. *et al. Mycobacterium marinum* infection of adult zebrafish causes caseating granulomatous tuberculosis and is moderated by adaptive immunity. *Infect. Immun.* **74,** 6108–6117 (2006).

34. Kwan, C. & Ernst, J. D. HIV and tuberculosis: A deadly human syndemic. *Clin. Microbiol. Rev.* **24,** 351–376 (2011).

35. MacMicking, J. D. *et al.* Identification of nitric oxide synthase as a protective locus against tuberculosis. *Proc. Natl. Acad. Sci. U. S. A.* **94,** 5243–8 (1997).

36. Mayer, B. & Hemmens, B. Biosynthesis and action of nitric oxide in mammalian cells. *Trends Biochem. Sci.* **22,** 477–481 (1997).

37. Kuo, H. P. *et al.* Nitric oxide modulates interleukin-1beta and tumor necrosis factor-alpha synthesis by alveolar macrophages in pulmonary tuberculosis. *Am J Respir Crit Care Med* **161,** 192–199 (2000).

38. Aston, C., Rom, W. N., Talbot, A. T. & Reibman, J. Early Inhibition of Mycobacterial Growth by Human Alveolar Macrophages is not Due to Nitric Oxide. *Am. J. Respir. Crit. Care Med.* **157,** 1943–1950 (1998).

39. Bustamante, J. *et al.* BCG-osis and tuberculosis in a child with chronic granulomatous disease. *J. Allergy Clin. Immunol.* **120,** 32–38 (2007).

40. Lee, P. P. W. *et al.* Susceptibility to Mycobacterial Infections in Children With X-

Linked Chronic Granulomatous Disease. *Pediatr. Infect. Dis. J.* **27,** 224–230 (2008).

41. Cooper, A. M. *et al.* Transient Loss of Resistance to Pulmonary Tuberculosis in p47 phox − / − Mice. *Infect. Immun.* **68,** 1231–1234 (2000).

42. Ng, V. H., Cox, J. S., Sousa, A. O., MacMicking, J. D. & McKinney, J. D. Role of KatG catalase-peroxidase in mycobacterial pathogenesis: countering the phagocyte oxidative burst. *Mol. Microbiol.* **52,** 1291–302 (2004).

43. British Medical Research Council. Controlled clinical trial for four short-course (6-month) regimens of chemotherapy for treatment of pulmonary tuberculosis: Third Report. *Lancet* 237–240 (1974).

44. East African/British Medical Research Councils. Controlled clinical trial of four short-course (6-month) regimens of chemotherapy for treatment of pulmonary tuberculosis. Second report. *Lancet* **301,** 1331–1338 (1973).

45. Rozwarski, D. A. *et al.* Modification of the NADH of the isoniazid target (InhA) from *Mycobacterium tuberculosis*. *Science* **279,** 98–102 (2016).

46. Telenti, A. *et al.* The emb operon, a gene cluster of *Mycobacterium tuberculosis* involved in resistance to ethambutol. *Nat. Med.* **3,** 567–70 (1997).

47. Frontali, L., Leoni, L. & Giorgio, T. Action of rifamycin on incorporation of amino-acids into protein in cell-free systems from *B. subtilis*. *Nature* **203,** 84–85 (1964).

48. Udwadia, Z. F., Amale, R. A., Ajbani, K. K. & Rodrigues, C. Totally Drug-Resistant Tuberculosis in India. *Clin. Infect. Dis.* **54,** 579–581 (2006).

49. Velayati, A. A. *et al.* Emergence of new forms of totally drug-resistant tuberculosis bacilli: super extensively drug-resistant tuberculosis or totally drug-resistant strains in iran. *Chest* **136,** 420–5 (2009).

50. Iseman, M. D. Tuberculosis therapy: past, present and future. *Eur. Respir. J.* **20,** 87S–94s (2002).

51. Tiemersma, E. W., van der Werf, M. J., Borgdorff, M. W., Williams, B. G. & Nagelkerke, N. J. D. Natural history of tuberculosis: Duration and fatality of untreated pulmonary tuberculosis in HIV negative patients: A systematic review. *PLoS One* **6,** (2011).

52. Floyd, K. Global Tuberculosis Report 2012. *WHO Rep.* 1–100 (2012).

53. Murray, M. F. Nicotinamide: an oral antimicrobial agent with activity against both *Mycobacterium tuberculosis* and human immunodeficiency virus. *Clin. Infect. Dis.* **36,** 453–60 (2003).

54. Schatz, a., Bugle, E. & Waksman, S. a. Streptomycin, a Substance Exhibiting Antibiotic Activity Against Gram-Positive and Gram-Negative Bacteria.* . *Exp. Biol. Med.* **55,** 66–69 (1944).

55. BERNSTEIN, J.; LOTT, W. A.; STEINBERG, B. A.; YALE, H. L. Chemotherapy of experimental tuberculosis. V. Isonicotinic acid hydrazide (Nydrazid) and related compounds. *Am. Rev. Tuberc. Pulm. Dis.* **65,** 357–364 (1952).

56. Malone L, Schurr A, Lindh H, McKenzie D, Kiser JS, W. J. The effect of pyrazinamide (aldinamide) on experimental tuberculosis in mice. *Am. Rev. Tuberc.* **65,** 511–518 (1952).

57. Dessau, F., Yeager, R., Burger, F. & Williams, J. Pyrazinamide (aldinamide) in experimental tuberculosis of the guinea pig. *Am. Rev. Tuberc.* **65,** 519–522 (1952).

58. Solotorovsky, M. *et al.* Pyrazinoic acid amide-an agent active against experimental murine tuberculosis. *Exp. Biol. Med.* **79,** 563–565 (1952).

59. Yeager, R. L., Munroe, W. G. C. & Dessau, F. I. Pyrazinamide (aldinamide) in the treatment of pulmonary tuberculosis. *Am. Rev. Tuberc.* **65,** 523–546 (1952).

60. McDermott W, T. R. Activation of pyrazinamide and nicotinamide in acidic environments in vitro. *Am. Rev. Tuberc.* **70,** 748–754 (1954).

61. Scorpio, A. & Zhang, Y. Mutations in pncA, a gene encoding pyrazinamidase/nicotinamidase, cause resistance to the antituberculous drug pyrazinamide in tubercle bacillus. *Nat. Med.* **2,** 662–667 (1996).

62. Stoffels, K., Mathys, V., Fauville-Dufaux, M., Wintjens, R. & Bifania, P. Systematic analysis of pyrazinamide-resistant spontaneous mutants and clinical isolates of *Mycobacterium tuberculosis*. *Antimicrob. Agents Chemother.* **56,** 5186–5193 (2012).

63. Konno K, Feldmann FM, M. W. Pyrazinamide susceptibility and amidase activity of tubercle bacilli. *Am Rev Respir Dis.* **95,** 461–469 (1967).

64. Begley, T. P., Kinsland, C., Mehl, R. A., Osterman, A. & Dorrestein, P. The biosynthesis of nicotinamide adenine dinucleotides in bacteria. *Vitam. Horm.* **61,** 103–19 (2001).

65. Boshoff, H. I. M. *et al.* Biosynthesis and recycling of nicotinamide cofactors in *Mycobacterium tuberculosis*. An essential role for NAD in nonreplicating bacilli.

J. Biol. Chem. **283,** 19329–41 (2008).

66. Zhang, S. *et al.* Mutations in *panD* encoding aspartate decarboxylase are associated with pyrazinamide resistance in *Mycobacterium tuberculosis*. *Emerg. Microbes Infect.* **2,** e34 (2013).

67. Gu, Y. *et al.* Pyrazinamide resistance among multidrug-resistant tuberculosis clinical isolates in a national referral center of China and its correlations with pncA, rpsA, and panD gene mutations. *Diagn. Microbiol. Infect. Dis.* **84,** 207–211 (2016).

68. Zimhony, O., Cox, J. S., Welch, J. T., Vilchèze, C. & Jacobs, W. R. Pyrazinamide inhibits the eukaryotic-like fatty acid synthetase I (FASI) of *Mycobacterium tuberculosis*. *Nat. Med.* **6,** 1043–7 (2000).

69. Zhang, Y., Zhang, H. & Sun, Z. Susceptibility of *Mycobacterium tuberculosis* to weak acids. *J. Antimicrob. Chemother.* **52,** 56–60 (2003).

70. Zhang, Y. & Mitchison, D. The curious characteristics of pyrazinamide: a review. *Int. J. Tuberc. Lung Dis.* **7,** 6–21 (2003).

71. Shi, W. *et al.* Pyrazinamide inhibits trans-translation in *Mycobacterium tuberculosis*. *Science* **333,** 1630–2 (2011).

72. Shi, W. *et al.* Aspartate decarboxylase (PanD) as a new target of pyrazinamide in *Mycobacterium tuberculosis*. *Emerg. Microbes Infect.* **3,** e58 (2014).

73. Boshoff, H. I., Mizrahi, V. & III, C. E. B. Effects of Pyrazinamide on Fatty Acid Synthesis by Whole Mycobacterial Cells and Purified Fatty Acid Synthase I. *J. Bacteriol.* **184,** 2167–2172 (2002).

74. Ngo, S. C. *et al.* Inhibition of isolated *Mycobacterium tuberculosis* fatty acid synthase I by pyrazinamide analogs. *Antimicrob. Agents Chemother.* **51,** 2430–5 (2007).

75. Baughn, A. D. *et al.* Mutually exclusive genotypes for pyrazinamide and 5-chloropyrazinamide resistance reveal a potential resistance-proofing strategy. *Antimicrob. Agents Chemother.* **54,** 5323–8 (2010).

76. McDermott, W. & Tompsett, R. Activation of pyrazinamide and nicotinamide in acid environments in vitro. *Am. Rev. Tuberc.* **70,** 748–754 (1954).

77. Zhang, Y., Wade, M. M., Scorpio, A., Zhang, H. & Sun, Z. Mode of action of pyrazinamide: disruption of *Mycobacterium tuberculosis* membrane transport and energetics by pyrazinoic acid. *J. Antimicrob. Chemother.* **52,** 790–5 (2003).

78. Lu, P. *et al.* Pyrazinoic acid decreases the proton motive force, respiratory ATP synthesis activity, and cellular ATP levels. *Antimicrob. Agents Chemother.* **55,** 5354–7 (2011).

79. Gopal, P. *et al.* Pyrazinamide Resistance Is Caused by Two Distinct Mechanisms: Prevention of Coenzyme A Depletion and Loss of Virulence Factor Synthesis. *ACS Infect. Dis.* A-K (2016). doi:10.1021/acsinfecdis.6b00070

80. Zhang, Y., Scorpio, A., Nikaido, H. & Sun, Z. Role of acid pH and deficient efflux of pyrazinoic acid in unique susceptibility of *Mycobacterium tuberculosis* to pyrazinamide. *J. Bacteriol.* **181,** 2044–9 (1999).

81. Zhang, Y., Permar, S. & Sun, Z. Conditions that may affect the results of susceptibility testing of *Mycobacterium tuberculosis* to pyrazinamide. *J. Med.*

Microbiol. **51,** 42–9 (2002).

82. Somner, A. & Angel, J. A controlled trial of six months chemotherapy in pulmonary tuberculosis: first report: results during chemotherapy. *Br. J. Dis. Chest* **75,** 141–153 (1981).

83. Floyd, K. Global Tuberculosis report 2014. *WHO Rep.* (2014).

84. Angelo Scorpio & Ying Zhang. Mutations in *pncA*, a gene encoding pyrazinamidase/nicotinamidase, cause resistance to the antituberculous drug pyrazinamide in tubercle bacillus. *Nat. Med.* **2,** 662–667 (1996).

85. Vilchèze, C., Weinrick, B., Wong, K. W., Chen, B. & Jacobs, W. NAD+ auxotrophy is bacteriocidal for the tubercle bacilli. *Mol. Microbiol.* **76,** 365–377 (2010).

86. Zhang, Y., Shi, W., Zhang, W. & Mitchison, D. Mechanisms of Pyrazinamide Action and Resistance. *Microbiol Spectr* **2,** 1–12 (2013).

87. Dillon, N. A., Peterson, N. D., Rosen, B. C. & Baughn, A. D. Pantothenate and pantetheine antagonize the antitubercular activity of pyrazinamide. *Antimicrob. Agents Chemother.* **58,** 7258–63 (2014).

88. Tarshis, M. & Weed, W. Lack of significant in vitro sensitivity of *Mycobacterium tuberculosis* to pyrazinamide on three dif- ferent solid media. *Am. Rev. Tuberc.* **67,** 391–395 (1953).

89. McDermott, W. & Tompsett, R. Activation of pyrazinamide and nicotinamide in acid environments in vitro. *Am. Rev. Tuberc.* **70,** 748–754 (1954).

90. Huang, Q. *et al.* Nutrient-Starved Incubation Conditions Enhance Pyrazinamide

Activity against *Mycobacterium tuberculosis*. *Chemotherapy* **53,** 338–343 (2007).

91. Wade, M. M. Anaerobic incubation conditions enhance pyrazinamide activity against *Mycobacterium tuberculosis*. *J. Med. Microbiol.* **53,** 769–773 (2004).

92. Miotto, P., Cirillo, D. M. & Migliori, G. B. Drug resistance in *Mycobacterium tuberculosis*: Molecular mechanisms challenging fluoroquinolones and pyrazinamide effectiveness. *Chest* **147,** 1135–1143 (2015).

93. Heifets, L. Susceptibility testing of *Mycobacterium tuberculosis* to pyrazinamide. *J. Med. Microbiol.* **51,** 11–12 (2002).

94. Vandal, O. H., Pierini, L. M., Schnappinger, D., Nathan, C. F. & Ehrt, S. A membrane protein preserves intrabacterial pH in intraphagosomal *Mycobacterium tuberculosis*. *Nat. Med.* **14,** 849–854 (2009).

95. Eoh, H. & Rhee, K. Y. Multifunctional essentiality of succinate metabolism in adaptation to hypoxia in *Mycobacterium tuberculosis*. *Proc. Natl. Acad. Sci. U. S. A.* **110,** 6554–9 (2013).

96. Ehrt, S. *et al.* Controlling gene expression in mycobacteria with anhydrotetracycline and Tet repressor. *Nucleic Acids Res.* **33,** e21 (2005).

97. Boshoff, H. I. M. & Mizrahi, V. Expression of *Mycobacterium smegmatis* pyrazinamidase in mycobacterium tuberculosis confers hypersensitivity to pyrazinamide and related amides. *J. Bacteriol.* **182,** 5479–5485 (2000).

98. Miesenböck, G., De Angelis, D. a & Rothman, J. E. Visualizing secretion and synaptic transmission with pH-sensitive green fluorescent proteins. *Nature* **394,** 192–5 (1998).

99. Kasianowicz, J., Benz, R. & McLaughlin, S. The kinetic mechanism by which CCCP (carbonyl cyanide m-Chlorophenylhydrazone) transports protons across membranes. *J. Membr. Biol.* **82,** 179–190 (1984).

100. Huczyński, A., Janczak, J., Łowicki, D. & Brzezinski, B. Monensin a acid complexes as a model of electrogenic transport of sodium cation. *Biochim. Biophys. Acta - Biomembr.* **1818,** 2108–2119 (2012).

101. Russell, J. B. Resistance of Streptococcus bovis to acetic acid at low pH : relationship between Resistance of *Streptococcus bovis* to Acetic Acid at Low pH : Relationship between Intracellular pH and Anion Accumulation. **57,** 255–259 (1991).

102. Lee, J. S. *et al.* Mutation in the Transcriptional Regulator PhoP Contributes to Avirulence of *Mycobacterium tuberculosis* H37Ra Strain. *Cell Host Microbe* **3,** 97–103 (2008).

103. Badalà, F., Nouri-mahdavi, K. & Raoof, D. A. Slow growth of *Mycobacterium tuberculosis* at acidic pH is regulated by phoPR and host-associated carbon sources. *Mol Microbiol* **84,** 56–69 (2014).

104. Darby, C. M. *et al.* Whole cell screen for inhibitors of pH homeostasis in *Mycobacterium tuberculosis*. *PLoS One* **8,** e68942 (2013).

105. East African/British Medical Research Councils. Controlled Clinical Trial of Four Short-Course (6-month) Regimens of Chemotherapy for Treatment of Pulmonary Tuberculosis. *Lancet* 237–240 (1974).

106. Stoffels, K., Mathys, V., Fauville-Dufaux, M., Wintjens, R. & Bifani, P.

Systematic analysis of pyrazinamide-resistant spontaneous mutants and clinical isolates of *Mycobacterium tuberculosis*. *Antimicrob. Agents Chemother.* **56,** 5186–5193 (2012).

107. Peterson, N. D., Rosen, B. C., Dillon, N. a. & Baughn, A. D. Uncoupling environmental pH and intrabacterial acidification from pyrazinamide susceptibility in *Mycobacterium tuberculosis*. *Antimicrob. Agents Chemother.* AAC.00967-15 (2015). doi:10.1128/AAC.00967-15

108. Via, L. E. *et al.* Host-Mediated Bioactivation of Pyrazinamide: Implications for Efficacy, Resistance, and Therapeutic Alternatives. *ACS Infect. Dis.* 150323101837007 (2015). doi:10.1021/id500028m

109. Keiler, K. C. & Feaga, H. A. Resolving nonstop translation complexes is a matter of life or death. *J. Bacteriol.* **196,** 2123–2130 (2014).

110. Luidalepp, H., Hallier, M. & Felden, B. tmRNA Decreases the bactericidal activity of aminoglycosides and the susceptibility to inhibitors of cell wall synthesis. *RNA Biol.* **2,** 70–74 (2005).

111. Thibonnier, M., Thiberge, J.-M. & De Reuse, H. Trans-translation in *Helicobacter pylori*: essentiality of ribosome rescue and requirement of protein tagging for stress resistance and competence. *PLoS One* **3,** e3810 (2008).

112. Svetlanov, A., Puri, N., Mena, P., Koller, A. & Karzai, a W. *Francisella tularensis* tmRNA system mutants are vulnerable to stress, avirulent in mice, and provide effective immune protection. *Mol. Microbiol.* **85,** 122–41 (2012).

113. McGinness, K. E. & Sauer, R. T. Ribosomal protein S1 binds mRNA and tmRNA

similarly but plays distinct roles in translation of these molecules. *Proc. Natl. Acad. Sci. U. S. A.* **101,** 13454–9 (2004).

114. Takada, K. *et al. Thermus thermophilus* tmRNA and trans-translation. *Nucleic Acids Symp. Ser. (Oxf).* 369–70 (2007). doi:10.1093/nass/nrm185

115. Qi, H., Shimizu, Y. & Ueda, T. Ribosomal protein S1 is not essential for the trans-translation machinery. *J. Mol. Biol.* **368,** 845–52 (2007).

116. Klemens, S. P., Sharpe, C. A. & Cynamon, M. H. Activity of pyrazinamide in a murine model against *Mycobacterium tuberculosis* isolates with various levels of in vitro susceptibility. **40,** (1996).

117. Speirs, R. J., Welch, J. T. & Cynamon, M. H. Activity of n-propyl pyrazinoate against pyrazinamide-resistant *Mycobacterium tuberculosis* : investigations into mechanism of action of and mechanism of resistance to Activity of n -Propyl Pyrazinoate against Pyrazinamide-Resistant Mycobacterium tu. *Antimicrob. Agents Chemother.* **39,** 6–9 (1995).

118. Personne, Y. & Parish, T. *Mycobacterium tuberculosis* possesses an unusual tmRNA rescue system. *Tuberculosis (Edinb).* **94,** 34–42 (2014).

119. Ramadoss, N. S. *et al.* Small molecule inhibitors of trans-translation have broad-spectrum antibiotic activity. *Proc. Natl. Acad. Sci. U. S. A.* **110,** 10282–7 (2013).

120. Vilchèze, C. *et al.* Transfer of a point mutation in *Mycobacterium tuberculosis inhA* resolves the target of isoniazid. *Nat. Med.* **12,** 1027–1029 (2006).

121. Qu, X., Lancaster, L., Noller, H. F., Bustamante, C. & Tinoco, I. Ribosomal protein S1 unwinds double-stranded RNA in multiple steps. *PNAS* 1–6 (2012).

doi:10.1073/pnas.1208950109/-/DCSupplemental.www.pnas.org/cgi/doi/10.1073/pnas.1208950109

122. Draper, D. E. & von Hippel, P. H. Nucleic acid binding properties of *Escherichia coli* ribosomal protein S1. I. Structure and interactions of binding site I. *J. Mol. Biol.* **122,** 321–38 (1978).

123. Kalapos, M. P., Paulus, H. & Sarkar, N. Identification of ribosomal protein S1 as a poly(A) binding protein in *Escherichia coli*. *Biochemie* **79,** 493–502 (1997).

124. Ormerod, L. P. & Horsfield, N. Short-course antituberculous chemotherapy for pulmonary and pleural disease: 5 years' experience in clinical practice. *Br. J. Dis. Chest* **81,** 268–271 (1987).

125. Diacon, A. H. *et al.* 14-day bactericidal activity of PA-824, bedaquiline, pyrazinamide, and moxifl oxacin combinations: A randomised trial. *Lancet* **380,** 986–993 (2012).

126. Via, L. E. *et al.* Tuberculous granulomas are hypoxic in guinea pigs, rabbits, and nonhuman primates. *Infect. Immun.* **76,** 2333–2340 (2008).

127. Scorpio, A. *et al.* Characterization of pncA mutations in pyrazinamide-resistant *Mycobacterium tuberculosis*. *Antimicrob. Agents Chemother.* 540–543 (1997). doi:10.1128/AAC.49.1.444-446.2005

128. Stansly, P. G., Schlosser, M. E. & Schlosser, E. The biological activity of pantolactone and pantoic acid. *J. Biol. Chem.* **161,** 513–515 (1945).

129. Eissenstat, R., Wyse, W. & Gaurth, R. Pantothenic acid status of adolescents. *Am. J. Clin. Nutr.* **44,** 931–937 (1986).

130. Teufel, M. *et al.* Sequence identification and characterization of human carnosinase and a closely related non-specific dipeptidase. *J. Biol. Chem.* **278,** 6521–6531 (2003).

131. Cole, S. T. *et al.* Deciphering the biology of *Mycobacterium tuberculosis* from the complete genome sequence. *Nature* **393,** 537–544 (1998).

132. Zimhony, O., Vilchèze, C., Arai, M., Welch, J. T. & Jacobs, W. R. Pyrazinoic acid and its n-propyl ester inhibit fatty acid synthase type I in replicating tubercle bacilli. *Antimicrob. Agents Chemother.* **51,** 752–4 (2007).

133. Wittwer, C. T., Gahl, W. a, Butler, J. D., Zatz, M. & Thoene, J. G. Metabolism of pantethine in cystinosis. *J. Clin. Invest.* **76,** 1665–72 (1985).

134. Yang, M. *et al.* A randomized, double-blind, placebo-controlled study of a novel pantothenic Acid-based dietary supplement in subjects with mild to moderate facial acne. *Dermatol. Ther. (Heidelb).* **4,** 93–101 (2014).

135. Nomura, H., Kimura, Y. & Okamoto, O. Effects of Antihyperlipidemic Drugs and Diet Plus Exercise Therapy in the Treatment of Patients with Moderate Hypercholesterolemia. **18,** 477–482

136. Coll, F. *et al.* Rapid determination of anti-tuberculosis drug resistance from whole-genome sequences. *Genome Med.* **7,** 51 (2015).

137. McDermott W, T. R. Activation of pyrazinamide and nicotinamide in acidic environments in vitro. *Am. Rev. Tuberc.* **70,** 748–754 (1954).

138. Coleman, D., Waddell, S. J. & Mitchison, D. A. Effects of low incubation temperatures on the bactericidal activity of anti-tuberculosis drugs. *J. Antimicrob.*

Chemother. **66,** 146–150 (2011).

139. Martin, M. Cutadapt removes adapter sequences from high-throughput sequencing reads. *EMBnet.journal* **17,** 10–12 (2011).

140. Langmead, B., Trapnell, C., Pop, M. & Salzberg, S. Ultrafast and memory-efficient alignment of short DNA sequences to the human genome. *Genome Biol.* **10,** R25 (2009).

141. Pritchard, J. R. *et al.* ARTIST: High-Resolution Genome-Wide Assessment of Fitness Using Transposon-Insertion Sequencing. *PLoS Genet.* **10,** (2014).

142. Zuzarte, P. C. *et al.* A two-dimensional pooling strategy for rare variant detection on next-generation sequencing platforms. *PLoS One* **9,** (2014).

143. Yee, M., Gopal, P. & Dick, T. Missense mutations in the unfoldase ClpC1 of the caseinolytic protease complex are associated with pyrazinamide resistance in *Mycobacterium tuberculosis*. *Antimicrob. Agents Chemother.* AAC.02342-16 (2016). doi:10.1128/AAC.02342-16

144. Barik, S., Sureka, K., Mukherjee, P., Basu, J. & Kundu, M. RseA, the SigE specific anti-sigma factor of *Mycobacterium tuberculosis*, is inactivated by phosphorylation-dependent ClpC1P2 proteolysis. *Mol. Microbiol.* **75,** 592–606 (2010).

145. Manganelli, R. & Provvedi, R. An integrated regulatory network including two positive feedback loops to modulate the activity σ^E in mycobacteria. *Mol. Microbiol.* **75,** 538–542 (2010).

146. Sassetti, C. M., Boyd, D. H. & Rubin, E. J. Genes required for mycobacterial

growth defined by high density mutagenesis. *Mol Microbiol* **48,** 77—84 (2003).

147. Manganelli, R., Voskuil, M. I., Schoolnik, G. K. & Smith, I. The *Mycobacterium tuberculosis* ECF sigma factor sigmaE: role in global gene expression and survival in macrophages. *Mol. Microbiol.* **41,** 423–37 (2001).

148. Fontán, P. A. *et al. Mycobacterium tuberculosis* Sigma Factor E Regulon Modulates the Host Inflammatory Response. *J. Infect. Dis.* **198,** 877–885 (2008).

149. Lanoix, J.-P. *et al.* Heterogeneous disease progression and treatment response in a C3HeB/FeJ mouse model of tuberculosis. *Dis. Model. Mech.* **8,** 603–10 (2015).

150. Lanoix, J. P. *et al.* Selective inactivity of pyrazinamide against tuberculosis in C3HeB/FeJ mice is best explained by neutral pH of caseum. *Antimicrob. Agents Chemother.* **60,** 735–743 (2016).

151. Almeida, D. V *et al.* Revisiting Anti-tuberculosis Activity of Pyrazinamide in Mice. *Mycobact. Dis. Tuberc. Lepr.* **4,** 145 (2014).

152. Mccune, B. Y. R. M., Tompsett, R. & Mcdermott, W. The fate of *Mycobacterium tuberculosis* in mouse tissues as determined by the microbial enumeration technique. *J. Exp. Med.* **104,** 763–802 (1956).

153. Cooper, a M., Segal, B. H., Frank, a a, Holland, S. M. & Orme, I. M. Transient loss of resistance to pulmonary tuberculosis in p47(phox-/-) mice. *Infection and immunity* **68,** 1231–4 (2000).

154. Shul'pin, G. B., Attanasion, D. & Suber, L. Efficient H2O2 oxidation of alkanes and arenes to alkyl peroxides and phenols catalyzed by the system vanadate – pyrazine-2-carboxylic acid.pdf. *J. Catal.* **142,** 147–152 (1993).

155. Kirillov, A. M. & Shul'pin, G. B. Pyrazinecarboxylic acid and analogs: Highly efficient co-catalysts in the metal-complex-catalyzed oxidation of organic compounds. *Coord. Chem. Rev.* **257,** 732–754 (2013).

156. Heldt, D. & Biaglow, J. E. Courmarin-3-Carboxylic Acid as a Detector for Hydroxyl Radicals Generated Chemically and by Gamma Radiation. *Radiat. Res.* **148,** 580–591 (1997).

157. Wehr, N. B. & Levine, R. L. Quantification of Protein Carbonylation. *Cell Senescence Methods Protoc.* **965,** 265–281 (2013).

158. VanderVen, B. C., Yates, R. M. & Russell, D. G. Intraphagosomal Measurement of the Magnitude and Duration of the Oxidative Burst. *Traffic* **10,** 372–378 (2009).

159. Odds, F. C. Synergy , antagonism , and what the chequerboard puts between them. *Antimicrob. Agents Chemother.* **52,** 1 (2003).

160. Yano, T. *et al.* Reduction of clofazimine by mycobacterial type 2 NADH:quinone oxidoreductase: a pathway for the generation of bactericidal levels of reactive oxygen species. *J. Biol. Chem.* **286,** 10276–87 (2011).

161. Akhtar, P. *et al.* Rv3303c of *Mycobacterium tuberculosis* protects tubercle bacilli against oxidative stress in vivo and contributes to virulence in mice. *Microbes Infect.* **8,** 2855–62 (2006).

162. Jackett, P. S., Aber, V. R. & Lowrie, D. B. Virulence and resistance to superoxide, low pH and hydrogen peroxide among strains of *Mycobacterium tuberculosis*. *J. Gen. Microbiol.* **104,** 37–45 (1978).

163. Vandal, O. H. *et al.* Acid-susceptible mutants of *Mycobacterium tuberculosis* share

hypersusceptibility to cell wall and oxidative stress and to the host environment. *J. Bacteriol.* **191,** 625–31 (2009).

164. Tyagi, P., Dharmaraja, A. T., Bhaskar, A., Chakrapani, H. & Singh, A. *Mycobacterium tuberculosis* has diminished capacity to counteract redox stress induced by elevated levels of endogenous superoxide. *Free Radic. Biol. Med.* **84,** 344–54 (2015).

165. Loomis, L. D. & Raymond, K. N. Solution equilibria of enterobactin and metal-enterobactin complexes. *Inorg. Chem.* **30,** 906–911 (1991).

166. Somoskovi, A., Wade, M. M., Sun, Z. & Zhang, Y. Iron enhances the antituberculous activity of pyrazinamide. *J. Antimicrob. Chemother.* **53,** 192–6 (2004).

167. Raynaud, C. *et al.* Mechanisms of pyrazinamide resistance in mycobacteria: importance of lack of uptake in addition to lack of pyrazinamidase activity. *Microbiology* **145 (Pt 6,** 1359–67 (1999).

168. Speirs, R. J., Welch, J. T. & Cynamon, M. H. Activity of n-propyl pyrazinoate against pyrazinamide-resistant *Mycobacterium tuberculosis* : investigations into mechanism of action of and mechanism of resistance to pyrazinamide. *Antimicrob. Agents Chemother.* **39,** 1269–1271 (1995).

169. Sambandamurthy, V. *et al.* A pantothenate auxotroph of *Mycobacterium tuberculosis* is highly attenuated and protects mice against tuberculosis. *Nat. Med.* **8,** 1171–1174 (2002).

170. Sambandamurthy, V. K. *et al.* Long-term protection against tuberculosis following

vaccination with a severely attenuated double lysine and pantothenate auxotroph of *Mycobacterium tuberculosis*. *Infect. Immun.* **73,** 1196–1203 (2005).

171. Bornemann, C., Jardine, M. A., Spies, H. S. C. & Steenkamp, D. J. Biosynthesis of mycothiol: elucidation of the sequence of steps in *Mycobacterium smegmatis*. *Biochem. J.* **629,** 623–629 (1997).

172. Effects, N. *et al.* Noxioius effects of oxygen reactive species on energy-coupling processes in Ehrlich ascites tumor mitochondria and the protection by pantothenic acid. *Free Radic. Biol. Med.* **20,** 793–800 (1996).

173. Wojtczak, L. & Slyshenkov, V. S. Protection by pantothenic acid against apoptosis and cell damage by oxygen free radicals--the role of glutathione. *Biofactors* **17,** 61–73 (2003).